AN ABSTRACT OF THE THESIS OF

Prasan Chintawongvanich for the Master of Science Degree in Chemistry presented on April 12, 1979

Title: Diffusion Coefficients of Cd^{++} and Co^{++} at 20°C by Polarography

Abstract approved: Charles M. Gramlich

The limiting diffusion coefficients of Cd^{++} and Co^{++} at 20°C, determined from concentration overvoltage at a dropping mercury electrode, are $(6.08 \pm 0.09) \times 10^{-6}$ cm^2sec^{-1} and $(6.28 \pm 0.17) \times 10^{-6}$ cm^2sec^{-1}, respectively.

The apparent diffusion coefficients of Cd^{++} and Co^{++} in the supporting electrolytes used, $NaNO_3$ and Na_2SO_4, decrease as the ionic strengths and the viscosities of the solutions increase.

A plot of the apparent diffusion coefficient of either Cd^{++} or Co^{++} at zero concentration of the supporting electrolyte as a function of the concentration of Cd^{++} or Co^{++}, under the experimental conditions, has a positive slope.

DIFFUSION COEFFICIENTS OF Cd^{++} AND Co^{++} AT 20°C BY POLAROGRAPHY

A Thesis

Presented to

the Department of Chemistry

EMPORIA STATE UNIVERSITY

In Partial Fulfillment

of the Requirements for the Degree

Master of Science

by

Prasan Chintawongvanich

April 1979

Charles M. Grinstead

Approved for the Major Department

Harold E. Durst

Approved for the Graduate Council

CONTENTS

SECTION		PAGE
1	INTRODUCTION	1
1.1	Electrode Process	1
1.2	Overvoltage	2
1.3	Diffusion Coefficient by Polarography	2
1.4	Reasons for Study	3
2	THEORETICAL FRAMEWORK	5
2.1	Mathematics of Diffusion	5
2.2	Linear Diffusion at a Plane Electrode Surface	6
2.3	Diffusion Controlled Process	7
2.4	Influence of Supporting Electrolyte on the Diffusion Current	8
2.5	Polarography	12
2.6	The Modified Ilkovic Equation	16
2.7	Dependence of Diffusion Current on Flow-rate and Drop-time	19
2.7.1	Flow-rate	20
2.7.2	Drop-time	21
2.8	Diffusion Coefficient as a Function of the Ionic Strength	23
2.8.1	Changes in the Effective Force Causing Diffusion	25
2.8.2	The Retarding Force	26
2.8.2.1	The Relaxation Effect	27
2.8.2.2	The Electrophoretic Effect	29
2.9	The Effect of Viscosity on the Diffusion Coefficient	29
3	METHOD	32
3.1	Diffusion Controlled Process at a Dropping Mercury Electrode	32

SECTION		PAGE
3.2	The Instantaneous Currents of Cadmium and Cobalt(II) Ions on Single Mercury Drops	32
3.2.1	Correction for Charging Current	32
3.2.2	Suppression of Maxima	33
3.2.3	Determination of the Flow-rate	35
3.2.4	Determination of the Drop-time	35
3.2.5	Determination of the Apparent Diffusion Coefficients of Cadmium and Cobalt (II) Ions	37
3.3	Determination of Limiting Diffusion Coefficient	38
4	APPARATUS AND INSTRUMENTATION	40
4.1	The Polarography System	40
4.1.1	The Dropping Mercury Electrode Apparatus	40
4.1.2	The Polarography Module and the Operational Amplifier System	41
4.1.3	The Chart Recorder	47
4.2	Calibration	47
4.3	Temperature Controlled System	48
5	PROCEDURE AND EXPERIMENTAL TECHNIQUE	51
5.1	Preparation of Standard Solutions	51
5.1.1	Cadmium Nitrate Standard Solution	51
5.1.2	Cobalt (II) Nitrate Standard Solution	52
5.1.3	Cobalt (II) Sulfate Standard Solution	52
5.1.4	Sodium Nitrate Standard Solution	52
5.1.5	Sodium Sulfate Standard Solution	53
5.1.6	Gelatin Solution	53
5.2.1	Preparation of Sample	53
5.2.2	Removal of the Dissolved Oxygen	54
5.2.3	Temperature Control	55
5.3	Measurements	55

LIST OF TABLES

TABLE		PAGE
1	Influence of Various Concentrations of Potassium Chloride, Potassium Nitrate, and Hydrochloric Acid of the Ratio of the Limiting Current Density of Lead Chloride	13
2	Comparison of Observed and Calculated Rates of Flow of Mercury From a Capillary Tube Under Various Pressures at 25°C	22
3	Dependence of Instantaneous Current on Drop-time at Various Applied Potentials at 20°C	24
4	Diffusion Coefficients of Cadmium Ion in Various Viscous Solution of Sulfuric Acid at 25°C	31
5	Diffusion Coefficient of Cobalt (II) Ion in 0.12 M Sodium Sulfate as a Function of Gelatin Concentration at 20°C	34
6	Determinations of Capillary Radius and Length	36
7	The Limiting Diffusion Coefficient of Cadmium Ion at 20°C	58
8	The Limiting Diffusion Coefficient of Cobalt (II) Ion at 20°C	62
9	Percent Magnitude of Random Errors	71
10	The Most Probable Error of the Apparent Diffusion Coefficients	72
11	Standard Deviations of the Diffusion Coefficients of Cadmium and Cobalt (II) Ions at Some Finite Concentrations of the Metal Ions and at Zero Concentration of the Supporting Electrolyte	73
12	The Apparent Diffusion Coefficients of Cd^{++} in $NaNO_3$ Solutions at 20.0 $\pm$ 0.1°C	84
13	The Apparent Diffusion Coefficients of Cd^{++} in Na_2SO_4 Solutions at 20.0 $\pm$ 0.1°C	88
14	The Apparent Diffusion Coefficients of Co^{++} in $NaNO_3$ Solutions at 20.0 $\pm$ 0.1°C	92
15	The Apparent Diffusion Coefficients of Co^{++} in Na_2SO_4 Solutions at 20.0 $\pm$ 0.1°C	95

TABLE		PAGE
16	The Diffusion Coefficients of Cd^{++} at Some Finite Concentrations of Cd^{++} and at Zero Concentration of the Supporting Electrolyte at 20°C	100
17	The Diffusion Coefficients of Co^{++} at Some Finite Concentrations of Co^{++} and at Zero Concentration of the Supporting Electrolyte at 20°C	101

LIST OF FIGURES

FIGURE		PAGE
1	Simple Polarographic Circuit	14
2	Dropping Mercury Electrode	15
3	Reduction Wave of 0.5 mM Co^{++} in 0.12 M Na_2SO_4 and 0.001% Gelatin Solution at 20°C	17
4	Dropping Mercury Electrode Apparatus	42
5	Front View of the D.M.E. Stand	43
6	Back View of the D.M.E. Stand	44
7	Simplified Schematic of the Polarography System	45
8	Air Bath	49
9	The Diffusion Coefficient of Cd^{++} at Zero Concentration of $NaNO_3$ as a Function of Concentration at 20°C	59
10	The Diffusion Coefficient of Cd^{++} at Zero Concentration of Na_2SO_4 as a Function of Concentration at 20°C	60
11	The Diffusion Coefficient of Co^{++} at Zero Concentration of $NaNO_3$ as a Function of Concentration at 20°C	63
12	The Diffusion Coefficient of Co^{++} at Zero Concentration of Na_2SO_4 as a Function of Concentration at 20°C	64
13	The Apparent Diffusion Coefficient of 0.5003 mM Cd^{++} in $NaNO_3$ as a Function of Concentration at 20°C	103
14	The Apparent Diffusion Coefficient of 1.0006 mM Cd^{++} in $NaNO_3$ as a Function of Concentration at 20°C	104
15	The Apparent Diffusion Coefficient of 2.0012 mM Cd^{++} in $NaNO_3$ as a Function of Concentration at 20°C	105
16	The Apparent Diffusion Coefficient of 3.0018 mM Cd^{++} in $NaNO_3$ as a Function of Concentration at 20°C	106
17	The Apparent Diffusion Coefficient of 4.0024 mM Cd^{++} in $NaNO_3$ as a Function of Concentration at 20°C	107
18	The Apparent Diffusion Coefficient of 5.0030 mM Cd^{++} in $NaNO_3$ as a Function of Concentration at 20°C	108
19	The Apparent Diffusion Coefficient of 6.0036 mM Cd^{++} in $NaNO_3$ as a Function of Concentration at 20°C	109

FIGURE		PAGE
20	The Apparent Diffusion Coefficient of 0.5007 mM Cd^{++} in Na_2SO_4 as a Function of Concentration at 20°C	110
21	The Apparent Diffusion Coefficient of 1.0014 mM Cd^{++} in Na_2SO_4 as a Function of Concentration at 20°C	111
22	The Apparent Diffusion Coefficient of 2.0028 mM Cd^{++} in Na_2SO_4 as a Function of Concentration at 20°C	112
23	The Apparent Diffusion Coefficient of 3.0043 mM Cd^{++} in Na_2SO_4 as a Function of Concentration at 20°C	113
24	The Apparent Diffusion Coefficient of 4.0056 mM Cd^{++} in Na_2SO_4 as a Function of Concentration at 20°C	114
25	The Apparent Diffusion Coefficient of 5.0171 mM Cd^{++} in Na_2SO_4 as a Function of Concentration at 20°C	115
26	The Apparent Diffusion Coefficient of 6.0085 mM Cd^{++} in Na_2SO_4 as a Function of Concentration at 20°C	116
27	The Apparent Diffusion Coefficient of 0.5017 mM Co^{++} in $NaNO_3$ as a Function of Concentration at 20°C	117
28	The Apparent Diffusion Coefficient of 1.0034 mM Co^{++} in $NaNO_3$ as a Function of Concentration at 20°C	118
29	The Apparent Diffusion Coefficient of 2.0068 mM Co^{++} in $NaNO_3$ as a Function of Concentration at 20°C	119
30	The Apparent Diffusion Coefficient of 3.0102 mM Co^{++} in $NaNO_3$ as a Function of Concentration at 20°C	120
31	The Apparent Diffusion Coefficient of 4.0136 mM Co^{++} in $NaNO_3$ as a Function of Concentration at 20°C	121
32	The Apparent Diffusion Coefficient of 5.0170 mM Co^{++} in $NaNO_3$ as a Function of Concentration at 20°C	122
33	The Apparent Diffusion Coefficient of 6.0204 mM Co^{++} in $NaNO_3$ as a Function of Concentration at 20°C	123
34	The Apparent Diffusion Coefficient of 0.5004 mM Co^{++} in Na_2SO_4 as a Function of Concentration at 20°C	124
35	The Apparent Diffusion Coefficient of 1.0008 mM Co^{++} in Na_2SO_4 as a Function of Concentration at 20°C	125
36	The Apparent Diffusion Coefficient of 2.0016 mM Co^{++} in Na_2SO_4 as a Function of Concentration at 20°C	126
37	The Apparent Diffusion Coefficient of 3.0024 mM Co^{++} in Na_2SO_4 as a Function of Concentration at 20°C	127

FIGURE PAGE

38 The Apparent Diffusion Coefficient of 4.0032 mM Co^{++} in Na_2SO_4 as a Function of Concentration at 20°C 128

39 The Apparent Diffusion Coefficient of 5.0040 mM Co^{++} in Na_2SO_4 as a Function of Concentration at 20°C 129

40 The Apparent Diffusion Coefficient of 6.0048 mM Co^{++} in Na_2SO_4 as a Function of Concentration at 20°C 130

ACKNOWLEDGEMENT

Upon five years of seeking my degrees at E.S.U., I feel indebted to Professor Charles M. Greenlief who advised me throughout the years. Besides Physical Chemistry, something rather "special", that I learned from Professor Greenlief is his personality. Perhaps I need not describe his personality since everyone in Cram Science Hall knows well that Professor Greenlief has the very "best" in all respects. He is polite, intelligent, and wise.

Professor Greenlief also gave his time and effort to assist me throughout the investigation of this manuscript. I feel infinitely indebted and forever grateful for his kindness.

SECTION 1

INTRODUCTION

1.1 Electrode Processes

There are many interesting aspects about the electrode processes and the reactions at the electrode surface. In general, these processes may be categorized in the following manner.[1-3]

1. The mass transfer process which involves the transference of matter through a solution towards and away from the electrode.

2. Charge transfer reaction in which a charge carrier (ion or electron) is transported, against the potential controlled activation energy, from one phase into another across the electrical double layer. The charge transfer reaction is of fundamental importance in electrochemistry, since it is the only reaction directly affected by the electrode potential, and the rate of reaction is determined by the potential difference across the electrical double layer.

3. The chemical reaction, which is a reaction in the interior of the electrical double layer, whose rate depends only on the concentrations and is independent of the electrode potential.

4. The crystallization reaction by which the atoms deposited during the transfer reaction are incorporated into the crystal lattice, or, conversely, removed from the lattice.

Among these processes (1-4), in situations where reactions (2-4) are sufficiently rapid compared to (1), the overall rate of the electrode reaction will be controlled by the mass transfer process. Furthermore, if diffusion is the only effective factor controlling mass transfer, the overall electrode processes are said to be "diffusion controlled".

1.2 Overvoltage

When current flows through an electrode, its potential E_i, assumes a value different from that in the absence of current. The deviation of the electrode potential, E_i, from the zero current potential, E_0, is called the overvoltage, η'. Thus

$$\eta' = E_i - E_0 \qquad (1.2\text{-}1)$$

The diffusion overvoltage is therefore the deviation of electrode potential between the zero current potential and the potential E_i attained when current flows as a result of the changed concentrations, or, more accurately, the changed activities of electroreducible or electrooxidizable substances at the electrode surface. However, during current flow, slow reactions also lead to changes in the concentrations or activities at the electrode surface. The sum of the diffusion overvoltage and this reaction overvoltage is often called "concentration overvoltage".[4-6]

Concentration overvoltage at a dropping mercury electrode (D.M.E.) is recognized as polarography, which is a subject that has been extensively studied. The scope of polarography is thus based on the situation of mass transfer being rate determining. Furthermore, it is considered mathematically difficult to include migration, where the overvoltage is a complicated function of transference number, and convection, into the process of mass transfer. Therefore, polarographic studies and those systems investigated by polarography are studies of a diffusion controlled process.

1.3 Diffusion Coefficient by Polarography

The limiting current obtained by polarography is proportional to the concentration and the diffusion coefficient of the substance under investigation.[7-13] In more accurate work, the activity should be used

in place of the concentration since the variation of the concentration causes changes in the ionic strength of the solution. Therefore, the limiting current is characterized by indifferent electrolytes as well.

In this study, a series of diffusion coefficients D_j of the metal M_j are obtained by changing the ionic strength of the system by changing the concentrations C_{M_j} and C_{S_j} of the metal M_j and the indifferent electrolyte S_j respectively. The diffusion coefficient may be expressed as a function of the concentrations of the electrolytes as

$$D_j = F(C_{M_j}, C_{S_j}) \tag{1.3-1}$$

The variation of the diffusion coefficient has been studied by changing the concentrations of the electrolytes, and it may be written in the form of

$$dD_j = \left(\frac{\partial D_j}{\partial C_{M_j}}\right) dC_{M_j} + \left(\frac{\partial D_j}{\partial C_{S_j}}\right) dC_{S_j} \tag{1.3-2}$$

1.4 Reasons for Study

The determination of the diffusion coefficients by polarography has been extensively carried out by many investigators.[14-26] A study of the results obtained by these investigators shows inconsistencies between them.

In the present study, a correction for the effect of ion-ion interactions, which was neglected in the previous studies, is made for the determination of the limiting diffusion coefficients obtained by polarography.

As an ideal ion for polarographic work, Cd^{++} was chosen for study as a "calibration ion" since its overvoltage in frequently used indifferent electrolytes, e.g., KCl, KNO_3, $NaNO_3$, and Na_2SO_4, has no "maxima".[27-32] Co^{++}, on the other hand, was chosen because the diffusion coefficient of

this ion has never been successfully investigated by the polarographic method. No experimental value of the diffusion coefficient of Co++ by polarography has yet been published.

Perhaps the most suitable indifferent electrolytes for this study are $NaNO_3$ and Na_2SO_4. The ionic strengths of these electrolytes at the same molar concentrations are different by a factor of $\sqrt{3}$, and consequently the changes in the magnitude of the diffusion coefficients from one medium to another due to the interionic interactions may be studied as changes in the ionic strengths of the solutions.

A temperature of 20°C is assigned to be a "working temperature" for this study since this temperature can be precisely controlled with the available instruments. There are literature values of the diffusion coefficients of Cd^{++} and Co^{++} obtained by other methods available at 20°C, and thus a comparison of the results between methods can be made.

SECTION 2

THEORETICAL FRAMEWORK

2.1 Mathematics of Diffusion

As heat conduction deals with the transfer of heat through a temperature gradient due to the random motions of the conducting matter, diffusion is the process by which matter is transported through a concentration gradient as a result of random motions.[33-36] The mathematical expression of diffusion is therefore based on the hypothesis that the rate of transfer of diffusing substances, in the number of moles per second, through a given cross-sectional plane of area A is proportional to the concentration gradient measured in a direction normal to the cross-sectional plane, and it is expressed by

$$\frac{dN}{dt} = - DA\left(\frac{\partial C}{\partial x}\right) \tag{2.1-1}$$

where D is the diffusion coefficient, and has the dimensions of $cm^2 sec^{-1}$.

Equation (2.1-1) is usually referred to as Fick's First Law.

It is often convenient to express Eq. (2.1-1) as a flux, f, which is defined as the time rate of transfer of diffusing substances per unit area. The flux across a plane at a distance x from the origin, f_x, is thus

$$f_x = - D \left(\frac{\partial C}{\partial x}\right) \tag{2.1-2}$$

The time rate of change of concentration between two planes separated by an infinitesimal distance dx is equal to the difference between the number of moles which leave across the plane at x and the number of moles which enter across the plane at x + dx, divided by the volume enclosed between the planes. That is

$$\frac{\partial C}{\partial t} = \frac{f_x - f_{x+dx}}{dx} \tag{2.1-3}$$

The expansion of f_{x+dx} about the plane at x in a Taylor series is

$$f_{x+dx} = f_x + \left(\frac{\partial f_x}{\partial x}\right)_{x=x} dx \qquad (2.1\text{-}4)$$

Differentiation of Eq. (2.1-2) gives

$$\frac{\partial f}{\partial x} = - D \left(\frac{\partial^2 C}{\partial x^2}\right) \qquad (2.1\text{-}5)$$

Substituting Eqs. (2.1-4) and (2.1-5) into Eq. (2.1-3) gives the time rate of change of the concentration at a given plane at a given instant.

$$\left(\frac{\partial C}{\partial t}\right)_x = D \left(\frac{\partial^2 C}{\partial x^2}\right)_t \qquad (2.1\text{-}6)$$

Equation (2.1-6) is frequently referred to as Fick's Second Law.

2.2 Linear Diffusion at a Plane Electrode Surface

An overall redox electrode reaction at a plane electrode surface of metal species M_{ox_i} and M_{red_i} with n electrons transferred may be written as

$$(-\nu_{red_1})M_{red_1} + (-\nu_{red_2})M_{red_2} + \ldots = \nu_{ox_1} M_{ox_1} + \nu_{ox_2} M_{ox_2} + \ldots + ne^- \qquad (2.2\text{-}1)$$

where the stoichiometric factors ν_j are positive for oxidized components and are negative for reduced components.

The electrode reaction (Eq. 2.2-1) at a plane electrode surface constitutes a diffusion layer of thickness dx as a result of depletion of the diffusing species at the electrode surface. The diffusion current at any instant, i_t, is therefore governed by the flux of the electroreducible or electrooxidizable metal, M_j, at the plane electrode surface where x = 0, and may be written as

$$i_{t,j} = \frac{n}{\nu_j}(FAf_{j,x=0,t}) = - \frac{n}{\nu_j}(FAD_j)\left(\frac{\partial C_j}{\partial x}\right)_{x=0,t} \qquad (2.2\text{-}2)$$

where F is the Faraday.

It is often convenient to rewrite Eq. (2.2-2) in terms of the flux f, thus

$$f_j = \frac{i_{d,j}\nu_j}{nF} = -D_j \left(\frac{\partial C_j}{\partial x}\right)_{x=0,t} \qquad (2.2\text{-}3)$$

where $i_{d,j}$ is the current density at the electrode surface.

In the stationary state and in the absence of homogeneous chemical equilibria (nonsteady state) through the entire diffusion layer of thickness dx, the flow of the component M_j is a constant. That is $\left(\frac{\partial C_j}{\partial x}\right)$ has a nonzero value, and is equal to $-\frac{(C_j - \bar{C}_j)}{x}$ for $0<dx<x$. Eq. (2.2-3) may thus be written as

$$f_j = D_j \frac{(C_j - \bar{C}_j)}{x} \qquad (2.2\text{-}4)$$

where C_j is the molar concentration at the electrode surface, and $\bar{C}_j$ is the molar concentration of M_j at distance x from the electrode surface, i.e., bulk concentration.

The limiting current density, $\bar{i}_{d,j}$, is obtained when the concentration gradient has a maximum value. That is, the condition when the component M_j at the electrode surface is completely depleted and C_j is equal to zero.

$$\bar{i}_{d,j} = -\frac{n}{\nu_j} FD_j \left(\frac{\bar{C}_j}{x}\right) \qquad (2.2\text{-}5)$$

2.3 Diffusion Controlled Process

The transference of matter through a solution towards and away from an electrode involves the following consideration:

1. diffusion, which has been discussed in the previous sections.

2. migration, which is referred to as the motion of the diffusing species due to the electrical potential gradient (this electrical field is generated by the limited conductivity in the diffusion layer, i.e., the property of maintenance of electroneutrality within the diffusion layer).

3. convection, which is the motions of matter under the influence of stirring, mechanical agitation, and/or temperature gradient.

In polarographic work, convection is often eliminated by proper arrangement of the apparatus used. While migration is often minimized by adding an "indifferent electrolyte"[37] in excess[38-41] (fifty or more times greater than the concentration of the electroactive component). Under this condition, the electrochemical process is assumed to be solely controlled by diffusion, upon which polarography is based.

2.4 Influence of Supporting Electrolyte on the Diffusion Current

In this section, some theories and their general treatment are given to demonstrate, in parallel, the two extreme cases of diffusion, namely, those taking place in the absence and in the presence of the supporting electrolyte. These two cases are then used to compare with free diffusion -- that is, diffusion without the migration effect.

The force causing diffusion arises from the concentration gradient and the electrical gradient within the diffusion field.[42,43] It is most convenient to express this force in terms of the gradient of the electrochemical potential, η''_j, which is composed of the molar chemical potential, μ_j, and the reversible electrical work, $zF\Psi$. The electrical potential is given by

$$\begin{aligned}\eta''_j &= \mu_j + z_j F\Psi \\ &= \bar{\mu}_j + RT\ln C_j + z_j F\Psi \end{aligned} \qquad (2.4\text{-}1)$$

where $\bar{\mu}_j$ is the chemical potential of the component M_j in the standard state, R is the molar gas constant, T is the absolute temperature, z_j is the signed charge ($z_j \equiv \frac{n}{\nu_j}$), and Ψ is the Galvanic potential.
The gradient of the electrochemical potential is equal to the force causing diffusion, $\bar{F}_j$. Thus differentiation of Eq. (2.4-1) with respect to x gives

$$\frac{\partial \eta''_j}{\partial x} = \left(\frac{RT}{C_j}\right)\left(\frac{\partial C_j}{\partial x}\right) + z_j F\left(\frac{\partial \Psi}{\partial x}\right) = \overline{F}_j \tag{2.4-2}$$

The flux of the diffusing component M_j is given by Eq. (2.1-1) to be

$$f_j = \left(\frac{1}{A}\right)\left(\frac{dN_j}{dt}\right) = \frac{C_j \overline{v}_j}{K} \tag{2.4-3}$$

where C_j is the molar concentration, $\overline{v}_j$ is the velocity acquired by each ion or molecule of M_j moving through the diffusion field, and K is Avogadro's number. The velocity $\overline{v}_j$ is often expressed in terms of the mobility δ_j, whose dimensions are those of velocity divided by force, or $\overline{v}_j = \overline{F}_j \delta_j$. Combining Eqs. (2.4-2) and (2.4-3) with this relationship, the flux now may be written as

$$f_j = \left[(RT)\left(\frac{\partial C_j}{\partial x}\right) + (z_j C_j F)\left(\frac{\partial \Psi}{\partial x}\right)\right] \frac{\delta_j}{K} \tag{2.4-4}$$

Since $\delta_j = \frac{K}{RT}(D_j)$,[44-46] the flux may also be written in terms of the diffusion coefficient D_j.

$$f_j = D_j\left[\frac{\partial C_j}{\partial x} + z_j C_j \left(\frac{F}{RT}\right)\left(\frac{\partial \Psi}{\partial x}\right)\right]$$

$$= -\frac{i_{d,j}\nu_j}{nF} \tag{2.4-5}$$

Eq. (2.4-5) is also valid for the components which are not involved in the electrode reaction, namely, $\nu_j = 0$, and thus

$$\frac{RT}{C_j}\left(\frac{\partial C_j}{\partial x}\right) = -z_j F\left(\frac{\partial \Psi}{\partial x}\right) \tag{2.4-6}$$

The integration of Eq. (2.4-6) with respect to the thickness of the layer dx,

from x = 0, where the concentration is C_j and the potential difference is $\Delta \Psi$,

to x = x, where the concentration is $\overline{C}_j$ and the potential difference is zero

gives

$$C_j = \overline{C}_j \exp(-\frac{z_j F}{RT} \Delta \Psi) \qquad (2.4\text{-}7)$$

A simple example will be given together with previously published data to demonstrate the influence of the supporting electrolyte on the diffusion current.

Electrolyte: C_1 - mole/liter of $PbCl_2$, C_2 - mole/liter of KCl

Charge transfer reaction: $Pb^{++} + 2e^- = Pb$

thus; n = 2

$$\nu_{Pb^{++}} = -1, \quad z_{Pb^{++}} = +2, \quad \overline{C}_{Pb^{++}} = C_1$$

$$\nu_{K^+} = 0, \quad z_{K^+} = +1, \quad \overline{C}_{K^+} = C_2$$

$$\nu_{Cl^-} = 0, \quad z_{Cl^-} = -1, \quad \overline{C}_{Cl^-} = 2C_1 + C_2$$

It follows from Eq. (2.4-7) that

$$C_{K^+} = C_2 \exp[(-\frac{F}{RT}) \Delta \Psi] \qquad (2.4\text{-}8.1)$$

$$C_{Cl^-} = (2C_1 + C_2) \exp[(\frac{F}{RT}) \Delta \Psi] \qquad (2.4\text{-}8.2)$$

Since there exists the condition of electroneutrality within the diffusion layer, the following expression must be valid.

$$2C_{Pb^{++}} + C_{K^+} = C_{Cl^-} \qquad (2.4\text{-}9)$$

Applying Eq. (2.4-5) to Pb^{++} with $\nu_{Pb^{++}} = -1$ and n = 2 gives

$$\frac{i_{d,Pb^{++}}}{FD_{Pb^{++}}} = 2[\frac{\partial C_{Pb^{++}}}{\partial x} + C_{Pb^{++}}(\frac{F}{RT})(\frac{\partial \Psi}{\partial x})] \qquad (2.4\text{-}10)$$

Substitution of Eq. (2.4-8) into Eq. (2.4-9) gives

$$C_{Pb^{++}} = [\frac{(2C_1 + C_2)}{2}] \exp[(\frac{F}{RT}) \Delta \Psi] - \frac{C_2}{2} \exp[(-\frac{F}{RT}) \Delta \Psi] \qquad (2.4\text{-}11)$$

While the differentiation of Eq. (2.4-11) with respect to x gives

$$\frac{\partial C_{Pb^{++}}}{\partial x} = [\frac{(2C_1 + C_2)}{2}(\frac{F}{RT})] \exp[(\frac{F}{RT}) \Delta \Psi] + [(\frac{C_2}{2})(\frac{F}{RT})] \exp[(-\frac{F}{RT}) \Delta \Psi] \qquad (2.4\text{-}12)$$

Substitution of these expressions for $C_{Pb^{++}}$ and $\frac{\partial C_{Pb^{++}}}{\partial x}$ into Eq. (2.4-10) yields

$$\frac{i_{d,Pb^{++}}}{FD_{Pb^{++}}} = \left(\frac{2F}{RT}\right)\left(\frac{\partial \Psi}{\partial x}\right)(2C_1 + C_2)\exp\left[\left(\frac{F}{RT}\right)\Delta \Psi\right] \qquad (2.4\text{-}13)$$

Upon the integration of Eq. (2.4-13) with respect to x, the following expression is obtained.

$$\frac{i_{d,Pb^{++}}}{FD_{Pb^{++}}} = \frac{2}{x}(2C_1 + C_2)\left[1 - \exp\left(\frac{F}{RT}\Delta \Psi\right)\right] \qquad (2.4\text{-}14)$$

The limiting current density, $\bar{i}_{d,Pb^{++}}$, is obtained by substituting into Eq. (2.4-14) the expression, $\exp[(F/RT)\Delta \Psi] = [C_2/(2C_1 + C_2)]$ which is derived from Eq. (2.4-11) for $C_{Pb^{++}} = 0$.

$$\begin{aligned}\bar{i}_{d,Pb^{++}} &= \left(\frac{2F}{x}\right)D_{Pb^{++}}(2C_1 + C_2)\left[1 - \left(\frac{C_2}{2C_1 + C_2}\right)^{1/2}\right] \\ &= \left(\frac{2F}{x}\right)D_{Pb^{++}}C_{Pb^{++}}\left(2 + \frac{C_2}{C_1}\right)\left[1 - \left(\frac{C_2/C_1}{2 + C_2/C_1}\right)^{1/2}\right] \qquad (2.4\text{-}15)\end{aligned}$$

According to Eq. (2.4-15), the limiting current density $\bar{i}_{d,Pb^{++}}$ in the absence of KCl is $[4FD_{Pb^{++}}(\bar{C}_{Pb^{++}}/x)]$, which is exactly double of its value for free diffusion which depends only upon the concentration gradient as seen from Eq. (2.2-5). However, $\bar{i}_{d,Pb^{++}}$ decreases rapidly with increases in the ratio of C_2/C_1, and eventually converges to the limiting value for free diffusion as $C_2/C_1 \to \infty$.

The data given below is for the ratio of $\bar{i}_{d,Pb^{++}}/\bar{i}_{d,Pb^{++}\infty}$ as a function of the ratio C_2/C_1 obtained from Eq. (2.4-15). The symbol $\bar{i}_{d,Pb^{++}\infty}$ denotes the limiting current density for free diffusion.

C_2/C_1	$\bar{i}_{d,Pb^{++}}/\bar{i}_{d,Pb^{++}\infty}$
0	2.0000
0.1	1.6417
0.2	1.5367
0.5	1.3820

C_2/C_1	$i_{d,Pb^{++}}/i_{d,Pb^{++}\infty}$
1.0	1.2679
5.0	1.0839
50.0	1.0098
100.0	1.0050
1000.0	1.0006
∞	1

Experimental data obtained by Lingane and Kolthoff[47] showing the agreement with Eq. (2.4-15) is given in Table 1.

2.5 Polarography

Basically, polarography consists of the electrolytic solution (the electroactive component and the supporting electrolyte) between a reference electrode and a dropping mercury electrode (D.M.E.) which usually functions as the cathode. Figure 1 shows the classical arrangement of a simple polarographic circuit. The applied potential across the electrodes is varied by means of a potentiometer while the current flow is indicated on a sensitive galvanometer.

The D.M.E., shown in Figure 2, consists of a series of small mercury droplets which emerge, at a constant flow-rate m, from the tip of a capillary attached to a constant head device. The duration, or drop-time t_d, of each drop normally lies between 2-5 seconds for most practical applications.

In Figure 1, the reference electrode has been shown for simplicity as a large mercury pool on the bottom of the electrolytic cell. Due to its large area and the small magnitude of current normally encountered, the potential of such an electrode remains fairly constant. However, for most measurements, it is normal to replace this electrode by a saturated calomel electrode (S.C.E.).

Before any potential is applied, it is necessary to remove the

TABLE 1

INFLUENCE OF VARIOUS CONCENTRATIONS OF POTASSIUM CHLORIDE, POTASSIUM NITRATE, AND HYDROCHLORIC ACID ON THE RATIO OF THE LIMITING CURRENT DENSITY OF LEAD CHLORIDE[a]

C_2/C_1[b]	$i_{d,Pb^{++}}/i_{d,Pb^{++}_{\infty}}$		
	KCl	KNO_3	HCl
0	2.0000	2.0000	2.0000
0.1	1.8523	1.8409	1.7841
0.2	1.6932	1.7045	1.6591
0.5	1.5114	1.5227	1.4432
1.0	1.3409	1.3636	1.2727
5.0	1.1136	1.1136	1.0795
100.0	0.9489	0.9602	-
1000.0	0.9091	0.9602	-

[a] Reference 47.

[b] C_2/C_1 is the ratio of the concentration of $PbCl_2$ to that of the supporting electrolyte.

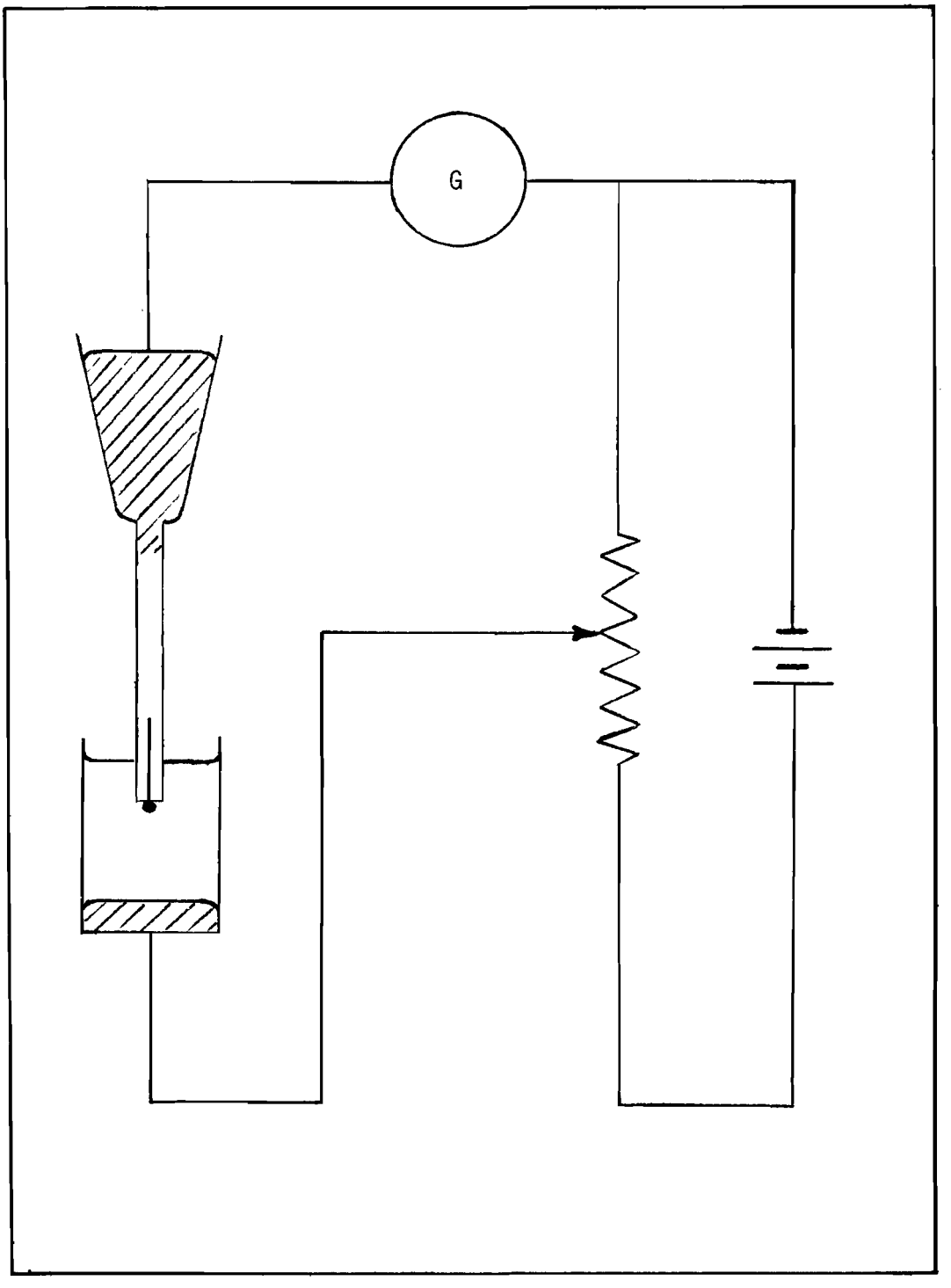

Figure 1

Simple Polarographic Circuit

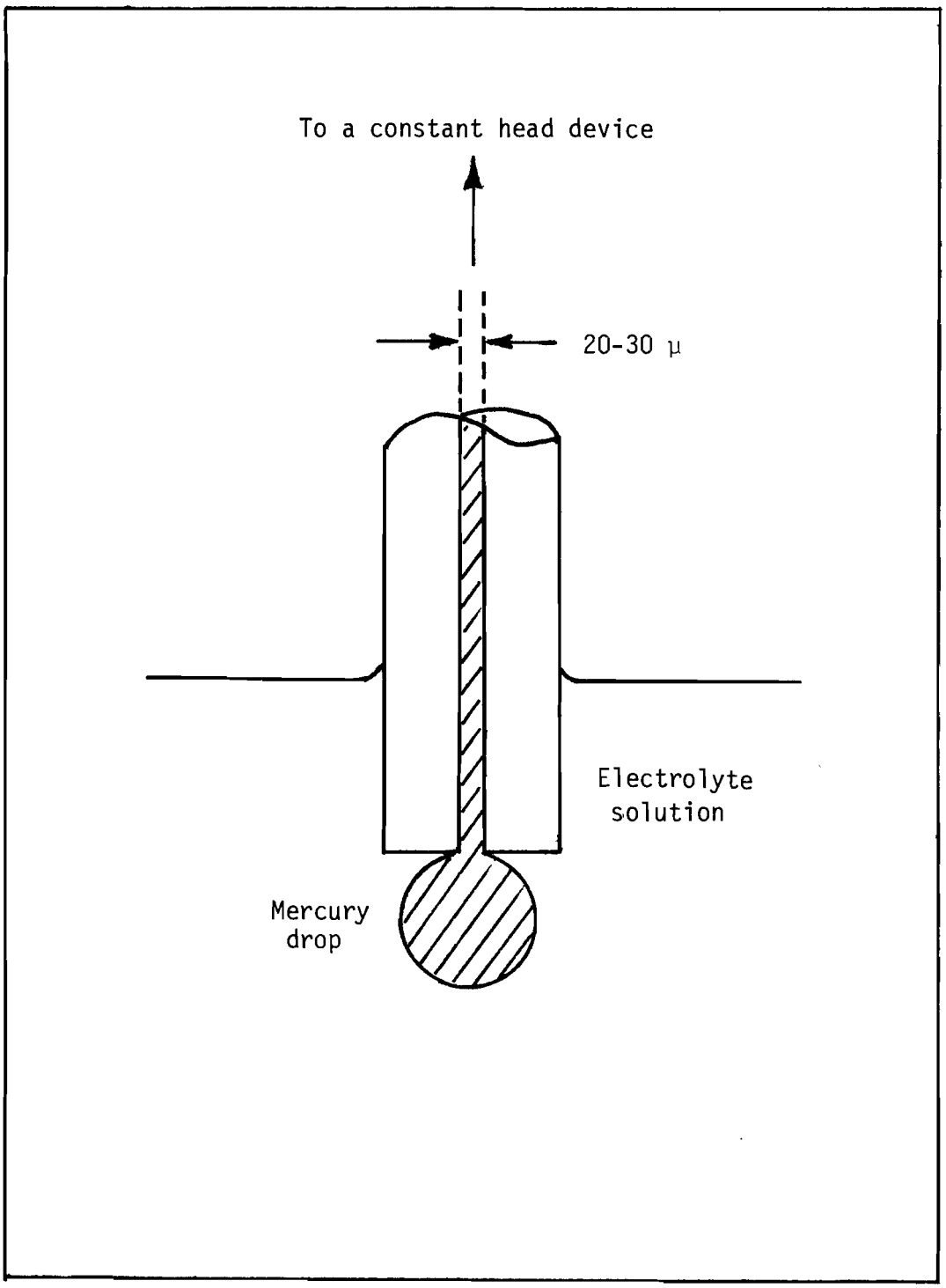

Figure 2

Dropping Mercury Electrode

dissolved oxygen which causes interference, which is accomplished by passing an inert gas, such as nitrogen, through the solution.

The current-voltage curve, or polarographic wave, as it is often called, is usually recorded by a chart recorder for convenience. Figure 3 shows an example of polarographic waves obtained in this study, the reduction wave of Co^{++} in Na_2SO_4-gelatin solution. As each mercury drop grows and falls, the current oscillates between a minimum and a maximum. The overall rise from the base line of this curve is called the limiting current, and is governed by the flux of Co^{++} to the surface of the growing mercury drop. The base line which also appears to oscillate as each mercury drop grows and falls is called a charging current, and it is a linear function of the applied potential.[48-50]

The potential corresponding to the mid-point of the wave shown in Figure 3, where the diffusion current is one-half of its maximum value, is often referred to as the "half-wave potential", $E_{1/2}$. At constant temperature, the half-wave potential is a characteristic property of a given electroactive component under fixed solution conditions. Measurement of half-wave potentials may therefore serve as a means of identification of different reducible species.

2.6 The Modified Ilkovic Equation

For an overall redox electrode reaction of Eq. (2.2-1) at the D.M.E., the instantaneous current i_t is given by Eq. (2.2-2).

$$i_{j,t} = (-\frac{n}{\nu_j})FAD\ (\frac{\partial C_j}{\partial r})_{r=r_0,t} \qquad (2.6\text{-}1)$$

Fick's Second Law for a spherical coordinated system has the form[51]

$$\frac{\partial C_j}{\partial t} = D_j(\frac{\partial^2 C_j}{\partial r^2} + \frac{2}{r}\frac{\partial C_j}{\partial r}) \qquad (2.6\text{-}2)$$

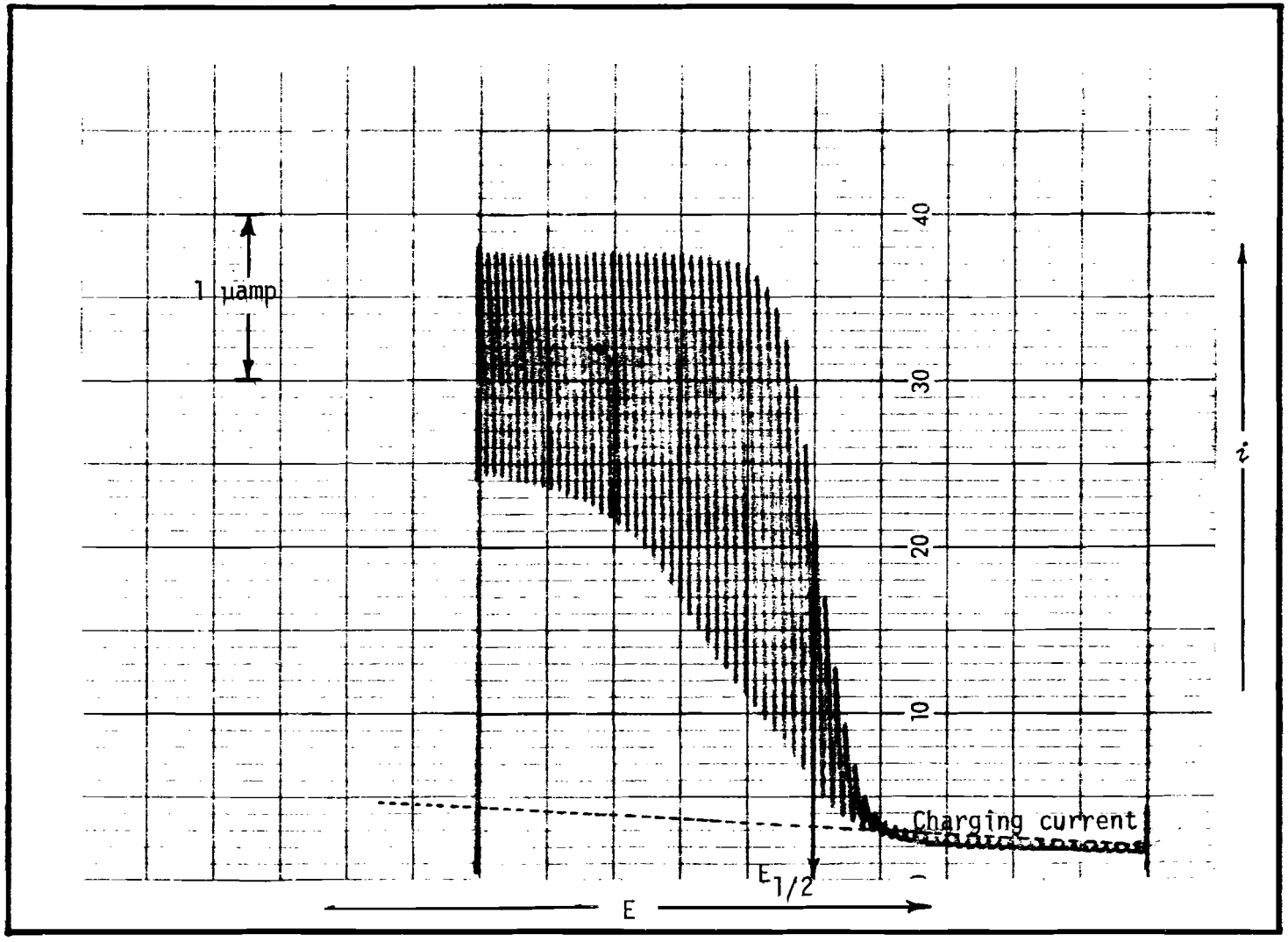

Figure 3

Reduction Wave of 0.5 mM Co^{++} in 0.12 M Na_2SO_4 and 0.001% Gelatin Solution at 20°C

The solution of Eq. (2.6-2) can be carried out with an appropriate initial and boundary conditions.[52-54] Before the electrode reaction of Eq. (2.2-1) takes place (t = 0), the concentration C_j at any distance from the center of the mercury drop, r, is that of the bulk concentration, $\overline{C}_j$. While the electrode reaction of Eq. (2.2-1) is taking place (t > 0), the concentration at the electrode surface, a distance r_0 from the center of the mercury drop, is equal to zero for the limiting diffusion current. That is, when the initial and boundary conditions are such that

$$t = 0,\ C_j = \overline{C}_j$$

$$t > 0,\ C_j = 0$$

Thus,

$$C_{j,t} = \overline{C}_j\left(\frac{r_0}{r}\right)\left(\frac{2}{\sqrt{\pi}}\right)\mathrm{erf}\left(\frac{r - r_0}{2\sqrt{D_j t}}\right) + \overline{C}_j\left(1 - \frac{r_0}{r}\right) \qquad (2.6\text{-}3)$$

Differentiation of Eq. (2.6-3) gives

$$\frac{\partial C_j}{\partial r} = \left(\frac{2}{\sqrt{\pi}}\right)\overline{C}_j\left(\frac{r_0}{r}\right)\mathrm{erf}\left(\frac{r - r_0}{2\sqrt{D_j t}}\right) + \left[\overline{C}_j\left(\frac{r_0}{r}\right)\left(\frac{1}{\sqrt{D_j \pi t}}\right)\right.$$

$$\left. \times \exp\left[\frac{-(r - r_0)^2}{4D_j t}\right]\right] + \overline{C}_j\left(\frac{r_0}{r^2}\right) \qquad (2.6\text{-}4)$$

The evaluation of Eq. (2.6-4) at the surface of the mercury drop, where $r = r_0$, gives

$$\left(\frac{\partial C_j}{\partial r}\right)_{r=r_0,t} = \frac{\overline{C}_j}{\sqrt{\pi D_j t}} + \frac{\overline{C}_j}{r_0} \qquad (2.6\text{-}5)$$

Substitution of this result into Eq. (2.6-1) yields

$$i_{j,t} = -\frac{n}{\nu_j} FAD_j\overline{C}_j\left(\frac{1}{\sqrt{\pi D_j t}} + \frac{1}{r_0}\right) \qquad (2.6\text{-}6)$$

The surface area and the radius of the growing mercury drop are functions of time t as well as the flow-rate m, since

$$A = 4\pi r_0^2 = 4\pi\left(\frac{3mt}{4\pi d}\right)^{2/3} \qquad (2.6\text{-}7.1)$$

$$r_0 = \left(\frac{3mt}{4\pi d}\right)^{1/3} \qquad (2.6\text{-}7.2)$$

where d is the density of mercury.

Substituting Eq. (2.6-7) into Eq. (2.6-6) gives

$$i_{j,t} = -\frac{n}{\nu_j} F4\pi\left(\frac{3mt}{4\pi d}\right)^{2/3} D_j\bar{C}_j\left[\left(\frac{7}{3\pi D_j t}\right)^{1/2} + \left(\frac{4\pi d}{3mt}\right)^{1/3}\right] \qquad (2.6\text{-}8)$$

where the factor $(7/3)^{1/2}$ has been introduced into the first term in the brackets of Eq. (2.6-8) to account for the curvature of the mercury surface.[55-57]

Introducing numerical values of the constants at 20°C into Eq. (2.6-8) yields

$$i_{j,t} = -\frac{n}{\nu_j}\bar{C}_j(708D_j^{1/2}m^{2/3}t^{1/6} + 31554D_j m^{1/3}t^{1/3}) \qquad (2.6\text{-}9)$$

where $i_{j,t}$ is in μamps, m is in mg·sec^{-1}, and t is in seconds.

Therefore, when t is equal to the drop-time t_d, Eq. (2.6-9) may be rewritten as

$$i_{j,t_d} = -\frac{n}{\nu_j}\bar{C}_j(708D_j^{1/2}m^{2/3}t_d^{1/6} + 31554D_j m^{1/3}t_d^{1/3}) \qquad (2.6\text{-}10)$$

which is known as the modified Ilkovic equation for an instantaneous current.

2.7 Dependence of Diffusion Current on Flow-rate and Drop-time

It is seen from the modified Ilkovic equation, Eq. (2.6-10), that the instantaneous current i_{j,t_d} is a function of the flow-rate m and the drop-time t_d, and it has the form

$$i_{j,t_d} = k'm^{2/3}t_d^{1/6} + k''m^{1/3}t_d^{1/3}$$

where k' and k" are constants.

The determination of the values m and t_d are of fundamental importance in polarography, and thus information concerning the determination

of values for m and t_d will be given.

2.7.1 Flow-rate

The flow-rate, m, may be directly determined by averaging the mass of the mercury drops over a period which normally lies between 10-15 minutes. However, it becomes very impractical to determine the flow-rate of a single mercury drop when the study of an instantaneous current on a single mercury drop is considered.

According to the Hagen-Poiseuille Law,[58] the following relationship holds for the flow-rate.

$$m = \frac{\pi r_c^4 dP}{8\eta l} = K'P \qquad (2.7.1\text{-}1)$$

where r_c is the internal radius of the capillary, d is the density of mercury, η is the viscosity coefficient of mercury, l is the capillary length, and P is the effective hydrostatic pressure acting on mercury at the capillary orifice.

The hydrostatic pressure at the capillary orifice, P_a, is proportional to the height of mercury from the capillary orifice to the mercury level in the reservoir.

$$P_a = dgh \qquad (2.7.1\text{-}2)$$

where h is the apparent height measured from the capillary orifice to the mercury level in the reservoir, and g is the gravitational constant.

Due to the interfacial tension, σ, between the mercury and the solution preventing the formation of a larger surface area, there is a pressure perpendicular to the surface of the growing drop and it opposes the growth of the drop. This pressure is so-called back pressure, P_b, and is given, according to Kucera,[59] by

$$P_b = \frac{2\sigma}{r} \qquad (2.7.1\text{-}3)$$

where r is the radius of the growing drop and is equal to $(\frac{3mt}{4\pi d})^{1/3}$ in accordance with Eq. (2.6-7.2).

The average value of the drop radius, $\bar{r}$, during the drop-time t_d is

$$\bar{r} = \frac{1}{t_d}\int_0^{t_d} r\,dt = \frac{1}{t_d}\int_0^{t_d} (\frac{3mt}{4\pi d})^{1/3}\,dt$$

$$= \frac{3}{4}(\frac{3mt_d}{4\pi d})^{1/3} \qquad (2.7.1\text{-}4)$$

The back pressure during the drop-time t_d is therefore defined from Eqs. (2.7.1-3) and (2.7.1-4).

$$P_b = 4.31\sigma(\frac{d}{mt_d})^{1/3} \qquad (2.7.1\text{-}5)$$

The effective hydrostatic pressure P is now defined by

$$P = P_a - P_b$$

$$= dgh - 4.31\sigma(\frac{d}{mt_d})^{1/3} \qquad (2.7.1\text{-}6)$$

Substitution of Eq. (2.7.1-6) into Eq. (2.7.1-1) gives the expression for the flow-rate during the drop-time t_d as

$$m = \frac{\pi r_c^4 d}{8l\eta}[dgh - 4.31\sigma(\frac{d}{mt_d})^{1/3}] \qquad (2.7.1\text{-}7)$$

Introducing the numerical values of the constants at 20°C and assuming $\sigma \simeq 400$ dyn·cm^{-1} in all electrolyte solutions yields

$$m = 4.545 \times 10^9 (\frac{r_c^4}{l})(h - \frac{3.1}{m^{1/3}t_d^{1/3}}) \qquad (2.7.1\text{-}8)$$

The experimental data obtained by Maas[60] showing the validity of the Hagen-Poiseuille Law for the flow-rate m is given in Table 2.

2.7.2 Drop-time

As seen from the modified Ilkovic equation, Eq. (2.6-10), the drop-time t_d affects the magnitude of $i_{j,t}$ directly, and therefore an

TABLE 2

COMPARISON OF OBSERVED AND CALCULATED RATES OF FLOWS OF MERCURY FROM A CAPILLARY TUBE UNDER VARIOUS PRESSURES AT 25°C[a]

Apparent Height h, cm	Drop-time t_d, sec	Flow-rate m (obs.) $mg \cdot sec^{-1}$	Calculated[b] Flow-rate m (calc.) $mg \cdot sec^{-1}$	Percent Difference Δ m, %
40.0	4.13	1.084	1.092	+ 0.7
60.0	2.69	1.653	1.668	+ 0.9
80.0	1.99	2.221	2.240	+ 0.9
100.0	1.59	2.789	2.816	+ 1.0

[a] Reference 60.

[b] Flow-rates are calculated from the equation

$$m = 4.64 \times 10^9 \left(\frac{r_c^4}{l}\right)\left(h - \frac{3.1}{m^{1/3} t_d^{1/3}}\right)$$

with r_c = 0.00189 cm, and l = 2.043 cm.

understanding of the role of drop-time on diffusion current is necessary in polarography.

The study of the electrocapillary curve[61-63] shows that the surface tension of a mercury drop is a function of the applied potential, and thus it is obvious that drop-time is a function of the applied potential as well. Experimental data, given in Table 3, obtained from a polarographic reduction wave of Co^{++} in $NaNO_3$ and gelatin solution shows the dependence of $i_{j,t}$ on drop-time as well as the dependence of drop-time on the applied potential.

The study of the data in Table 3 also provides the important conclusion that the diffusion current $i_{j,t}$ of the electroactive component M_j at the D.M.E. is dependent on the applied potential, but the diffusion coefficient D_j of the electroactive component M_j is independent of an applied potential.

2.8 Diffusion Coefficient as a Function of the Ionic Strength

After the brief introduction to diffusion and reviewing the fundamentals of polarography, it is now necessary to investigate the significance of the diffusion coefficient obtained from polarography.

It is understood that the interactions between ions are electrostatic in origin. Therefore, the change in the apparent diffusion coefficient D_j of the electroactive component M_j is assumed to be caused by the electrostatic interactions between M_j - M_j, and M_j and the supporting electrolyte.

For a diffusion controlled process, one is restricted to situations where the concentration of the supporting electrolyte is at least one to two orders of magnitude greater than that of the electroactive component M_j. Under this condition,[64] the change in the apparent diffusion

TABLE 3

DEPENDENCE OF INSTANTANEOUS CURRENT ON DROP-TIME AT VARIOUS APPLIED POTENTIALS AT 20°C

Applied Potential E, V	Instantaneous Current i_{j,t_d}, μamp	Drop-time t_d, sec	Apparent Height h, cm	Flow-rate m, $mg \cdot sec^{-1}$	Diffusion Coefficient D X 10^6 $cm^2 sec^{-1}$
- 1.187	3.69	3.57	41.54	1.986	5.787
- 1.268	3.66	3.42	41.54	1.985	5.786
- 1.349	3.63	3.29	41.54	1.984	5.777
- 1.430	3.60	3.12	41.54	1.983	5.795
- 1.511	3.56	2.93	41.54	1.981	5.806

Data obtained experimentally from 0.5017 mM $Co(NO_3)_2$ in 0.10 M $NaNO_3$ and 0.01% gelatin solution at 20.0 $\pm$ 0.1°C.

coefficient is mainly due to:

1. the change in the effective force causing diffusion due to the non-ideal behavior.
2. the retarding force which is referred to as the relaxation effect and the electrophoretic effect.

2.8.1 Changes in the Effective Force Causing Diffusion

According to the Debye-Huckle theory,[65-67] the chemical potential μ_j due to the ionic atmosphere is given by

$$\mu_j' = \frac{\partial G}{\partial n_j} = RT \ln(\gamma_j) \qquad (2.8.1\text{-}1)$$

where G is the extra free energy due to the ionic atmosphere, and γ_j is the activity coefficient of the component M_j.

The extra free energy G is equal to the extra potential due to the ionic atmosphere.

$$G = \frac{z_j q b}{4\pi\varepsilon_0\varepsilon} \qquad (2.8.1\text{-}2)$$

where q is the fundamental charge, b is the inverse of the Debye length, ε_0 and ε are the dielectric constants of vacuum and the electrolyte medium respectively.

The inverse of the Debye length, b, is related to other physical properties of the solution by

$$b^2 = \left(\frac{2}{k\varepsilon_0}\right)\left(\frac{q^2}{\varepsilon T}\right)\left[\frac{1}{2}\Sigma C_j z_j^2\right] \qquad (2.8.1\text{-}3)$$

where k is the Boltzmann constant, and the quantity in brackets is referred to as the ionic strength of the solution.

The thermodynamic expression for the chemical potential of a non-ideal electrolytic solution, μ_j'', is given by[68]

$$\mu_j'' = \mu_j' + \mu_j \qquad (2.8.1\text{-}4)$$

where μ_j is the chemical potential defined by Eq. (2.4-1) which is valid only for a very dilute solution.

Thus, the chemical potential μ_j'' of the component M_j is now correctly written as

$$\mu_j'' = \overline{\mu}_j + RT \ln(C_j) + RT \ln(\gamma_j)$$

$$= \overline{\mu}_j + RT \ln(a_j) \qquad (2.8.1\text{-}5)$$

where $a_j \equiv \gamma_j C_j$ is the activity of the component M_j.

It follows that the force causing the diffusion of the component M_j is equal to the gradient of the chemical potential μ_j''.

$$F_j'' = \frac{\partial \mu_j}{\partial x} = \frac{RT}{a_j} \ln(a_j) \qquad (2.8.1\text{-}6)$$

Therefore, the change in the effective force causing diffusion due to the non-ideal behavior is

$$\Delta \overline{F}_j = \overline{F}_j - F_j''$$

$$= RT \left(\frac{\ln C_j}{C_j} - \frac{\ln a_j}{a_j}\right) \qquad (2.8.1\text{-}7)$$

2.8.2 The Retarding Force

Due to the restrictive conditions for a diffusion controlled process, the concentration, or more correctly, the activities of the electroactive component M_j must be several times less than that of the supporting electrolyte added. Therefore, the electroactive component M_j is moving relative to a background of non-diffusing ions, whereas in one component electrolytic solutions all the ions are moving with the same velocity. Under this restriction, there is a retarding force on the electroactive component M_j which must be taken into account in order to deduce the diffusion coefficient D_j from its apparent value. This retarding force is referred

to as the relaxation effect and as the electrophoretic effect.

2.8.2.1 The Relaxation Effect

In the Debye-Huckle model, an ion is considered to be surrounded by an ionic atmosphere of opposite charge. Likewise for the situation of diffusion at the D.M.E., the electroactive ion M_j is surrounded by the ionic atmosphere of the opposite charge of the supporting electrolyte. The activity gradient causes the ion M_j to diffuse in the ionic atmosphere of the supporting electrolyte which is relatively localized. The movement of the ion M_j tends to distort the symmetry of the surrounded ionic atmosphere, and this causes the net surrounding charge to accumulate behind the diffusing ion M_j. Thus the distorted ionic atmosphere exerts an electrostatic drag on the diffusing ion M_j. This is referred to as the relaxation effect.

The force causing diffusion of the ion M_j under the relaxation effect is given, on the basis of the Onsager theory outlined for the diffusion of several electrolytes simultaneously present in a solution, by[69-73]

$$F_j^* = F_j'' \left[1 - \frac{bz_j^2 q^2}{3\varepsilon kT}\left(1 - \sqrt{d(\delta_j)}\right)\right] \qquad (2.8.2.1\text{-}1)$$

where F_j^* is the force causing diffusion under the relaxation effect, F_j'' is the apparent force causing diffusion previously defined by Eq. (2.8.1-6), and the quantity $d(\delta_j)$ is defined, for simplicity, as

$$d(\delta_1) = \frac{|z_1|}{|z_2| + |z_3|}\left(\frac{|z_2|\lambda_2^0}{|z_1|\lambda_2^0 + |z_2|\lambda_1^0} + \frac{|z_3|\lambda_3^0}{|z_1|\lambda_3^0 + |z_3|\lambda_1^0}\right)$$

where z_j is the signed charge, and λ_j^0 is the ionic conductance at infinite dilution. The subscript 1 now refers to the electroactive component, and the subscripts 2 and 3 refer to the components of the supporting

electrolyte.

Equation (2.8.2.1-1) may be written in terms of the gradient of the chemical potential of the electroactive component M_j.

$$F_j^* = \frac{\partial \mu_j''}{\partial x} (1 - bB) \qquad (2.8.2.1\text{-}2)$$

where $B \equiv \frac{z_j^2 q_j^2}{3\varepsilon kT} [1 - \sqrt{d(\delta_j)}]$

By following the pattern of Eqs. (2.4-2) to (2.4-5), the force causing diffusion F_j^* can be altered to give the expression for the flux f_j^* of the electroactive component M_j under the relaxation effect.

$$f_j^* = f_j(1 - bB)$$
$$= f_j(1 - \sqrt{d(C_j)}\ k^*B) \qquad (2.8.2.1\text{-}3)$$

where f_j is defined by Eq. (2.2-3), $d(C_j)$ is the ionic strength of the solution, and the constant k^* is equal to $b[d(C_j)]^{-1/2}$.

Equation (2.8.2.1-3) shows a linear relationship between the flux of the electroactive component M_j at the D.M.E. under the relaxation effect and the square root of the ionic strength.

Since the flux is equal to the diffusion coefficient multiplied by a negative gradient, it is important to define the following expression.

$$D_j^* = D_j(1 - \sqrt{d(C_j)}\ k^*B) \qquad (2.8.2.1\text{-}4)$$

where D_j^* is the diffusion coefficient of the electroactive component M_j under the relaxation effect, and D_j is the apparent diffusion coefficient of the electroactive component M_j.

It should be mentioned that, at infinite dilution the ionic strength becomes zero, and therefore, the relaxation effect will be removed.

2.8.2.2 The Electrophoretic Effect

Due to the electrostatic attraction, the electroactive ion M_j tends to "drag" other associated solvent molecules in its vicinity along with it. The effect of this action is equal to a net flow of the associated solvent molecules in the direction opposite to that of the electroactive ion M_j. This is referred to as the electrophoretic effect.[74]

The electrophoretic effect for the situation of the diffusion process at the D.M.E. may be negligible since it is dependent on the concentration of the electroactive component M_j which is normally low in polarographic work. Further, the electrophoretic effect will tend towards zero at infinite dilution.

2.9 The Effect of Viscosity on the Diffusion Coefficient

A frictional force that balances the diffusion force when some constant velocity of the diffusing component M_j is reached is referred to as a viscous force.[75-77] The viscous force may be expressed according to Stoke's Law by

$$F_\eta = 6\pi r_j \bar{v}_j \eta \qquad (2.9\text{-}1)$$

where F_η is the viscous force, r_j is the radius of the electroactive ion, $\bar{v}_j$ is its velocity, and η is the viscosity coefficient of the medium. Since the electroactive ion M_j moves with a constant velocity $\bar{v}_j$, the net force exerted on the ion M_j must be zero, thus the force causing diffusion F_j^* is equal to the viscous force F_η.

$$F_j^* = F_\eta = 6\pi r_j \bar{v}_j \eta \qquad (2.9\text{-}2)$$

Substituting $\bar{v}_j = (D_j F_j^*)/(kT)$ into Eq. (2.9-2) yields

$$D_j = \frac{kT}{6\pi r_j \eta} \qquad (2.9\text{-}3)$$

Equation (2.9-3) is known as the Stoke-Einstein equation relating

diffusion and viscosity.

Brasher and Jones[78] have successfully verified the validity of Eq. (2.9-3) by polarography. A portion of their data is given in Table 4.

TABLE 4

DIFFUSION COEFFICIENTS OF CADMIUM IONS IN VARIOUS VISCOUS SOLUTIONS OF SULFURIC ACID AT 25°C[a]

Viscosity $\eta \times 10^2$, P	Diffusion Coefficient $D \times 10^6$, $cm^2 sec^{-1}$	$\eta \cdot D \times 10^8$, $g \cdot cm \cdot sec^{-1}$
1.000	7.71	7.710
1.003	7.52	7.543
1.007	7.52	7.573
1.014	7.32	7.422
1.019	7.26	7.398
1.049	7.13	7.479
1.091	7.00	7.637
1.094	6.88	7.527
1.253	6.33	7.931
1.570	5.25	8.242
1.977	3.98	7.868
2.500	3.25	8.125
3.162	2.53	8.000
4.102	1.93	7.917
5.483	1.32	7.238

[a] Reference 78.

SECTION 3

METHOD

3.1 Diffusion Controlled Process at a Dropping Mercury Electrode

It can be shown as given in Section 2.4 that a diffusion controlled process at the D.M.E. for both Cd^{++} and Co^{++} may be achieved by having the concentration of the supporting electrolyte used, $NaNO_3$ or Na_2SO_4, several times greater than that of Cd^{++} and Co^{++}. In this work, the lower limit of the concentration of the supporting electrolytes was set at fifty times that of the electroactive components. The diffusion current obtained in this manner is then assumed to be free of the migration effect and solely controlled by the diffusion process.

3.2 The Instantaneous Currents of Cadium and Cobalt (II) Ions on Single Mercury Drops

The instantaneous currents of Cd^{++} and Co^{++} measured at any time t is related to their diffusion coefficients by means of Eq. (2.6-9). The choice of the time t for the measurements of such instantaneous currents is when t is equal to the drop-time t_d, namely, the measurement of an instantaneous current on a single mercury drop.

As it has been indicated in Section 2.7.2, the diffusion coefficient D_j is independent of the applied potential. The study of the diffusion coefficients of Cd^{++} and Co^{++} is therefore based on the information obtained from the instantaneous currents on single mercury drops in a "well defined" limiting current region. The determination of such instantaneous currents involves several considerations.

3.2.1 Correction for Charging Current

The charging current, which is a linear function of the applied

potential as mentioned in Section 2.5 and does not involve the electrode reaction, is superimposed on the diffusion current. In order to obtain the instantaneous current i_{j,t_d}, the charging current must be subtracted off from the limiting current.

The determination of the charging current as a function of the applied potential is necessary since the instantaneous current i_{j,t_d} may be taken at any applied potential along the overvoltage. The charging current at any applied potential may be determined by extending the base line of a polarographic wave such as that shown in Figure 3. This extended line represents the charging current as a function of the applied potential.

3.2.2 Suppression of Maxima

It is apparent that the reduction wave of Co^{++} in the supporting electrolyte used, $NaNO_3$ or Na_2SO_4, has "maxima". In order to obtain a useful measurement for Co^{++}, the maxima which masks the limiting current must be suppressed. The suppression of the maxima for Co^{++} was carried out by adding gelatin to the electrolyte solution.

Gelatin, one of the most frequent used maxima-suppressors, has been claimed to be effective by many investigators.[79,80] Although, among these, Kolthoff and Lingane[81] indicated that the use of gelatin with some heavy metals may lead to the possibility of complex formation.

In this work, only the minimum amount of gelatin was used so as to obtain a "well defined" wave. The experimental data in Table 5 show the magnitude of the diffusion cofficient of Co^{++} in Na_2SO_4 at various gelatin concentrations.

A study of Table 5 shows that 0.001% gelatin is the minimum amount required in Co^{++}-Na_2SO_4-gelatin solution for a "well defined" wave. On

TABLE 5

DIFFUSION COEFFICIENT OF COBALT (II) IN 0.12 M SODIUM SULFATE AS A FUNCTION OF GELATIN CONCENTRATION AT 20°C

Gelatin Concentration C, percent	Instantaneous Current i_{j,t_d}, μamp	Apparent Height h, cm	Flow-rate m, $mg \cdot sec^{-1}$	Drop-time t_d, sec	Diffusion Coefficient D X 10^6, $cm^2 sec^{-1}$
0	a	-	-	-	-
0.0002	a	-	-	-	-
0.0004	3.58	42.70	2.038	2.73	5.824
0.0005	3.46	42.70	2.038	2.73	5.471
0.0008	3.44	42.70	2.038	2.73	5.413
0.0010	3.43	42.70	2.038	2.74	5.390
0.0015	3.43	42.70	2.038	2.74	5.390
0.0020	3.43	42.70	2.038	2.73	5.355
0.0050	3.43	42.70	2.038	2.74	5.390
0.0100	3.42	42.70	2.038	2.73	5.355
0.0150	3.40	42.70	2.038	2.74	5.355
0.0200	3.38	42.70	2.038	2.74	5.247
0.0250	3.38	42.70	2.038	2.74	5.247

Data obtained experimentally from 0.5004 mM $CoSO_4$ in 0.12 M Na_2SO_4 and various concentrations of gelatin at 20.0± 0.1°C.

[a] Maxima masked the diffusion current, and the wave was not well defined.

electrolyte.

Equation (2.8.2.1-1) may be written in terms of the gradient of the chemical potential of the electroactive component M_j.

$$F_j^* = \frac{\partial \mu_j''}{\partial x} (1 - bB) \qquad (2.8.2.1\text{-}2)$$

where $B \equiv \frac{z_j^2 q_j^2}{3\varepsilon kT} [1 - \sqrt{d(\delta_j)}]$

By following the pattern of Eqs. (2.4-2) to (2.4-5), the force causing diffusion F_j^* can be altered to give the expression for the flux f_j^* of the electroactive component M_j under the relaxation effect.

$$\begin{aligned} f_j^* &= f_j(1 - bB) \\ &= f_j(1 - \sqrt{d(C_j)}\ k^*B) \end{aligned} \qquad (2.8.2.1\text{-}3)$$

where f_j is defined by Eq. (2.2-3), $d(C_j)$ is the ionic strength of the solution, and the constant k^* is equal to $b[d(C_j)]^{-1/2}$.

Equation (2.8.2.1-3) shows a linear relationship between the flux of the electroactive component M_j at the D.M.E. under the relaxation effect and the square root of the ionic strength.

Since the flux is equal to the diffusion coefficient multiplied by a negative gradient, it is important to define the following expression.

$$D_j^* = D_j(1 - \sqrt{d(C_j)}\ k^*B) \qquad (2.8.2.1\text{-}4)$$

where D_j^* is the diffusion coefficient of the electroactive component M_j under the relaxation effect, and D_j is the apparent diffusion coefficient of the electroactive component M_j.

It should be mentioned that, at infinite dilution the ionic strength becomes zero, and therefore, the relaxation effect will be removed.

2.8.2.2 The Electrophoretic Effect

Due to the electrostatic attraction, the electroactive ion M_j tends to "drag" other associated solvent molecules in its vicinity along with it. The effect of this action is equal to a net flow of the associated solvent molecules in the direction opposite to that of the electroactive ion M_j. This is referred to as the electrophoretic effect.[74]

The electrophoretic effect for the situation of the diffusion process at the D.M.E. may be negligible since it is dependent on the concentration of the electroactive component M_j which is normally low in polarographic work. Further, the electrophoretic effect will tend towards zero at infinite dilution.

2.9 The Effect of Viscosity on the Diffusion Coefficient

A frictional force that balances the diffusion force when some constant velocity of the diffusing component M_j is reached is referred to as a viscous force.[75-77] The viscous force may be expressed according to Stoke's Law by

$$F_\eta = 6\pi r_j \bar{v}_j \eta \qquad (2.9\text{-}1)$$

where F_η is the viscous force, r_j is the radius of the electroactive ion, $\bar{v}_j$ is its velocity, and η is the viscosity coefficient of the medium. Since the electroactive ion M_j moves with a constant velocity $\bar{v}_j$, the net force exerted on the ion M_j must be zero, thus the force causing diffusion F_j^* is equal to the viscous force F_η.

$$F_j^* = F_\eta = 6\pi r_j \bar{v}_j \eta \qquad (2.9\text{-}2)$$

Substituting $\bar{v}_j = (D_j F_j^*)/(kT)$ into Eq. (2.9-2) yields

$$D_j = \frac{kT}{6\pi r_j \eta} \qquad (2.9\text{-}3)$$

Equation (2.9-3) is known as the Stoke-Einstein equation relating

diffusion and viscosity.

Brasher and Jones[78] have successfully verified the validity of Eq. (2.9-3) by polarography. A portion of their data is given in Table 4.

TABLE 4

DIFFUSION COEFFICIENTS OF CADMIUM IONS IN VARIOUS VISCOUS SOLUTIONS OF SULFURIC ACID AT 25°C[a]

Viscosity $\eta \times 10^2$, P	Diffusion Coefficient $D \times 10^6$, $cm^2 sec^{-1}$	$\eta \cdot D \times 10^8$, $g \cdot cm \cdot sec^{-1}$
1.000	7.71	7.710
1.003	7.52	7.543
1.007	7.52	7.573
1.014	7.32	7.422
1.019	7.26	7.398
1.049	7.13	7.479
1.091	7.00	7.637
1.094	6.88	7.527
1.253	6.33	7.931
1.570	5.25	8.242
1.977	3.98	7.868
2.500	3.25	8.125
3.162	2.53	8.000
4.102	1.93	7.917
5.483	1.32	7.238

[a] Reference 78.

SECTION 3

METHOD

3.1 Diffusion Controlled Process at a Dropping Mercury Electrode

It can be shown as given in Section 2.4 that a diffusion controlled process at the D.M.E. for both Cd^{++} and Co^{++} may be achieved by having the concentration of the supporting electrolyte used, $NaNO_3$ or Na_2SO_4, several times greater than that of Cd^{++} and Co^{++}. In this work, the lower limit of the concentration of the supporting electrolytes was set at fifty times that of the electroactive components. The diffusion current obtained in this manner is then assumed to be free of the migration effect and solely controlled by the diffusion process.

3.2 The Instantaneous Currents of Cadium and Cobalt (II) Ions on Single Mercury Drops

The instantaneous currents of Cd^{++} and Co^{++} measured at any time t is related to their diffusion coefficients by means of Eq. (2.6-9). The choice of the time t for the measurements of such instantaneous currents is when t is equal to the drop-time t_d, namely, the measurement of an instantaneous current on a single mercury drop.

As it has been indicated in Section 2.7.2, the diffusion coefficient D_j is independent of the applied potential. The study of the diffusion coefficients of Cd^{++} and Co^{++} is therefore based on the information obtained from the instantaneous currents on single mercury drops in a "well defined" limiting current region. The determination of such instantaneous currents involves several considerations.

3.2.1 Correction for Charging Current

The charging current, which is a linear function of the applied

potential as mentioned in Section 2.5 and does not involve the electrode reaction, is superimposed on the diffusion current. In order to obtain the instantaneous current i_{j,t_d}, the charging current must be subtracted off from the limiting current.

The determination of the charging current as a function of the applied potential is necessary since the instantaneous current i_{j,t_d} may be taken at any applied potential along the overvoltage. The charging current at any applied potential may be determined by extending the base line of a polarographic wave such as that shown in Figure 3. This extended line represents the charging current as a function of the applied potential.

3.2.2 Suppression of Maxima

It is apparent that the reduction wave of Co^{++} in the supporting electrolyte used, $NaNO_3$ or Na_2SO_4, has "maxima". In order to obtain a useful measurement for Co^{++}, the maxima which masks the limiting current must be suppressed. The suppression of the maxima for Co^{++} was carried out by adding gelatin to the electrolyte solution.

Gelatin, one of the most frequent used maxima-suppressors, has been claimed to be effective by many investigators.[79,80] Although, among these, Kolthoff and Lingane[81] indicated that the use of gelatin with some heavy metals may lead to the possibility of complex formation.

In this work, only the minimum amount of gelatin was used so as to obtain a "well defined" wave. The experimental data in Table 5 show the magnitude of the diffusion cofficient of Co^{++} in Na_2SO_4 at various gelatin concentrations.

A study of Table 5 shows that 0.001% gelatin is the minimum amount required in Co^{++}-Na_2SO_4-gelatin solution for a "well defined" wave. On

TABLE 5

DIFFUSION COEFFICIENT OF COBALT (II) IN 0.12 M SODIUM SULFATE AS A FUNCTION OF GELATIN CONCENTRATION AT 20°C

Gelatin Concentration C, percent	Instantaneous Current i_{j,t_d}, μamp	Apparent Height h, cm	Flow-rate m, $mg \cdot sec^{-1}$	Drop-time t_d, sec	Diffusion Coefficient D X 10^6, $cm^2 sec^{-1}$
0	a	-	-	-	-
0.0002	a	-	-	-	-
0.0004	3.58	42.70	2.038	2.73	5.824
0.0005	3.46	42.70	2.038	2.73	5.471
0.0008	3.44	42.70	2.038	2.73	5.413
0.0010	3.43	42.70	2.038	2.74	5.390
0.0015	3.43	42.70	2.038	2.74	5.390
0.0020	3.43	42.70	2.038	2.73	5.355
0.0050	3.43	42.70	2.038	2.74	5.390
0.0100	3.42	42.70	2.038	2.73	5.355
0.0150	3.40	42.70	2.038	2.74	5.355
0.0200	3.38	42.70	2.038	2.74	5.247
0.0250	3.38	42.70	2.038	2.74	5.247

Data obtained experimentally from 0.5004 mM $CoSO_4$ in 0.12 M Na_2SO_4 and various concentrations of gelatin at 20.0± 0.1°C.

[a] Maxima masked the diffusion current, and the wave was not well defined.

the other hand, it was found experimentally from the study of the gelatin composition in Co^{++}-$NaNO_3$-gelatin solutions that 0.01% gelatin is the minimum amount required for a "well defined" wave. The increase of gelatin, ten fold, in the Co^{++}-$NaNO_3$-gelatin solutions over the Co^{++}-Na_2SO_4-gelatin solutions is due to the experimental fact that the hydrogen overvoltage in $NaNO_3$ medium decreases with an increase of the concentration of $NaNO_3$ at some constant concentration of gelatin, and increases with an increase of the concentration of gelatin at some constant concentration of $NaNO_3$.

The use of gelatin in this work for the best condition, i.e., minimum gelatin added for a "well defined" wave, is therefore 0.001% of gelatin concentration for all Co^{++}-Na_2SO_4-gelatin solutions, and 0.01% of gelatin concentration for all Co^{++}-$NaNO_3$-gelatin solutions.

3.2.3 Determination of the Flow-rate

The flow-rate m for a single mercury drop was determined by means of Eq. (2.7.1-8). The constants r_c and l of the capillary used were determined experimentally by means of a travelling microscope to be 3.007×10^{-3} cm and 7.468 cm respectively. The experimental data representing the determinations of r_c and l are given in Table 6.

It is convenient to introduce the numerical values of the constants r_c and l into Eq. (2.7.1-8), which gives

$$m = 4.976 \times 10^{-2} \left(h - \frac{3.1}{m^{1/3} t_d^{1/3}}\right) \qquad (3.2.3\text{-}1)$$

where m is expressed in $mg \cdot sec^{-1}$.

3.2.4 Determination of the Drop-time

In Section 2.7.2, the dependence of the limiting current on the applied potential and the significance of the electrocapillary curve in

TABLE 6

DETERMINATIONS OF CAPILLARY RADIUS AND LENGTHS

Room Temperature T, ^{o}C	Capillary Radius r_c, cm	Capillary Length ℓ, cm
21.5± 0.5	3.011	7.467
21.5	3.007	7.468
21.5	3.003	7.470
21.5	3.006	7.463
22.0± 0.5	3.012	7.468
22.0	3.011	7.470
22.0	3.005	7.468
22.0	3.009	7.471
23.0± 0.5	3.011	7.469
23.0	3.012	7.465
23.0	3.010	7.470
23.0	3.006	7.469
23.5± 0.5	3.017	7.470
23.5	3.001	7.470
23.5	3.010	7.468
23.5	2.986	7.464
24.0± 0.5	3.005	7.470
24.0	3.002	7.470
24.0	3.014	7.470
24.0	3.010	7.469

The capillary radius, r_c, in the temperature range 21.5 - 24.0^{o}C = $(3.007 \pm 0.006) \times 10^{-3}$ cm.

The capillary length, ℓ, in the temperature range 21.5 - 24.0^{o}C = 7.468 ± 0.003 cm.

polarographic work were discussed. From this information, it is clearly seen that the potential at which the instantaneous current i_{j,t_d} and the drop-time t_d are evaluated must be the same potential.

It will be explained later in Section 4.1.2 that the polarography module used in this work is equipped with a "hold" button to keep the applied potential constant at any selected value. The drop-time t_d was determined by keeping the potential at which i_{j,t_d} was evaluated constant and averaging the time over twenty mercury drops.

3.2.5 Determination of the Apparent Diffusion Coefficients of Cadmium and Cobalt (II) Ions

Referring to the modified Ilkovic equation for an instantaneous current, Eq. (2.6-10),

$$i_{j,t_d} = - \frac{n}{\nu_j} (\bar{C}_j) (708 D_j^{1/2} m^{2/3} t_d^{1/6} + 31554 D_j m^{1/3} t_d^{1/3})$$

where

i_{j,t_d} = the instantaneous current on a single mercury drop

n = the number of electrons transferred

ν_j = the stoichiometric factor

$\bar{C}_j$ = the bulk concentration of the electroactive component M_j

D_j = the apparent diffusion coefficient

m = the flow-rate

t_d = the drop-time

The diffusion coefficient D_j can be readily calculated from this equation when the parameters i_{j,t_d}, n, ν_j, $\bar{C}_j$, m, and t_d, are known.

For Cd^{++} and Co^{++}, both ions have the same form of the charge transfer reaction for a reduction wave

$$M_j^{++} + 2e^- = M_j$$

Thus, n = 2, and ν_j = -1. The specific form of the modified Ilkovic equation for a reduction wave for both Cd^{++} and Co^{++} can be written

$$i_{j,t_d} = 2\bar{C}_j\,(708D_j^{1/2}m^{2/3}t_d^{1/6} + 31554D_jm^{1/3}t_d^{1/3}) \qquad (3.2.5\text{-}1)$$

Equation (3.2.5-1) serves as the fundamental equation for calculating the diffusion coefficient D_j.

3.3 Determination of Limiting Diffusion Coefficient

Discussion in the previous sections shows the complexity of the diffusion process at the D.M.E. The diffusion coefficient is a complicated function of the concentrations of both the electroactive component M_j and the supporting electrolyte S_j. In order to deduce the true diffusion coefficient for the electroactive component M_j, the dependence of the diffusion coefficients on the concentrations must be removed, and this can be achieved at infinite dilution.

The determination of the limiting diffusion coefficient may be carried out graphically, by extrapolating to zero concentrations of both the electroactive component and the supporting electrolyte. According to Eq. (1.3-2),

$$dD_j = \left(\frac{\partial D_j}{\partial C_{M_j}}\right) dC_{M_j} + \left(\frac{\partial D_j}{\partial C_{S_j}}\right) dC_{S_j}$$

Thus, the variation in the concentrations of one component while the other is being kept constant will give a set of D_j with one component being constant.

The following procedures were employed for such determination:

1. a set of D_j, at some finite concentration of the electroactive component C_{M_j}, is obtained and plotted as a function of the square root of the concentration of the supporting electrolyte, $C_{S_j}^{1/2}$. A linear extrapolation to zero of $C_{S_j}^{1/2}$ will give the diffusion coefficient at some

finite concentration C_{M_j} and at zero concentration of the supporting electrolyte, $D_{j,1}$.

2. the diffusion coefficients $D_{j,1}$ are now plotted as a function of C_{M_j}. A linear extrapolation to zero of C_{M_j} will give the diffusion coefficient D_j° at zero concentrations of both the electroactive component and the supporting electrolyte.

Graphs were plotted by employing the Hewlett-Packard 9862A Plotter with programming through the Hewlett-Packard 9820A Calculator. The programs used, which will be explained in Section 7.1, are of the forms

$$D_j = aC_{S_j}^{1/2} + D_{j,1} \tag{3.3-1}$$

$$D_{j,1} = aC_{M_j} + D_j^\circ \tag{3.3-2}$$

where

D_j = the apparent diffusion coefficient obtained experimentally

a = a slope of the plot of Eqs. (3.3-1) or (3.3-2)

C_{S_j} = the concentration of the supporting electrolyte

$D_{j,1}$ = the diffusion coefficient at some finite concentration of the electroactive component M_j and at zero concentration of C_{S_j}

C_{M_j} = the concentration of the electroactive component M_j

D_j° = the limiting diffusion coefficient

SECTION 4

APPARATUS AND INSTRUMENTATION

4.1 The Polarography System

The polarography unit used in this experiment is a three-electrode system which had been specially designed to employ a true "controlled-potential". The use of the three-electrode system has been widely claimed to have a major advantage over the classical two-electrode system since the true "controlled-potential" design will measure whatever potential exists at the D.M.E. with respect to a reference electrode (open loop gains of Amplifiers 1 and 3 are 21,000, see Section 4.1.2).

Although, the exact potential is not a major required factor in this work, nevertheless, the functional operations of the three-electrode system provide better accuracy and such conveniences as:

1. the electrode can be stored in a "ready" condition since a convenient dip-type calomel electrode is used in place of the large calomel and frit electrode which requires continuous maintenance.

2. a large surface area of mercury for a non-polarizable electrode is not required. This, in turn, minimizes possible contaminations by means of the large amount of mercury.

The Heath Polarography System was employed for this work. The system consists of: 1) the D.M.E. apparatus, 2) the polarography module and the operational amplifier system. The output signals were fed into the chart recorder, Fisher Recordall Series 5000.

4.1.1 The Dropping Mercury Electrode Apparatus

The Heath Model EUA-19-6 Dropping Mercury Electrode apparatus was employed for this work. It consists of two major parts, the electrode system and the D.M.E. stand.

Figure 4 describes the electrode system in detail. As seen from this figure, the D.M.E. is placed at the center of the sample compartment, and close to it is a calomel reference electrode. A counter electrode made of platinum wire sealed in a glass tube is used in place of the mercury pool electrode. The thermometer used (not shown) was placed in position 1 of this figure, while the nitrogen bubbling tube was placed in position 2. The spacing between the edge of the sample compartment and the electrode gasket was arranged so that no nitrogen vent tube was needed.

Figures 5 and 6 give the front and back views of the D.M.E. stand. The D.M.E. apparatus was placed on a large fiber tray which was placed on the top of a rugged absorber, one-half inch thick, to eliminate vibrations.

4.1.2 The Polarography Module and the Operational Amplifier System

The Heath Model EUA-19-2 Polarography Module functions as a preamplifier and the signals were fed to the Heath Model EUW-19A Operational Amplifier System.

A simplified schematic of the polarography system is shown in Figure 7. The number in each amplifier symbol refers to the amplifier number in the EUW-19A Operational Amplifier System. Amplifier 1 is connected to a voltage follower with the reference calomel electrode as its input. The voltage at the follower output is thus the potential between the reference electrode and ground. Since the D.M.E. is connected to the vertical ground at the input to Amplifier 4, the follower measures the potential between the reference electrode and the D.M.E., $E_{ref} - E_{DME}$.

Amplifier 2 is used in the sweep generator circuit. A constant potential, shown as a battery for simplicity, is obtained from a stable 3.3 volt zener-diode-controlled reference supply. The sweep rate switch

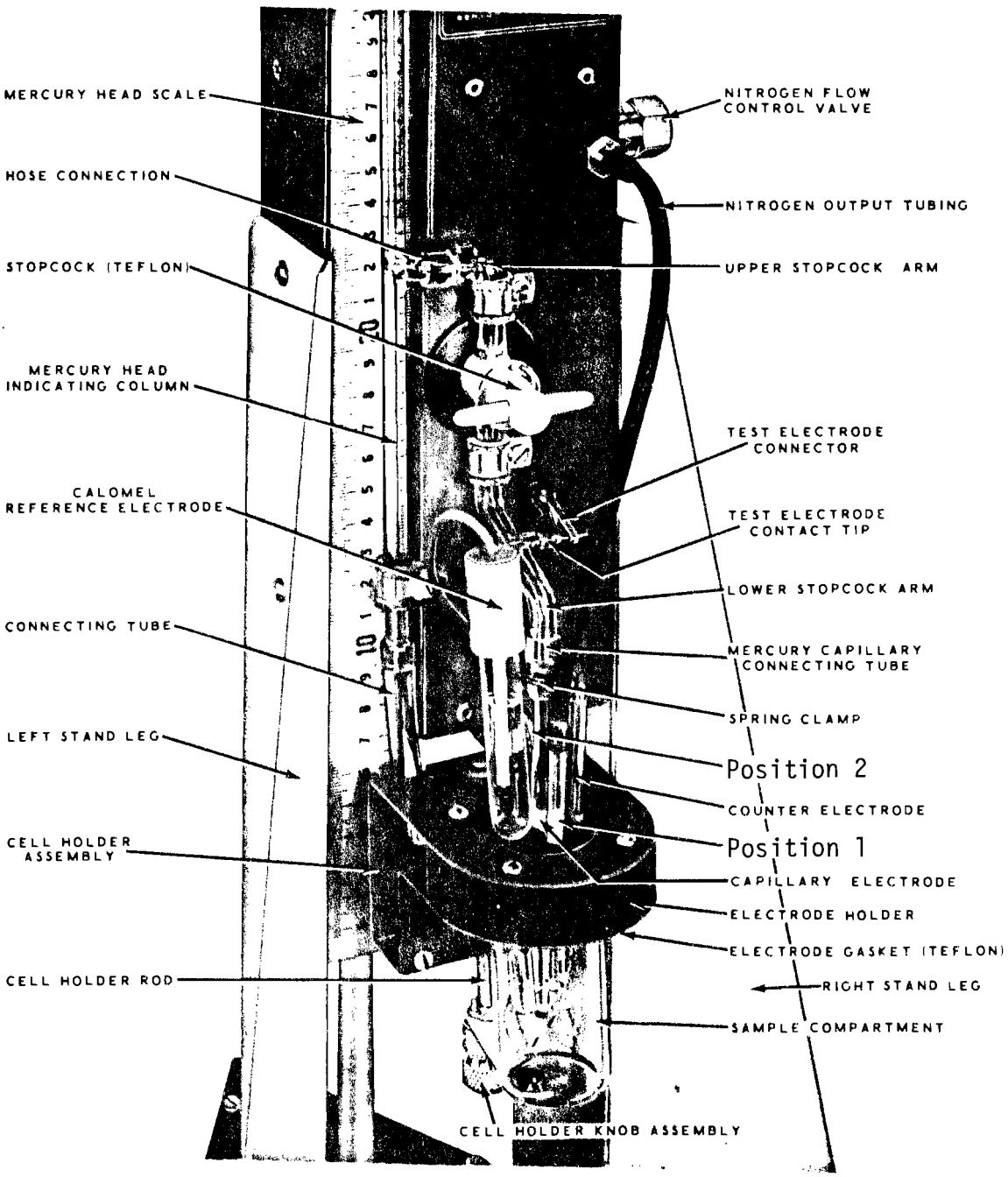

FIGURE 4

Dropping Mercury Electrode Apparatus

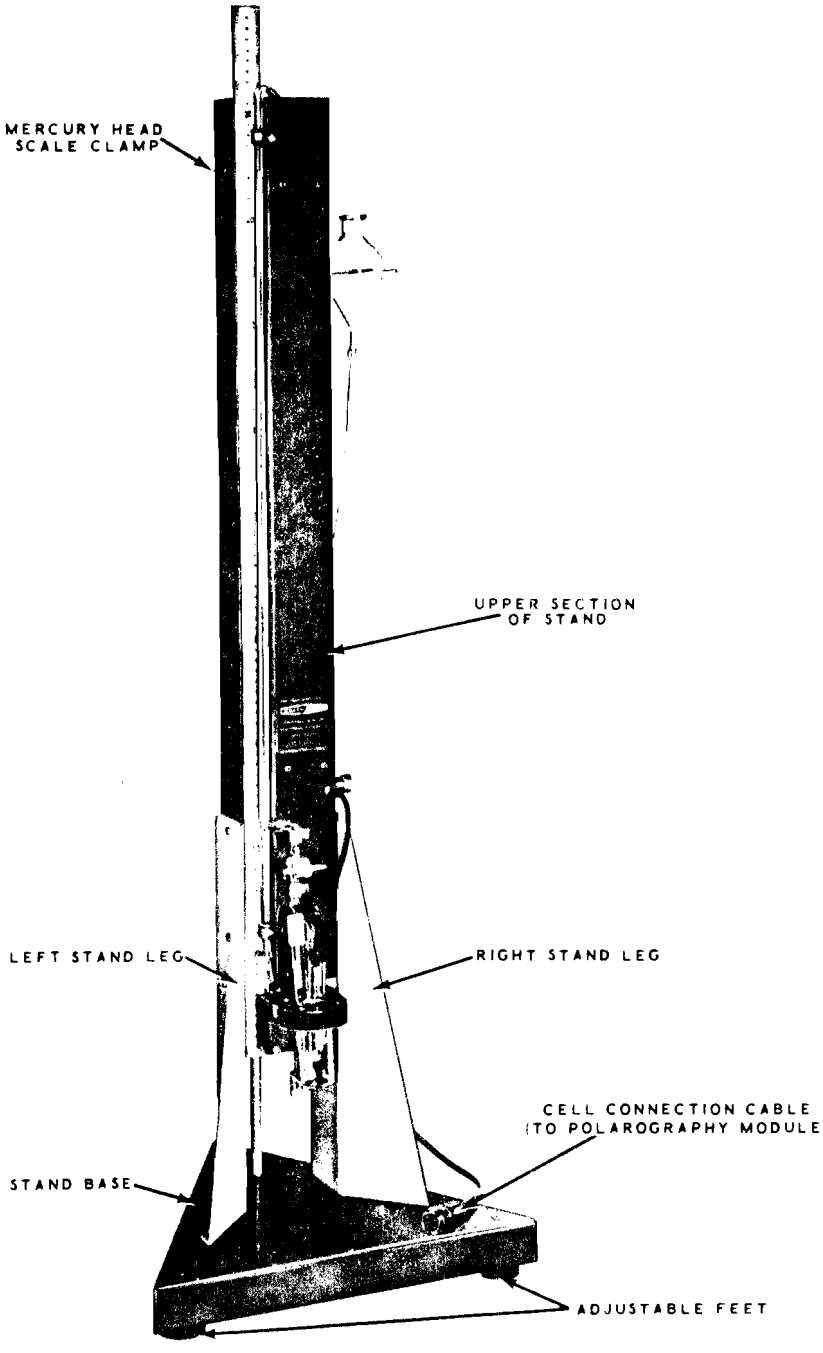

FIGURE 5

Front View of the D.M.E. Stand

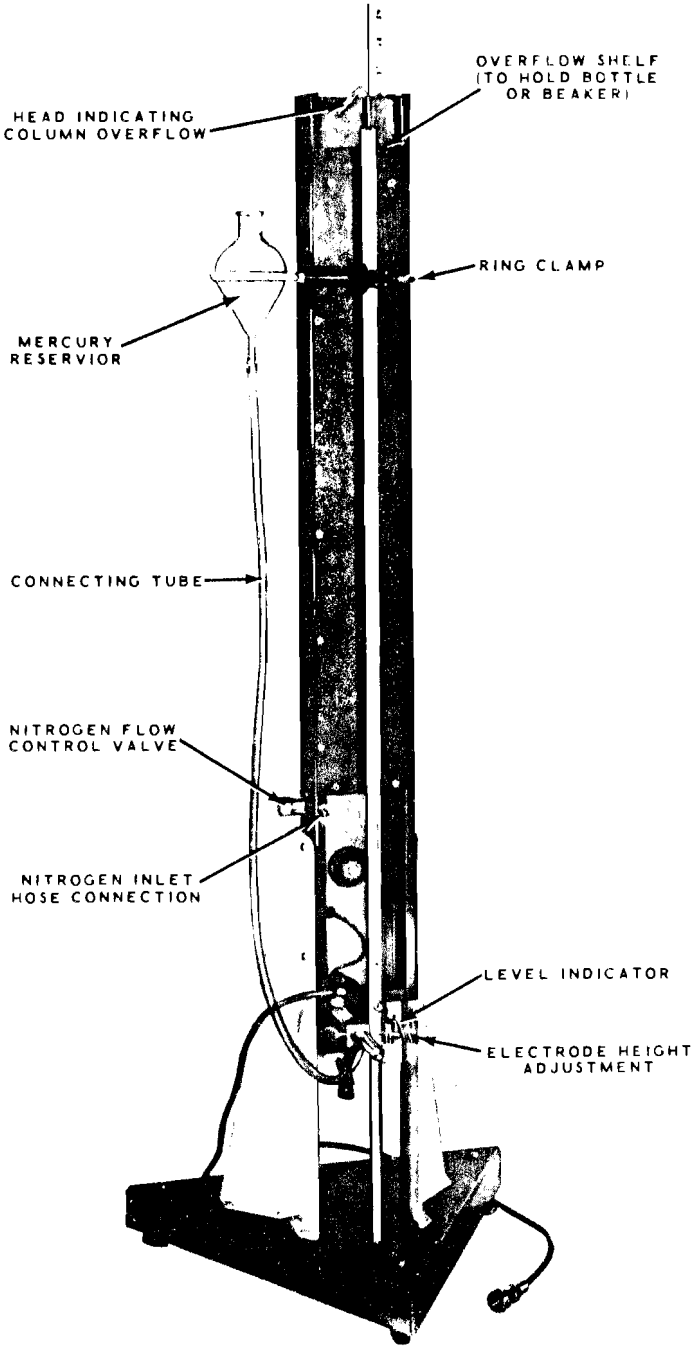

FIGURE 6

Back View of the D.M.E. Stand

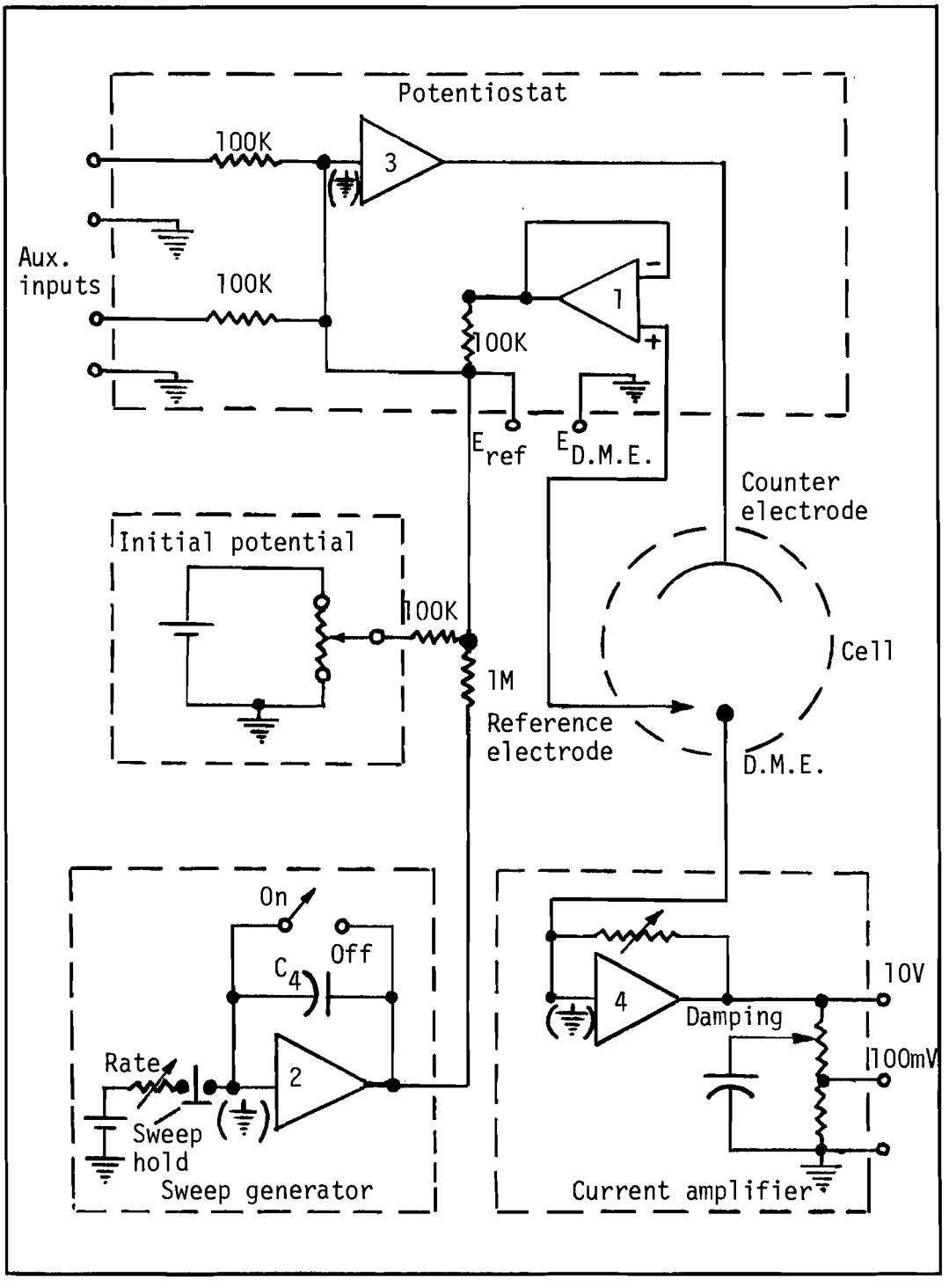

Figure 7

Simplified Schematic of the Polarography System

which appears on the front panel of the polarography module (EUA-19-2) varies the input resistance and thus charging C4.

The initial potential source, shown as a battery for simplicity, is a 3.0 volt zener-diode-controlled reference supply similar to that used in the sweep generator circuit.

All electrode potentials are summed at the input to the potential controlled amplifier, Amplifier 3. The output of Amplifier 3 is connected to the counter electrode to supply whatever current is required at the D.M.E. to keep the D.M.E. at a desired potential with respect to the reference electrode. Thus the cell and the follower, Amplifier 1, are in the feedback path of Amplifier 3. For the summing point of Amplifier 3 to be a virtual ground, the algebraic sum of all the currents to that point must be zero,[82,83] thus

$$\frac{E_{ref} - E_{DME}}{100K} + \frac{E_{aux1}}{100K} + \frac{E_{aux2}}{100K} + \frac{E_{int}}{100K} + \frac{E_{sweep}}{1M} = 0$$

or,

$$E_{DME} - E_{ref} = E_{aux1} + E_{aux2} + E_{int} + \frac{E_{sweep}}{10}$$

Therefore, the potential of the D.M.E. with respect to the reference electrode will be controlled to be the sum of all the potential control voltages.

The D.M.E., which must be at ground potential for proper potential control, is connected directly to the virtual ground at the input of Amplifier 4. This amplifier, Amplifier 4, is wired to be a current amplifier whose sensitivity depends on the feedback resistance selected by the switch on the front panel of EUA-19-2 Polarography Module.

4.1.3 The Chart Recorder

The output signal of the current amplifier, Amplifier 4, in Figure 7 is attenuated by means of EUA-19-2 Polarography Module. A chart recorder input is connected to the output of the polarography module for recording.

A Fisher Recordall Series 5000 recorder was used for recording polarographic waves. This chart recorder has a calibrated metric scale. The accuracy is better than $\pm$ 0.2% of any calibrated full scale, and scale readability is $\pm$ 0.1% of a full scale span.

4.2 Calibration

The sensitivity of the electrode current measurement depends on the feedback resistance of the current amplifier as described explicitly in Section 4.1.2. The control of this feedback resistance which appears as a switch on the front panel of the polarography module (EUA-19-2) is variable from 0.5, 1, 5, 10, . . ., 1000 μamps for a full signal output (100 mV). At some applied potential, a setting of the feedback controlled switch on a position such as 1 μamp or 10 μamps causes exactly 100 mV to appear at the output, on the polarography module, correspond to 1 μamp or 10 μamps of the electrode current.

The calibration on the current measurement was carried out by an indirect method. A sensitive VTVM, Heath Model EUW-24, which had been calibrated with a "working standard", the cadmium Weston cell whose cell had a value of 1.0183 international volts,[84] was used for the calibration.

At a setting of the feedback controlled switch on a 10 μamp position, 100 mV was searched through the VTVM by varying the applied potential. The chart recorder, whose attenuation was set at 100 mV for

a full span and at the same time connected in parallel with the VTVM at the output, was allowed to deflect. The peak signal on the chart recorder was taken as 10 μamps.

The scale reading on the chart recorder was adjusted to correspond with the calibration work by multiplying by a correction factor. The correction factor was found to be 0.980.

The calibration method described above is one method suggested by the manufacturer. However, to verify the consistency of the calibration work as well as testing the accuracy of the system used, the best available digital multi meter, Keithley 173 Autoranging DMM, was placed directly across the electrode terminals to observe an instantaneous current. The results between the two, the chart recorder and the digital multi meter, were in good agreement ($\pm$ 0.20%).

4.3 Temperature Controlled System

The temperature controlled system used in this work has been specially designed to employ a true "controlled-temperature" since the system controls the temperature of the sample compartment as well as controlling the temperature of the mercury reservoir on the D.M.E. stand.

The temperature controlled system consists of five elements.

1. Air bath. An air bath whose dimensions were designed to fit the D.M.E. apparatus was made of clear acrylic plastic of one-fourth inch thickness. Figure 8 shows the construction of the air bath. It was constructed into a tetragonal shape provided with two convenient windows in the front. On the backside of this enclosure, an open circle of four inches in diameter is provided for forcing air into the system. There are five drilled holes on the top of this air bath provided as an air bypass.

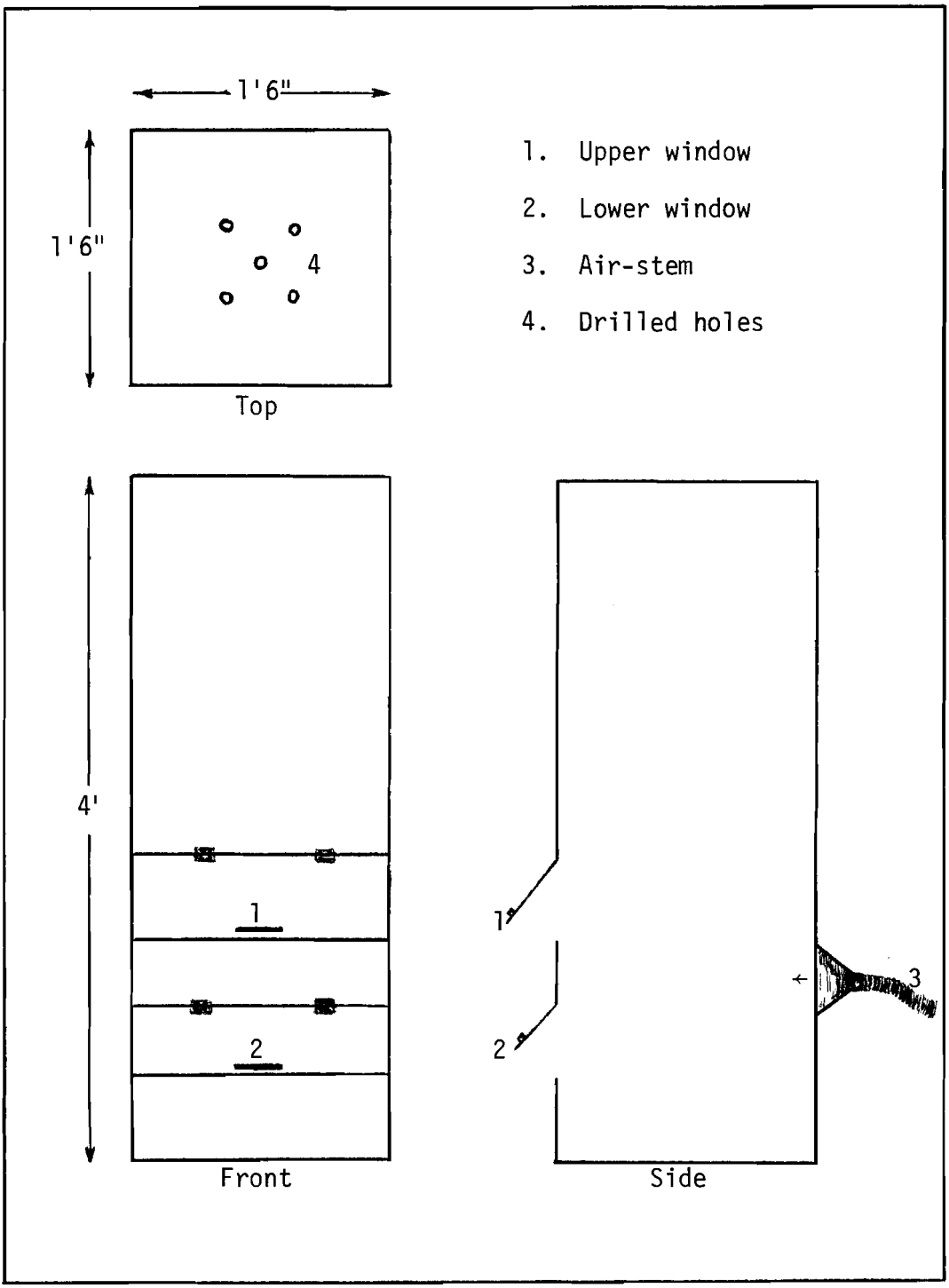

Figure 8

Air Bath

2. Heating strip. An eight foot long strip of heating element is used as a heater to heat the system up to a desired temperature. This strip is positioned so that heat can be evenly distributed inside the temperature housing.

3. Forced-air generator. A high torque motor with a three-element blade is used as a source of a forced-air generator unit. The generated air is forced into the air bath through an air-stem of two inches in diameter. The forced-air generator unit is used to circulate heat inside the air bath.

4. White light source. A 200 watt white light is used for fine temperature adjustment. The white light is shone directly into the sample compartment when a quick rise in the temperature is needed.

5. Thermometer. There are two thermometers used in this system. One, the Fisher 6C-8846 thermometer, is placed so that it is always dipped into a solution in the sample compartment, and the other, a Fisher 6C-8965 thermometer, is placed on the D.M.E. stand to measure the temperature around the sample compartment.

It was found that this temperature controlled system had the ability to control the temperature within a range of 15-30°C to a precision of $\pm$ 0.05°C for a few minutes, and to a precision of $\pm$ 0.20°C for several hours.

SECTION 5

PROCEDURE AND EXPERIMENTAL TECHNIQUE

5.1 Preparation of Standard Solutions

All reagents used for preparing standard solutions were Certified A.C.S. reagent grade from Fisher Scientific Company. Their purities were better than 99.9%.

The glassware used, volumetric flasks and pipettes, was Pyrex class A of NBS specification at 20°C. All glassware was thoroughly cleaned with nitric acid and rinsed with deionized water to remove possible contaminations.

5.1.1 Cadmium Nitrate Standard Solution

Approximately 30 grams of $Cd(NO_3)_2 \cdot 4H_2O$ had been dried in a desiccator (containing $CaSO_4$) for at least 48 hours. Two concentrated $Cd(NO_3)_2$ solutions, 0.20029 M and 0.20012 M, were made as primary standard solutions.

The standard $Cd(NO_3)_2$ solution of the concentration 0.20028 M was prepared by introducing 6.17804 grams of the dried $Cd(NO_3)_2 \cdot 4H_2O$ into a 100 ml volumetric flask and diluted to approximately 90 ml with deionized water. This diluted solution had been well shaken until the solute was completely dissolved, and proceeded temperature-control by placing the volumetric flask into a temperature controlled bath, setting at 20°C for at least two hours. It was finally diluted to a total volume of 100 ml with deionized water.

Seven different concentrated $Cd(NO_3)_2$ solutions, 0.5007×10^{-2} M, 1.0014×10^{-2} M, 2.0028×10^{-2} M, 3.0043×10^{-2} M, 4.0056×10^{-2} M, 5.0071×10^{-2} M, and 6.0085×10^{-2} M, were obtained from the standard 0.20028 M $Cd(NO_3)_2$ solution by successive dilution.

The standard 0.20012 M $Cd(NO_3)_2$ solution was prepared by the same procedure as above by introducing 6.17311 grams of the dried $Cd(NO_3)_2 \cdot 4H_2O$ into a 100 ml volumetric flask and diluting to 100 ml. Seven concentrated $Cd(NO_3)_2$ solutions, 0.5003×10^{-2} M, 1.0006×10^{-2} M, 2.0021×10^{-2} M, 3.0018×10^{-2} M, 4.0024×10^{-2} M, 5.0030×10^{-2} M, and 6.0036×10^{-2} M, were obtained from this standard solution by successive dilutions.

5.1.2 Cobalt (II) Nitrate Standard Solution

Approximately 20 grams of $Co(NO_3)_2 \cdot 6H_2O$ had been dried in a desiccator for at least 48 hours. The standard 0.20068 M $Co(NO_3)_2$ solution was prepared by introducing 5.84060 grams of the dried $Co(NO_3)_2 \cdot 6H_2O$ into a 100 ml volumetric flask and diluting to 100 ml by the procedure described in Section 5.1.1. Seven different concentrations, 0.5017×10^{-2} M, 1.0034×10^{-2} M, 2.0068×10^{-2} M, 3.0102×10^{-2} M, 4.0136×10^{-2} M, 5.0170×10^{-2} M, and 6.0204×10^{-2} M, of $Co(NO_3)_2$ solutions were obtained by successive dilutions.

5.1.3 Cobalt (II) Sulfate Standard Solution

Approximately 20 grams of $CoSO_4 \cdot 7H_2O$ had been dried in a desiccator for at least 48 hours. The standard 0.20016 M $CoSO_4$ solution was prepared by introducing 5,62650 grams of the dried $CoSO_4 \cdot 7H_2O$ into a 100 ml volumetric flask and diluting to 100 ml by the procedure described in Section 5.1.1. Seven different concentrations, 0.5004×10^{-2} M, 1.0008×10^{-2} M, 2.0016×10^{-2} M, 3.0024×10^{-2} M, 4.0032×10^{-2} M, 5.0040×10^{-2} M, and 6.0048×10^{-2} M, of $CoSO_4$ solutions were obtained by successive dilutions.

5.1.4 Sodium Nitrate Standard Solution

Approximately 200 grams of $NaNO_3$ had been dried in a oven setting at 90°C for at least 2 hours. The standard $NaNO_3$ solution of concentration

2.0013 M was prepared by introducing 170.0905 grams of the dried $NaNO_3$ into a 1000 ml volumetric flask and diluting to 1000 ml by the procedure described in Section 5.1.1.

5.1.5 Sodium Sulfate Standard Solution

Approximately 200 grams of Na_2SO_4 had been dried in an oven setting at 90°C for at least 2 hours. The standard Na_2SO_4 solution of concentration 1.2006 M was prepared by introducing 170.5332 grams of the dried Na_2SO_4 into a 1000 ml volumetric flask and diluting to 1000 ml by the procedure described in Section 5.1.1.

5.1.6 Gelatin Solution

Gelatin solutions used for the study of Co^{++} were freshly prepared. Two concentrations, 0.20110% and 0.20075%, of gelatin solutions were prepared as primary standard solutions.

The solution of 0.20110% gelatin was prepared by introducing 0.20110 grams of granulated gelatin into a 100 ml volumetric flask and diluting with deionized water to approximately 50 ml. The undissolved gelatin had been heated to approximately 50°C and agitated until it was completely dissolved. The solution was cooled to approximately 20°C in a temperature controlled bath and finally diluted to a total volume of 100 ml with deionized water.

A 0.01% gelatin solution was prepared by diluting the standard 0.20110% gelatin solution, and a 0.10% gelatin solution was prepared by diluting the standard 0.20075% gelatin solution.

5.2.1 Preparation of Sample

The amount of electrolyte to be introduced into the sample compartment for analysis was assigned to have a standard volume of 20 ml

since the sample compartment has a capacity of approximately 30 ml.

A 2 ml Pyrex class A glass pipette was used to deliver the electroactive component (Cd^{++} or Co^{++}) into the sample compartment, and this same pipette had been used for handling the electroactive component in each analysis throughout this investigation. The accuracy of this pipette was reported by the manufacturer to be $\pm$ 0.006 ml at 20°C.

Examples

A 0.5003 mM $Cd(NO_3)_2$ in 0.10 M $NaNO_3$ solution was prepared by;

pipette, 2 ml of 0.5003 X 10^{-2} M $Cd(NO_3)_2$, 1 ml of 2.0 M $NaNO_3$, and 17 ml of deionized water.

Thus a 5.0170 mM $CO(NO_3)_2$ in 0.30 M $NaNO_3$ and 0.01% gelatin solution was prepared by;

pipette, 2 ml of 5.0170 X 10^{-2} M $Co(NO_3)_2$, 3 ml of 2.0 M $NaNO_3$, 2 ml of 0.10% gelatin, and 13 ml of deionized water.

This technique of preparing samples is not the best technique available since it involves using several pipettes to yield a total volume of 20 ml. However, there were more than 250 different concentrations, and therefore, we adopted the above procedure. The error in the concentration $\overline{C}_j$ introduced by this technique should be less than $\pm$ 0.50%.

5.2.2 Removal of Dissolved Oxygen

The removal of the dissolved oxygen was carried out by passing purified nitrogen through the sample. The nitrogen gas was bubbled through each sample for 15 minutes with a sufficient flow-rate of nitrogen (approximately 10-15 bubbles per second). The dissolved oxygen was completely removed by this procedure.

5.2.3 Temperature Control

Although the temperature controlled system described in Section 4.3 can control temperature ranging from 15°C to 30°C to within a precision of ± 0.05°C for several minutes and to within a precision of ± 0.20°C for several hours, in all cases, it requires the temperature of the surroundings to be lower than that of the controlled temperature. Therefore, the temperature of the surrounding area was controlled as well.

When the temperature of the sample in the sample compartment exceeded 20°C during the investigation, a paper towel soaked with cold water was wrapped around the sample compartment in order to lower the temperature as necessary. During the cooling process (and/or heating process), nitrogen gas was passed into the sample to eliminate temperature gradients.

The temperature during each data point taken was able to be controlled to within a precision of ± 0.10°C by using the technique described above.

5.3 Measurements

In order to minimize drift of the operational amplifier system, the system had been turned "on" for a period of at least 4 hours before each day's operation. The system stabilized after a few hours of warming up. However, small drifts still occurred periodically, thus balancing each Amplifier (1-4), to ensure a zero output with a zero input was necessary for each data point taken.

The electrode system was thoroughly cleaned with deionized water prior to each day's use, between each data point, and at the end of each day. The sample compartment was filled with deionized water when the system was not in use.

Prior to taking data, the polarography module was turned from "stand by" to "on" position which caused the potential at the D.M.E. to decrease at a controlled rate. At the same moment of positioning "on" on the polarography module, the chart recorder was manually turned to "on" as well. The initial potentials of the D.M.E. with respect to the reference electrode were set at -0.30 V and -0.70 V for Cd^{++} and Co^{++} respectively. The rate of decreasing the potential at the D.M.E. was assigned a value of -0.20 V/min., and the chart drive was operated at a speed of 2.50 cm/min.

The magnitude of the instantaneous current i_{j,t_d} was directly read from the limiting current recorded on the chart. The magnitude of the instantaneous current is referred to as the instantaneous current which had been corrected for the charging current as discussed in Section 3.2.1, and which had been multiplied by the correction factor, 0.980, to correspond with the calibration work as discussed in Section 4.2.

The sweep hold button, shown in Figure 7, was used so as to give a constant potential during the determination of drop-time t_d. The drop-time was obtained by averaging the time over twenty mercury drops.

The mercury flow-rate, m, was determined by means of Eq. (3.2.3-1). The apparent height, h, was measured directly from the meter stick attached to the D.M.E. stand shown in Figures 4 and 5.

SECTION 6

EXPERIMENTAL RESULTS

6.1 The Limiting Diffusion Coefficient of Cadmium Ion at 20°C

The experimental values of the limiting diffusion coefficient of Cd^{++} at 20°C were determined graphically from linear plots of Eq. (3.3-2).

$$D_{j,1} = aC_{M_j} + D_j^\circ$$

where $D_{j,1}$ = the diffusion coefficients at some finite concentrations of Cd^{++} and at zero concentration of the supporting electrolyte used, $NaNO_3$ or Na_2SO_4

a = the slope of the linear plot of Eq. (3.3-2)

C_{M_j} = the concentration of Cd^{++} ($C_{M_j} \equiv \bar{C}_j$)

D_j° = the limiting diffusion coefficient of Cd^{++} obtained from extrapolation to zero concentration of Cd^{++}

There are two values of the limiting diffusion coefficient of Cd^{++} obtained experimentally according to the two supporting electrolytes used, namely, one was determined from the diffusion of Cd^{++} in $NaNO_3$ and the other was determined from the diffusion of Cd^{++} in Na_2SO_4. These two experimental values are tabulated in Table 7 together with their standard deviations.

Figures 9 and 10 are the plots of Eq. (3.3-2) for the determination of D_j° of Cd^{++}. The discussion of the characteristic slopes of these plots, which are positive, is given in Section 8.2.

A limiting diffusion coefficient of a species is an individual characteristic of each species and has a finite value at some constant temperature. Therefore, the arithmetic means of the two experimental values may be regarded as the result for the determination of the

TABLE 7

THE LIMITING DIFFUSION COEFFICIENT OF CADMIUM ION AT 20°C

Present Study		Literature Values	
$D^{\circ}_{Cd^{++}} \times 10^6$, $cm^2 sec^{-1}$	Remark	$D^{\circ}_{Cd^{++}} \times 10^6$, $cm^2 sec^{-1}$	Remark
6.17 ± 0.02	a,b,c	6.30	f,g,h
5.99 ± 0.02	a,c,d	6.30	f,g,i
6.08 ± 0.09	c,e	6.30	f,g,j
		6.3	f,g,k

[a] Polarographic method.

[b] Determined from Cd^{++} with $NaNO_3$ as supporting electrolyte.

[c] Error is that of the standard deviation.

[d] Determined from Cd^{++} with Na_2SO_4 as supporting electrolyte.

[e] The arithmetic means of the two experimental values above.

[f] Determined from conductivity measurements.

[g] Determined from Eq. (6.1-1).

[h] Reference 85, $D^{\circ}_{Cd^{++}} = 7.19 \times 10^{-6}$ $cm^2 sec^{-1}$ at 25°C.

[i] Reference 86, $D^{\circ}_{Cd^{++}} = 7.19 \times 10^{-6}$ $cm^2 sec^{-1}$ at 25°C.

[j] Reference 87, $D^{\circ}_{Cd^{++}} = 7.19 \times 10^{-6}$ $cm^2 sec^{-1}$ at 25°C.

[k] Reference 88, $D^{\circ}_{Cd^{++}} = 7.2 \times 10^{-6}$ $cm^2 sec^{-1}$ at 25°C.

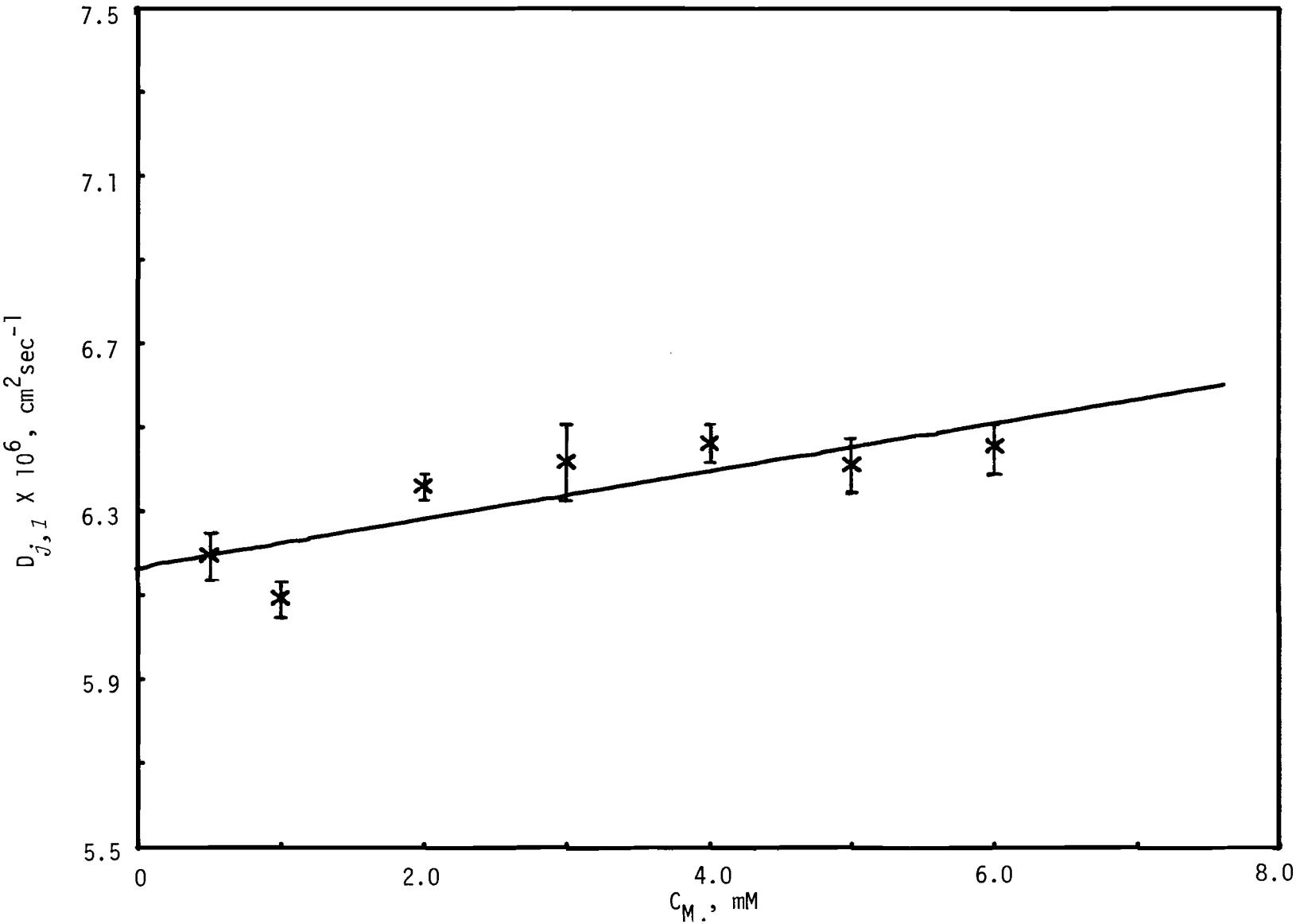

Figure 9. The Diffusion Coefficient of Cd^{++} at Zero Concentration of $NaNO_3$ as a Function of Concentration at 20°C.

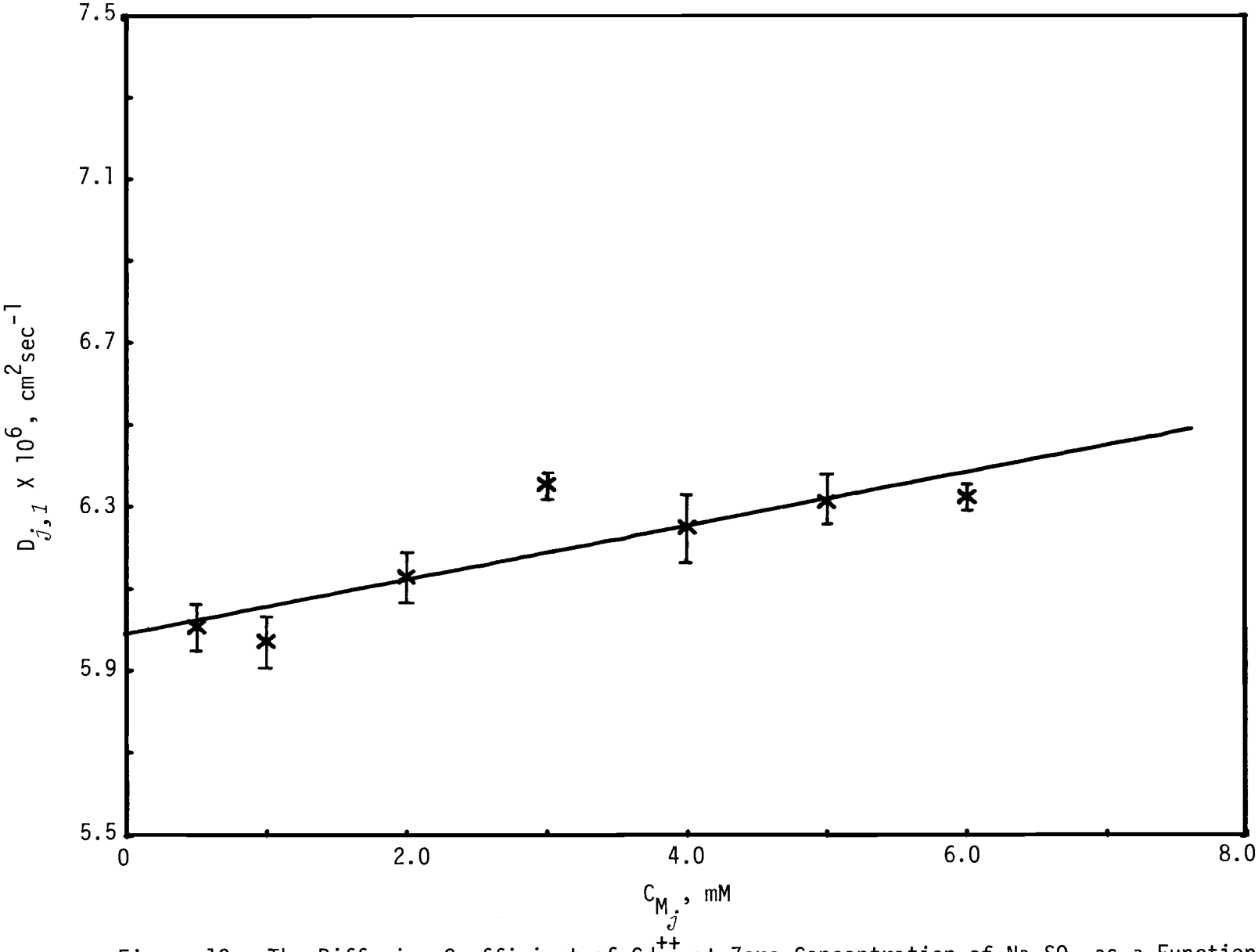

Figure 10. The Diffusion Coefficient of Cd^{++} at Zero Concentration of Na_2SO_4 as a Function of Concentration at 20°C.

limiting diffusion coefficient of Cd^{++} at 20°C. The result is tabulated in Table 7 together with the standard deviation.

The literature values of the limiting diffusion coefficient of Cd^{++} at 20°C are given in Table 7 for comparison.[85-88] These values were determined from the equation, given by Reid and Sherwood,[89] of the form

$$D^{\circ}_{T} = D^{\circ}_{25}\left(\frac{T}{334\mu_{T}}\right) \qquad (6.1\text{-}1)$$

where D°_{T} = the limiting diffusion coefficient at T°C

D°_{25} = the limiting diffusion coefficient at 25°C

T = the absolute temperature

μ_{T} = the viscosity of water at T°K (μ_{T} = 1.002 cP at 293.15°K[90-92])

6.2 The Limiting Diffusion Coefficient of Cobalt (II) Ion at 20°C

There are two experimental values of the limiting diffusion coefficient of Co^{++} at 20°C obtained graphically from the linear extrapolations of Eq. (3.3-2) analogous to those obtained for Cd^{++} in Section 6.1. These two experimental values are tabulated in Table 8 together with the standard deviations.

Figures 11 and 12, the plots of Eq. (3.3-2) for the determination of D°_{j} of Co^{++}, also have positive slopes as those of Figures 9 and 10. The discussion of the characteristic slopes of these figures is given in Section 8.2.

It should be mentioned, according to the use of gelatin (Section 3.3.2), that these two experimental values were determined from the diffusion of Co^{++} in diluted gelatin solutions, namely, one which employed $NaNO_3$ as the supporting electrolyte was determined from the diffusion of Co^{++} in 0.01% gelatin solution, and the other which employed Na_2SO_4 as the supporting electrolyte was determined from the diffusion of Co^{++} in 0.001% gelatin solution. However, the two compositions of

TABLE 8

THE LIMITING DIFFUSION COEFFICIENT OF COBALT (II) ION AT 20°C

Present Study		Literature Values	
$D^{\circ}_{Co^{++}} \times 10^6$, $cm^2 sec^{-1}$	Remark	$D^{\circ}_{Co^{++}} \times 10^6$, $cm^2 sec^{-1}$	Remark
6.11 ± 0.03	a,b,c	6.30	f,g,h
6.45 ± 0.02	a,c,d	6.18	f,g,i
6.28 ± 0.17	c,e	6.39	f,g,j

[a] Polarographic method.

[b] Determined from Co^{++} with $NaNO_3$ as supporting electrolyte.

[c] Error is that of the standard deviation.

[d] Determined from Co^{++} with Na_2SO_4 as supporting electrolyte.

[e] The arithmetic means of the two experimental values above.

[f] Determined from conductivity measurements.

[g] Determined from Eq. (6.1-1).

[h] Reference 93, $D^{\circ}_{Co^{++}} = 7.19 \times 10^{-6}$ $cm^2 sec^{-1}$ at 25°C.

[i] Reference 94, $D^{\circ}_{Co^{++}} = 7.06 \times 10^{-6}$ $cm^2 sec^{-1}$ at 25°C.

[j] Reference 95, $D^{\circ}_{Co^{++}} = 7.30 \times 10^{-6}$ $cm^2 sec^{-1}$ at 25°C.

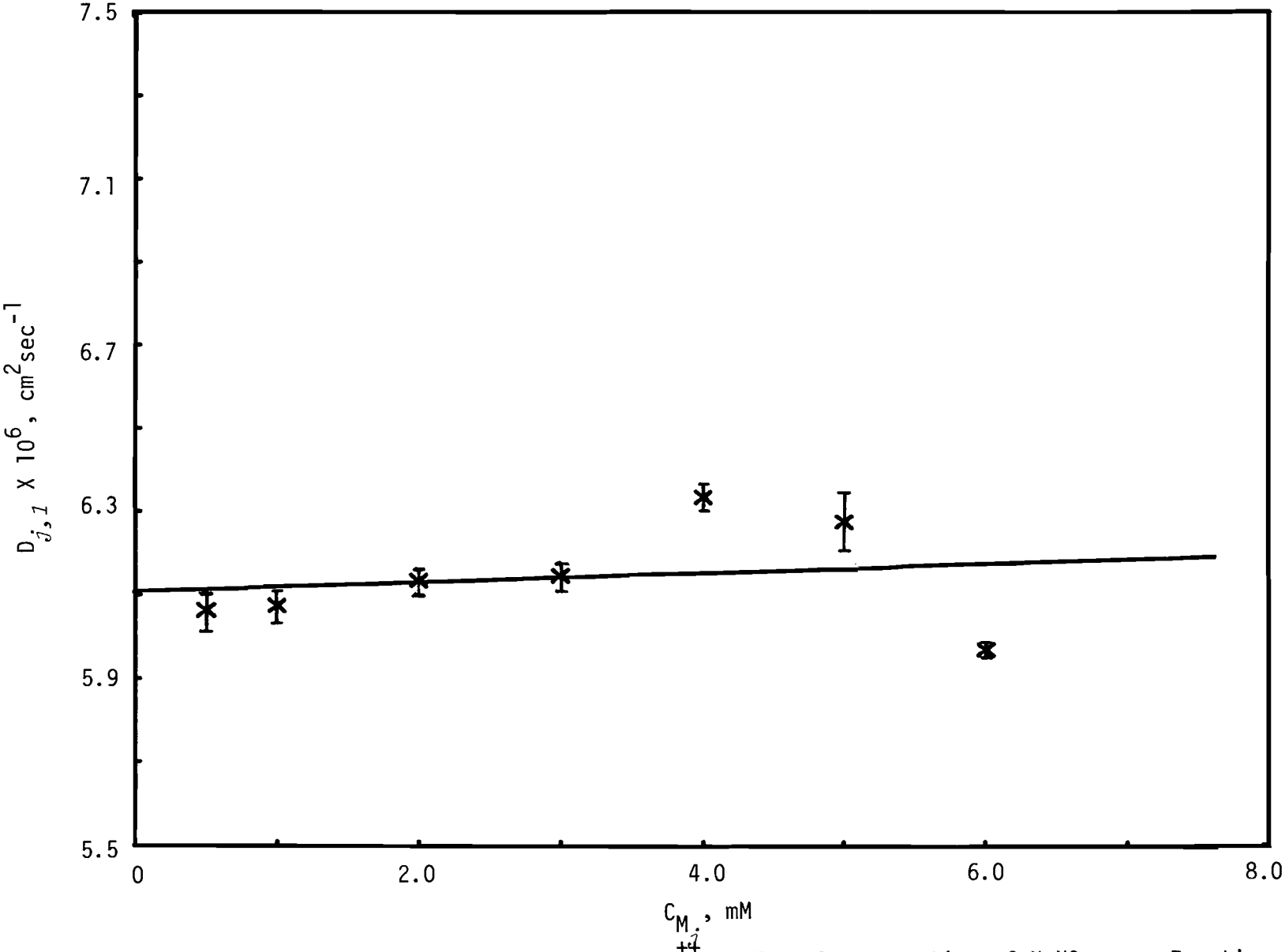

Figure 11. The Diffusion Coefficient of Co^{+4} at Zero Concentration of $NaNO_3$ as a Function of Concentration at 20°C.

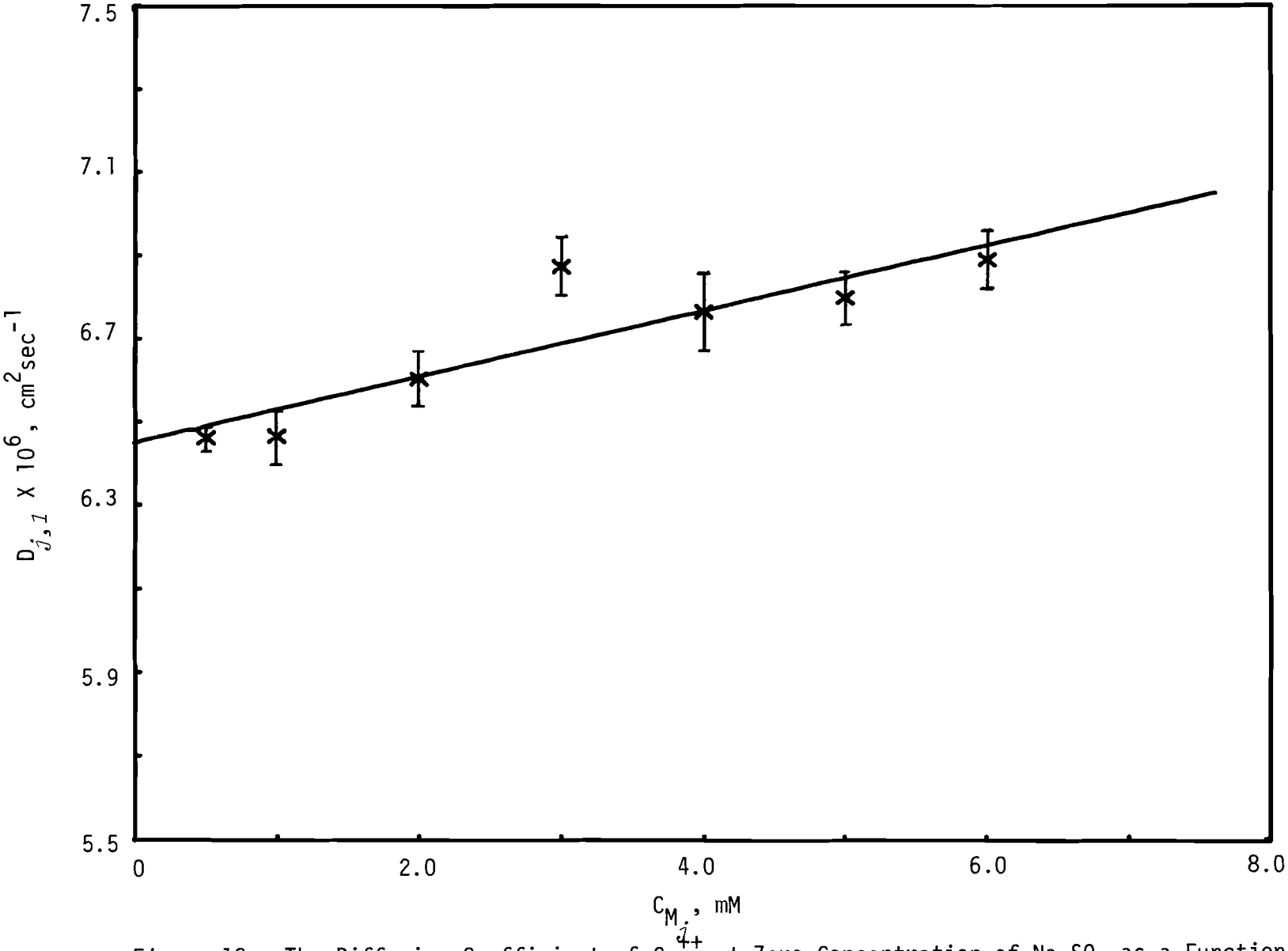

Figure 12. The Diffusion Coefficient of Co^{++} at Zero Concentration of Na_2SO_4 as a Function of Concentration at 20°C.

gelatin are small and therefore it is assumed that no irregular response of the diffusion of Co^{++} was caused by adding gelatin.

The experimental result of the limiting diffusion coefficient of Co^{++} at 20°C is thus the arithmetic means of the two experimental values. The result together with the standard deviation is tabulated in Table 8. The literature values of the limiting diffusion coefficient of Co^{++} at 20°C are also given in Table 8 for comparison.[93-95]

SECTION 7

DATA ANALYSIS

7.1 Determination of the Limiting Diffusion Coefficients of Cadmium and Cobalt (II) Ions

The determination of the limiting diffusion coefficients of Cd^{++} and Co^{++}, on the basis of the theories given in Section 2, involved these considerations.

1. Dependence of the apparent diffusion coefficient D_j on the ionic strength of the solution. The discussion given in Section 2.8 shows that changes in the apparent diffusion coefficient D_j is due to changes in the effective force causing diffusion and changes in the retarding force.

The change in the effective force causing diffusion may be regarded as the error resulting from the information used in the calculation of the diffusion coefficient, namely, the activity of the electroactive component M_j should be used in place of the concentration. However, the error generated in this manner is small at low ionic strength of the solution, and the value obtained from the extrapolation to zero concentration of the supporting electrolyte will still be correct. On the other hand, the retarding force, which is regarded as the relaxation effect, changes the mobility of the diffusion species.

Equation (2.8.2.1-4) suggests a linear relationship between the diffusion coefficient D_j and the square root of the concentrations of the electrolytes which may be regarded as the concentration of the supporting electrolyte since the concentration of the supporting electrolyte is imposed to be several times greater than that of the electroactive component. A linear extrapolation to zero concentration of the plot of this equation will remove the dependence of the diffusion

coefficient D_j on the ionic strength.

2. Dependence of the apparent diffusion coefficient D_j on the viscosity of the solution. The apparent diffusion coefficient D_j is an inverse function of the viscosity of the solution, therefore, the effect of the viscosity of the medium must be taken into consideration in order to deduce the limiting diffusion coefficient D_j°. Jones and Dole[96-98] expressed the relative viscosity, η/η_0, in terms of the concentration of the solution, and it is given by

$$\eta/\eta_0 = 1 + a_1 C_{S_j}^{1/2} + a_2 C_{S_j} \qquad (7.1\text{-}1)$$

where η is the viscosity of the solution, η_0 is the viscosity of the solvent, a_j are the viscosity coefficients, and C_{S_j} is referred to as the concentration of the supporting electrolyte.[99]

Eq. (7.1-1), which is expressed for η/η_0 as a function of C_{S_j} over a wide range of concentrations of C_{S_j}, reduces to the form of Eq. (7.1-2) at low concentrations of C_{S_j}.[100-102]

$$\eta/\eta_0 = 1 + aC_{S_j}^{1/2} \qquad (7.1\text{-}2)$$

which verifies that η/η_0 converges to one at zero concentration of the supporting electrolyte.

3. Dependence of the apparent diffusion coefficient D_j on the concentration of the electroactive component. The experimental data given in Appendix I show that at some constant concentration of the supporting electrolyte, the apparent diffusion coefficient D_j increases linearly with increases in the concentration of the electroactive component (the discussion of this phenomena is given in Section 8.2).

The dependence of the diffusion coefficient on the concentration C_{M_j} may be removed at zero concentration of the electroactive component,

and thus a linear extrapolation of a plot of Eq. (3.3-2) is considered for this purpose.

On the basis of these three considerations, the determination of the limiting diffusion coefficients of Cd^{++} and Co^{++} in this study is thus equivalent to that given in Section 3.3.

According to the discussion given in Section 3.3, the limiting diffusion coefficients D_j° of Cd^{++} and Co^{++} are those determined from the linear extrapolations of the plots of Eq. (3.3-2). The data of $D_{j,1}$, the diffusion coefficients at some finite concentrations of the electroactive components and at zero concentration of the supporting electrolyte, which were used for these linear extrapolations, are tabulated in Appendix II.

There are four sets of $D_{j,1}$ according to the two electroactive components and the two supporting electrolytes. These data sets are referred to as:

1. the diffusion coefficients at some finite concentrations of Cd^{++} and at zero concentration of $NaNO_3$,

2. the diffusion coefficients at some finite concentrations of Cd^{++} and at zero concentration of Na_2SO_4,

3. the diffusion coefficients at some finite concentrations of Co^{++} and at zero concentration of $NaNO_3$, and

4. the diffusion coefficients at some finite concentrations of Co^{++} and at zero concentration of Na_2SO_4.

The diffusion coefficents $D_{j,1}$ of both Cd^{++} and Co^{++} were determined on the same basis by the linear extrapolations of the plots of Eq. (3.3-1). The plots of Eq. (3.3-1), shown in Appendix III, are based on the experimental data of D_j and C_{S_j} which are given in Appendix I.

It should be mentioned that Eq. (3.3-1) is valid to the extent

of the limiting law, therefore the data of D_j and C_{S_j} for the plots of Eq. (3.3-1) are limited to be those obtained at low concentrations of the supporting electrolyte, $NaNO_3$ and Na_2SO_4. Taking this consideration into account, the experimental data of D_j and C_{S_j} for the plots of Eq. (3.3-1) are those obtained from the solutions where the concentrations C_{S_j} are less than one molar.

7.2 Errors

There are three main types of errors that change the magnitude of the results significantly.

1. Experimental error, which may be regarded as the errors in the parameters, $i_{t,j}$, $\overline{C}_j$, m, and t_d, used for calculating the apparent diffusion coefficient D_j.

2. Functional error, which is referred to as the error resulting from the form of the function used, Eq. (3.3-1), for the determination of the diffusion coefficients $D_{j,1}$. Equation (3.3-1) was chosen on the basis of Eqs. (2.8.2.1-4) and (7.1-2) which were derived on the basis of the limiting behavior. Therefore, data at high concentrations of C_{S_j} affected the overall results.

3. Systematic error, which is recognized as the error introduced into the system by transducers and calibration.

The experimental error was determined on the basis of two methods, the most probable error and a linear least square method.

The magnitude of the errors of the calculated diffusion coefficients D_j were determined by the method of the most probable error. The errors are approximately two percent of the magnitude of D_j. Figure 13, the apparent diffusion coefficient of 0.5003 mM Cd^{++} in $NaNO_3$ as a function of concentration at 20°C, provides an example of the error bars assigned on the basis of the most probable method. For more exact information of

the errors, percent magnitude of the random errors of the paramters, i_{j,t_d}, $\bar{C}_j$, m, and t_d, are given explicitly in Table 9. Table 10 gives the most probable errors of the diffusion coefficients in terms of percentages. This table is based on the information provided in Table 9.

The magnitude of the errors of $D_{j,1}$, the diffusion coefficients at some finite concentrations of the electroactive component M_j and at zero concentration of the supporting electrolyte, were determined from a linear least square method since $D_{j,1}$ were determined from the extrapolations of the best fit lines through all points in the linear plots of Eq. (3.3-1). The error bars that appear on Figure 9, 10, 11, and 12, the plots of Eq. (3.3-2) for the determination of D_j°, are based on the method of linear least square. Table 11 gives the standard deviations of $D_{j,1}$, σ.

TABLE 9

PERCENT MAGNITUDE OF RANDOM ERRORS

Source of Error	Concentration of the Electroactive Component, mM						
	0.5	1.0	2.0	3.0	4.0	5.0	6.0
$\frac{\Delta i_{j,t_d}}{i_{j,t_d}}$ [a]	0.50	0.50	0.30	0.30	0.25	0.20	0.20
$\frac{\Delta \overline{C}_j}{\overline{C}_j}$ [b]	0.50	0.50	0.30	0.30	0.30	0.30	0.20
$\frac{\Delta m}{m}$ [c]	1.42	1.42	1.42	1.42	1.42	1.42	1.42
$\frac{\Delta t_d}{t_d}$	0.50	0.50	0.50	0.50	0.50	0.50	0.50

[a] The errors of i_{j,t_d} were determined from the feedback resistant, scale readability, and thermal drift.

[b] Estimated from the number of dilutions.

[c] Estimated from the apparent height, fluctuation of the temperature, the standard deviations of the capillary radius and the capillary length.

TABLE 10

THE MOST PROBABLE ERROR OF THE APPARENT DIFFUSION COEFFICIENTS

Concentration $\overline{C}_j$, mM	The Most Probable Error $\frac{\Delta D_j}{D_j}$, percent
0.5	2.37
1.0	2.37
2.0	2.08
3.0	2.08
4.0	2.05
5.0	2.03
6.0	1.98

TABLE 11

STANDARD DEVIATIONS OF THE DIFFUSION COEFFICIENTS OF CADMIUM AND COBALT (II) IONS AT SOME FINITE CONCENTRATIONS OF THE METAL IONS AND AT ZERO CONCENTRATION OF THE SUPPORTING ELECTROLYTE

Concentration of the Electroactive Component $\bar{C}_j$, mM	$\sigma \times 10^6$, $cm^2 sec^{-1}$			
	Cd^{++}		Co^{++}	
	$NaNO_3$	Na_2SO_4	$NaNO_3$	Na_2SO_4
0.5	0.110	0.111	0.097	0.061
1.0	0.083	0.127	0.074	0.137
2.0	0.071	0.125	0.054	0.138
3.0	0.173	0.071	0.057	0.149
4.0	0.092	0.163	0.059	0.184
5.0	0.136	0.117	0.142	0.134
6.0	0.121	0.051	0.010	0.145

SECTION 8

DISCUSSION

8.1 The Limiting Diffusion Coefficients by Polarography

The limiting diffusion coefficients of Cd^{++} and Co^{++} at 20°C obtained by the polarographic method used in this study are in good agreement with the literature values which were determined from conductivity measurements. The limiting diffusion coefficient of Co^{++} in particular shows a consistency with the literature values to within the limit of the experimental error. On the other hand, the limiting diffusion coefficient obtained for Cd^{++} is comparable with the literature values to within a few standard deviation units.

8.2 The Apparent Diffusion Coefficients

The apparent diffusion coefficients of Cd^{++} and Co^{++} in the supporting electrolyte used, $NaNO_3$ or Na_2SO_4, were calculated from the modified Ilkovic equation. The apparent values of the diffusion coefficients D_j vary with the composition of the solutions.

Scheme 1, below, is given in order to give a full description of the dependence of D_j on the concentrations of the solutions. The plots in Scheme 1 are based on the assumption of no experimental errors.

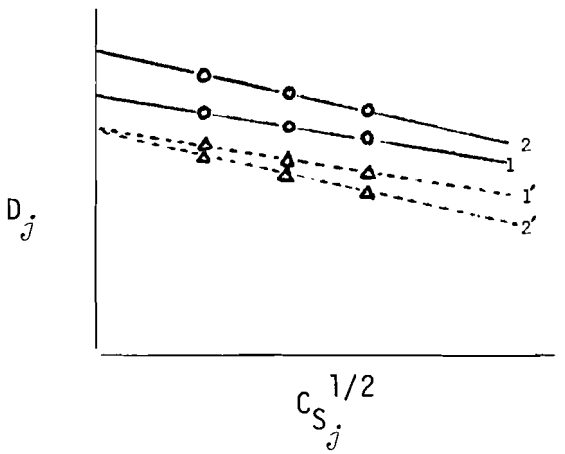

Scheme 1

The solid lines 1 and 2 are the plots of Eq. (3.3-1) under the experimental conditions.

The dotted lines 1' and 2' are the plots of Eq. (3.3-1) under a pure diffusion process.

According to Scheme 1, the solid lines labelled 1 and 2 refer to the plots of D_j versus $C_{S_j}^{1/2}$, Eq. (3.3-1), for the electroactive component M_j of concentrations $\overline{C}_j(1)$ and $\overline{C}_j(2)$ respectively [$\overline{C}_j(1) < \overline{C}_j(2)$]. Each circle on these plots represents a data point obtained under the experimental conditons. It can be seen from either plot of the solid line 1 or 2 that D_j decreases as C_{S_j} increases. The decreases of D_j as C_{S_j} increases are due to the fact that the increases of C_{S_j} cause increases in the ionic strength and the viscosity of the solution. The increases of the ionic strength of the solution cause a lowering in the effective force causing diffusion (Section 2.8.1) and an increase in the retarding force (Section 2.8.2.1). On the other hand, the viscosity of the solution is an inverse function of D_j, and thus increases of the viscosity of the solution decrease D_j.

In going from the solid line 1 to the solid line 2, where the concentration of the electroactive component C_{M_j} increases from $\overline{C}_j(1)$ to $\overline{C}_j(2)$, D_j at some finite concentration C_{S_j} increases significantly.

The dependence of the apparent diffusion coefficient D_j on C_{M_j}, under the experimental conditions in this work, perhaps owing to the reduced form of the electroactive component M_j, at the surface of the mercury drop, reacting with the hydrogen ions within their vicinity to give further oxidized forms of M_j which are themselves reducible. The magnitude of the instantaneous current i_{j,t_d} would therefore be larger than that obtained from a pure diffusion process. Clearly, the amount of the reduced form of M_j, that adsorbed on the surface of the mercury drop, is proportional to the amount of M_j that was reduced, namely, the amount of the reduced form of M_j is proportional to the bulk concentration $\overline{C}_j$.

The dotted lines 1' and 2' in Scheme 1 refer to the plots of D_j

versus $C_{S_j}^{1/2}$ for the electroactive component M_j of concentrations $\bar{C}_j(1)$ and $\bar{C}_j(2)$ analogous to that of the solid lines but under a pure diffusion process (without the discharge of hydrogen ions). The plots of these dotted lines are not experimentally obtainable since the experimental data in Appendix I show that D_j increases linearly with increases in the concentration C_{M_j}.

Scheme 2, given below, shows plots of Eq. (3.3-2), $D_{j,1}$ versus C_{M_j}. The solid line was plotted from the data of $D_{j,1}$ which were obtained from the extrapolations of the solid lines 1 and 2 in Scheme 1. The slope of this plot is positive, possibly owing to the reaction of the reduced form of the electroactive component with the hydrogen ions as explained above. The dotted line in Scheme 2 is the plot of Eq. (3.3-2) analogous to that of the solid line in the same scheme. The dotted line has a zero slope since it was plotted from the data of $D_{j,1}$ for a pure diffusion process which were obtained from the extrapolations of the dotted lines 1' and 2' in Scheme 1.

103

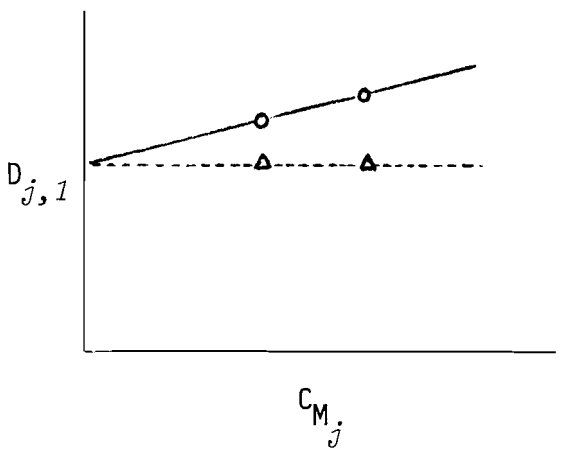

Scheme 2

The solid line is the plot of Eq. (3.3-2) under the experimental conditions.

The dotted line is the plot of Eq. (3.3-2) under a pure diffusion process.

8.3 Summary

1. The limiting diffusion coefficients of Cd^{++} and Co^{++} at 20°C, determined by polarography, are (6.08 $\pm$ 0.09) X 10^{-6} cm^2sec^{-1} and (6.28 $\pm$ 0.17) X 10^{-6} cm^2sec^{-1}, respectively.

2. The apparent diffusion coefficients D_j of Cd^{++} and Co^{++} in the supporting electrolyte used, $NaNO_3$ or Na_2SO_4, were studied as functions of the ionic strengths and the concentrations of the electroactive components.

3. The apparent diffusion coefficients D_j decrease with increases in the ionic strengths and the viscosities of the solutions.

4. The characteristic slopes obtained experimentally from the plots of $D_{j,1}$ versus C_{M_j} for the determination of the limiting diffusion coefficients of Cd^{++} and Co^{++} at 20°C are positive, possibly due to the discharge of hydrogen ions.

REFERENCES

1. K.J. Vetter, Electrochemical Kinetics (Academic Press, New York, 1967), Ch. 2.

2. K.J. Laidler, J. Chem. Ed. 47, 600 (1970).

3. R. Weston and H.A. Schwarz, Chemical Kinetics (Prentice-Hall, New Jersey, 1972), Ch. 1.

4. K.J. Vetter, Electrochemical Kinetics, Ch. 1.

5. J.J. Lingane, Electroanalytical Chemistry, 2nd ed. (Interscience, New York, 1958), Ch. 10.

6. H.A. Laitinen and W.E. Harris, Chemical Analysis, 2nd ed. (McGraw-Hill, New York, 1975), Ch. 14.

7. I.M. Kolthoff and J.J. Lingane, Polarography, Vol. 1, 2nd ed. (Interscience, New York, 1965).

8. J. Heyrovsky and J. Kuta, Principles of Polarography (Academic Press, New York, 1966).

9. J.J. Lingane, Electroanalytical Chemistry, Ch. 11.

10. L. Meites, Polarographic Techniques (Interscience, New York, 1955).

11. D.R. Crow, Polarography of Metal Complexes (Academic Press, New York, 1969), Ch. 2.

12. J.B. Headridge, Electrochemical Techniques for Inorganic Chemists (Academic Press, New York, 1969), Ch. 2.

13. G. Charlot, J. Badoz-Lambling and B. Tremillon, Electrochemical Reactions (Elsevier, Amsterdam, 1962), Ch. 1.

14. D.M. Brasher and F.R. Jones, Trans. Faraday Soc. 42, 775 (1946).

15. C.L. Rulfs, J. Amer. Chem. Soc. 76, 2071 (1954).

16. I. Vavruch, Collection Czechoslov. Chem. Communs. 12, 429 (1947).

17. N.H. Furman and W.C. Cooper, J. Amer. Chem. Soc. 72, 5667 (1950).

18. W.C. Cooper and N.H. Furman, J. Amer. Chem. Soc. 74, 6185 (1952).

19. M.v. Stackelberg, M. Pilgram and V. Toome, Z. Elektrochem. 57, 342 (1953).

20. M.v. Stackelberg and V. Toome, Z. Elektrochem. 58, 226 (1954).

21. I. Shain and K.J. Martin, J. Phys. Chem. 65, 254 (1961).

22. I. Shain and D.S. Polcyn, J. Phys. Chem. 65, 1649 (1961).

23. D.J. Macero and C.L. Rulfs, J. Amer. Chem. Soc. 81, 2942 (1959).

24. D.J. Macero and C.L. Rulfs, J. Amer. Chem. Soc. 81, 2944 (1959).

25. H. Rubin and F.C. Collins, J. Phys. Chem. 58, 958 (1954).

26. J. Koryta, Collection Czechoslov. Chem. Communs. 19, 433 (1954).

27. J.J. Lingane, Electroanalytical Chemistry, Ch. 11.

28. F. Buckley and J.K. Taylor, J. res. Nat. Bur. Stand. 34, 97 (1945).

29. H.A. Laitinen and I.M. Kolthoff, J. Phys. Chem. 45, 1061 (1941).

30. J. Heyrovsky and J. Kuta, Principles of Polarography, Ch. 19.

31. I.M. Kolthoff and J.J. Lingane, Polarography, Ch. 10.

32. L. Meites, Polarographic Techniques, Ch. 6.

33. J. Clank, The Mathematics of Diffusion (Clarendon, Oxford, 1956), Ch. 1.

34. L. Cady, Chem. Rev. 14, 171 (1934).

35. J.R. Welty, C.E. Wicks and R.E. Wilson, Fundamentals of Momentum, Heat and Mass Transfer (John Wiley and Sons, New York, 1969), Ch. 24.

36. R. Weston and H.A. Schwarz, Chemical Kinetics, Ch. 6.

37. This added component is often referred to as the supporting electrolyte.

38. K.J. Vetter, Electrochemical Kinetics, Ch. 2.

39. J.J. Lingane and I.M. Kolthoff, J. Amer. Chem. Soc. 61, 1045 (1939).

40. L. Meites, Polarographic Techniques, p. 42.

41. J. Heyrovsky and J. Kuta, Principles of Polarography, Ch. 5.

42. J. Robbins, Ions in Solution(2) an Introduction to Electrochemistry (Clarendon, Oxford, 1972), Ch. 3.

43. E.A. Guggenhein, J. Phys. Chem. 33, 842 (1929).

44. J. Robbins, Ions in Solution(2) an Introduction to Electrochemistry, p. 46.

45. R.A. Robinson and R.H. Stokes, Electrolyte Solutions, 2nd ed. (Academic Press, New York, 1959), Ch. 11.

46. S. Bretsznajder, Prediction of Transport and Other Physical Properties of Fluids, Vol. 11, P.V. Danckwerts ed. (Pergamon, Oxford, 1971), p. 385.

47. J.J. Lingane and I.M. Kolthoff, J. Amer. Chem. Soc. 61, 1045 (1939).

48. D.C. Grahame, Chem. Rev. 41, 441 (1947).

49. L. Meites, Polarographic Techniques, Ch. 3.

50. I.M. Kolthoff and J.J. Lingane, Polarography, Ch. 9.

51. J. Clank, The Mathematics of Diffusion, Ch. 3.

52. E.D. Rainville and P.E. Bedient, Elementary Differential Equations, 5th ed. (Macmillan, New York, 1974), Ch. 24.

53. M.L. Boas, Mathematical Methods in the Physical Sciences (John Wiley and Sons, New York, 1966), Ch. 14.

54. J. Koryta, J. Dvorak and V. Bohackova, Electrochemistry (Metheun, London, 1970), p. 116.

55. J.J. Lingane and B.A. Loveridge, J. Amer. Chem. Soc. 72, 438 (1950).

56. J. Kontecky, Czech. J. Phys. 2, 50 (1953).

57. J.M. Markowitz and P.J. Elving, Chem. Rev. 58, 1047 (1958).

58. J. Heyrovsky and J. Kuta, Principles of Polarography, p. 35.

59. J. Heyrovsky and J. Kuta, Principles of Polarography, p. 35.

60. I.M. Kolthoff and J.J. Lingane, Polarography, p. 82.

61. D.C. Grahame, Chem. Rev. 41, 441 (1947).

62. J. Kuta, J. Dvorak and V. Bohackova, Electrochemistry, p. 214.

63. K.J. Vetter, Electrochemical Kinetics, p. 73.

64. This condition is equivalent to the situation of tracer diffusion. For more details on tracer diffusion, see references 69-73.

65. H.S. Harned and B.B. Owen, Physical Chemistry of Electrolysis Solutions, 3rd ed. (Reinhold, New York, 1958).

66. R.A. Robinson and R.H. Stokes, Electrolyte Solutions, Ch. 4.

67. J. Robbins, Ions in Solution(2) an Introduction to Electrochemistry, Ch. 1.

68. I.M. Klotz and R.M. Rosenberg, Chemical Thermodynamics, 3rd ed. (W.A. Benjamin, Massachusetts, 1972), Ch. 14.

69. L. Onsager, Phys. Rev. 37, 405 (1937).

70. L.C. Gosting and H.S. Harned, J. Amer. Chem. Soc. 73, 159 (1951).

71. R.A. Robinson and R.H. Stokes, Electrolyte Solutions, p. 314.

72. J. Kuta, J. Dvorak and V. Bohackova, Electrochemistry.

73. T. Erdey-Gruz, Transport Phenomena in Aqueous Solutions (Wiley, New York, 1974), p. 235.

74. R.A. Robinson and R.H. Stokes, Electrolyte Solutions, p. 133.

75. J. Robbins, Ions in Solution(2) an Introduction to Electrochemistry, p. 46.

76. T. Erdey-Gruz, Transport Phenomena in Aqueous Solutions, Ch. 2.

77. R.H. Stokes and R. Mills, Viscosity of Electrolytes and Related Properties (Pergamon Press, New York, 1965).

78. D.M. Brasher and F.R. Jones, Trans. Faraday Soc. 42, 775 (1946).

79. F. Buckley and J.K. Taylor, J. res. Nat. Bur. Stand. 34, 97 (1945).

80. I.M. Kolthoff and J.J. Lingane, Chem. Rev. 24, 1 (1939).

81. I.M. Kolthoff and J.J. Lingane, Chem. Rev. 24, 1 (1939).

82. C.G. Enke and R.A. Baxter, J. Chem. Ed. 41, 202 (1964).

83. H.V. Malmstadt, C.G. Enke and S.R. Crouch, Electronic Analog Measurements and Transducers, Module 1 (W.A. Benjamin, Massachusetts, 1973), p. 110.

84. The international volt as a working standard is defined as: 1 V = 1/1.0183 of the emf of the Weston Normal (saturated) cell at 20°C. See reference 83, page 45.

85. S. Bretsznajder, Prediction of Transport and Other Physical Properties of Fluids, p. 386.

86. John A. Dean, Ed., Hand Book of Chemistry, 11th ed. (McGraw-Hill, New York, 1965), p. 6-30.

87. J. Robbins, Ions in Solution(2) an Introduction to Electrochemistry, p. 24.

88. I.M. Kolthoff and J.J. Lingane, Polarography, p. 52.

89. S. Bretsznajder, Prediction of Transport and Other Physical Properties of Fluids, p. 388.

90. L. Korson, J. Phys. Chem. 73, 34 (1969).

91. R.H. Stokes and R. Mills, Viscosity of Electrolytes and Related Properties.

92. Swindells, Coe and Godfrey, J. res. Nat. Bur. Stand. 48, 1 (1952).

93. S. Bretsznajder, Prediction of Transport and Other Physical Properties of Fluids, p. 386.

94. John A. Dean, Ed., Hand Book of Chemistry, 11th ed. (McGraw-Hill, New York, 1965), p. 6-30.

95. R.A. Robinson and R.H. Stokes, Electrolyte Solutions, p. 463.

96. R.H. Stokes and R. Mills, Viscosity of Electrolytes and Related Properties.

97. T. Erdey-Gruz, Transport Phenomena in Aqueous Solutions, p. 112.

98. R.A. Robinson and R.H. Stokes, Electrolyte Solutions, p. 304.

99. Equation (7.1-1) is expressed for one component electrolyte. However, the concentration of the supporting electrolyte is several times that of the electroactive component, therefore it may be assumed that changes in the viscosity of the solution are only affected by changes in the concentration of the supporting electrolyte.

100. R.H. Stokes and R. Mills, Viscosity of Electrolytes and Related Properties.

101. T. Erdey-Gruz, Transport Phenomena in Aqueous Solutions, Ch. 2.

102. R.A. Robinson and R.H. Stokes, Electrolyte Solutions, p. 304.

103. The concentrations of the electroactive component are in the order of magnitude of 10^{-3} M, hence the activity coefficients are close to unity.

APPENDIX I

Experimental Data

TABLE 12

THE APPARENT DIFFUSION COEFFICIENTS OF Cd^{++} IN $NaNO_3$ SOLUTIONS AT 20.0 ± 0.1°C

Concentration $NaNO_3$ C_{S_j}, M	Half-wave Potential $E_{1/2}$, V	Drop-time [a,b] t_d, sec	Instantaneous Current [a] i_{j,t_d}, μamp	Diffusion Coefficient $D_j \times 10^6$, $cm^2 sec^{-1}$
0.100	- 0.560	4.16	3.81	5.894
0.200	- 0.560	4.16	3.81	5.894
0.300	- 0.560	4.16	3.72	5.642
0.400	- 0.560	4.16	3.71	5.615
0.500	- 0.560	4.16	3.69	5.560
0.600	- 0.560	4.16	3.65	5.450
0.700	- 0.560	4.16	3.65	5.450
0.800	- 0.560	4.16	3.65	5.450
1.000	- 0.560	4.16	3.64	5.423
1.200	- 0.560	4.16	3.64	5.423

0.5003 mM $Cd(NO_3)_2$ in $NaNO_3$ solutions.

[a] Evaluated at E = -0.702 V with respect to SCE.

[b] Flow-rate determined from Eq. (3.2.3-1), with h = 41.26 cm, to be 1.976 $mg \cdot sec^{-1}$.

Concentration $NaNO_3$ C_{S_j}, M	Half-wave Potential $E_{1/2}$, V	Drop-time [a,b] t_d, sec	Instantaneous Current [a] i_{j,t_d}, μamp	Diffusion Coefficient $D_j \times 10^6$, $cm^2 sec^{-1}$
0.100	- 0.560	4.16	7.62	5.888
0.200	- 0.560	4.16	7.62	5.888
0.300	- 0.560	4.16	7.49	5.706
0.400	- 0.560	4.16	7.48	5.692
0.500	- 0.560	4.16	7.43	5.623
0.600	- 0.560	4.16	7.40	5.582
0.700	- 0.560	4.16	7.40	5.582
0.800	- 0.560	4.16	7.40	5.582
1.000	- 0.560	4.16	7.38	5.554
1.200	- 0.560	4.16	7.36	5.527

1.006 mM $Cd(NO_3)_2$ in $NaNO_3$ solutions.

[a] Evaluated at E = -0.702 V with respect to SCE.

[b] Flow-rate determined from Eq. (3.2.3-1), with h = 41.26 cm, to be 1.976 $mg \cdot sec^{-1}$.

TABLE 12 (continued)

C_{S_j}, M	$E_{1/2}$, V	t_d[a,b], sec	i_{j,t_d}[a], μamp	$D_j \times 10^6$, $cm^2 sec^{-1}$
0.100	- 0.560	4.19	15.42	6.056
0.200	- 0.560	4.19	15.34	5.999
0.300	- 0.560	4.19	15.10	5.829
0.400	- 0.560	4.19	14.96	5.731
0.500	- 0.560	4.19	14.86	5.662
0.600	- 0.560	4.19	14.80	5.620
0.700	- 0.560	4.19	14.74	5.578
0.800	- 0.560	4.19	14.72	5.565
1.000	- 0.560	4.19	14.66	5.523
1.200	- 0.560	4.19	14.64	5.510

2.0012 mM $Cd(NO_3)_2$ in $NaNO_3$ solutions.

[a] Evaluated at E = -0.702 V with respect to SCE.

[b] Flow-rate determined from Eq. (3.2.3-1), with h = 40.97 cm, to be 1.962 $mg \cdot sec^{-1}$.

C_{S_j}, M	$E_{1/2}$, V	t_d[a,b], sec	i_{j,t_d}[a], μamp	$D_j \times 10^6$, $cm^2 sec^{-1}$
0.200	- 0.560	4.19	23.20	6.089
0.300	- 0.560	4.19	22.70	5.853
0.400	- 0.560	4.19	22.50	5.759
0.500	- 0.560	4.19	22.40	5.713
0.600	- 0.560	4.19	22.25	5.645
0.700	- 0.560	4.19	22.25	5.643
0.800	- 0.560	4.19	22.25	5.643
1.000	- 0.560	4.19	22.10	5.574
1.200	- 0.560	4.19	22.00	5.528

3.0018 mM $Cd(NO_3)_2$ in $NaNO_3$ solutions.

[a] Evaluated at E = -0.702 V with respect to SCE.

[b] Flow-rate determined from Eq. (3.2.3-1), with h = 40.97 cm, to be 1.962 $mg \cdot sec^{-1}$.

TABLE 12 (continued)

C_{S_j}, M	$E_{1/2}$, V	t_d[a,b], sec	i_{j,t_d}[a], μamp	$D_j \times 10^6$, $cm^2 sec^{-1}$
0.200	- 0.560	4.22	30.65	6.031
0.300	- 0.560	4.22	30.25	5,889
0.400	- 0.560	4.22	30.00	5.800
0.500	- 0.560	4.22	29.70	5.695
0.600	- 0.560	4.22	29.50	5.625
0.700	- 0.560	4.22	29.40	5.590
0.800	- 0.560	4.22	29.40	5.590
1.000	- 0.560	4.22	29.35	5.573
1.200	- 0.560	4.22	29.20	5.521

4.0024 mM $Cd(NO_3)_2$ in $NaNO_3$ solutions.

[a] Evaluated at E = -0.702 V with respect to SCE.

[b] Flow-rate determined from Eq. (3.2.3-1), with h = 40.66 cm, to be 1.946 $mg \cdot sec^{-1}$.

C_{S_j}, M	$E_{1/2}$, V	t_d[a,b], sec	i_{j,t_d}[a], μamp	$D_j \times 10^6$, $cm^2 sec^{-1}$
0.300	- 0.560	4.06	38.70	5.904
0.400	- 0.560	4.06	38.40	5.821
0.500	- 0.560	4.06	38.00	5.711
0.600	- 0.560	4.06	37.65	5.615
0.700	- 0.560	4.06	37.60	5.601
0.800	- 0.560	4.06	37.60	5.601
1.000	- 0.560	4.06	37.40	5.547
1.200	- 0.560	4.06	37.30	5.520

5.0030 mM $Cd(NO_3)_2$ in $NaNO_3$ solutions.

[a] Evaluated at E = -0.702 V with respect to SCE.

[b] Flow-rate determined from Eq. (3.2.3-1), with h = 42.21 cm, to be 2.024 $mg \cdot sec^{-1}$.

TABLE 12 (continued)

C_{S_j}, M	$E_{1/2}$, V	t_d[a,b], sec	i_{j,t_d}[a], μamp	$D_j \times 10^6$, $cm^2 sec^{-1}$
0.300	- 0.560	4.06	47.00	6.034
0.400	- 0.560	4.06	46.50	5.918
0.500	- 0.560	4.06	46.10	5.825
0.600	- 0.560	4.06	46.10	5.825
0.700	- 0.560	4.06	46.00	5.802
0.800	- 0.560	4.06	45.60	5.710
1.000	- 0.560	4.06	45.30	5.642
1.200	- 0.560	4.06	45.20	5.619

6.0036 mM $Cd(NO_3)_2$ in $NaNO_3$ solutions.

[a] Evaluated at E = -0.702 V with respect to SCE.

[b] Flow-rate determined from Eq. (3.2.3-1), with h = 42.21 cm, to be 2.024 $mg \cdot sec^{-1}$.

TABLE 13

THE APPARENT DIFFUSION COEFFICIENTS OF Cd^{++} IN Na_2SO_4 SOLUTIONS AT 20.0 ± 0.1°C

Concentration Na_2SO_4 C_{S_j}, M	Half-wave Potential $E_{1/2}$, V	Drop-time [a,b] t_d, sec	Instantaneous Current [a] i_{j,t_d}, μamp	Diffusion Coefficient $D_j \times 10^6$, $cm^2 sec^{-1}$
0.030	- 0.578	3.96	3.74	5.465
0.060	- 0.578	3.96	3.69	5.332
0.120	- 0.578	3.95	3.62	5.152
0.240	- 0.582	3.95	3.51	4.869
0.360	- 0.582	3.95	3.43	4.666
0.480	- 0.582	3.95	3.28	4.297
0.600	- 0.586	3.95	3.20	4.106
0.720	- 0.586	3.95	3.11	3.894
0.840	- 0.586	3.95	2.99	3.620
0.960	- 0.586	3.95	2.91	3.442
1.080	- 0.586	3.95	2.85	3.312

0.5007 mM $Cd(NO_3)_2$ in Na_2SO_4 solutions.

[a] Evaluated at E = -0.710 V with respect to SCE.

[b] Flow-rate determined from Eq. (3.2.3-1), with h = 43.25 cm, to be 2.075 $mg \cdot sec^{-1}$.

Concentration Na_2SO_4 C_{S_j}, M	Half-wave Potential $E_{1/2}$, V	Drop-time [a,b] t_d, sec	Instantaneous Current [a] i_{j,t_d}, μamp	Diffusion Coefficient $D_j \times 10^6$, $cm^2 sec^{-1}$
0.060	- 0.578	3.96	7.32	5.280
0.120	- 0.578	3.95	7.22	5.152
0.240	- 0.582	3.94	6.98	4.847
0.360	- 0.582	3.94	6.89	4.732
0.480	- 0.582	3.94	6.58	4.348
0.600	- 0.586	3.94	6.37	4.095
0.720	- 0.586	3.94	6.28	3.988
0.840	- 0.586	3.94	6.13	3.814
0.960	- 0.586	3.94	5.90	3.552
1.080	- 0.586	3.95	5.70	3.329

1.0014 mM $Cd(NO_3)_2$ in Na_2SO_4 solutions.

[a] Evaluated at E = -0.710 V with respect to SCE.

[b] Flow-rate determined from Eq. (3.2.3-1), with h = 43.06 cm, to be 2.066 $mg \cdot sec^{-1}$.

TABLE 13 (continued)

C_{S_j}, M	$E_{1/2}$, V	t_d[a,b], sec	i_{j,t_d}[a], μamp	$D_j \times 10^6$, $cm^2 sec^{-1}$
0.120	- 0.582	3.95	14.48	5.191
0.240	- 0.582	3.94	13.93	4.838
0.360	- 0.582	3.94	13.70	4.692
0.480	- 0.582	3.94	13.33	4.462
0.600	- 0.586	3.94	12.89	4.194
0.720	- 0.586	3.94	12.60	4.021
0.840	- 0.586	3.94	12.14	3.753
0.960	- 0.586	3.96	11.84	3.577
1.080	- 0.586	3.97	11.54	3.407

2.0028 mM $Cd(NO_3)_2$ in Na_2SO_4 solutions.

[a] Evaluated at E = -0.710 V with respect to SCE.

[b] Flow-rate determined from Eq. (3.2.3-1), with h = 42.98 cm, to be 2.062 $mg \cdot sec^{-1}$.

C_{S_j}, M	$E_{1/2}$, V	t_d[a,b], sec	i_{j,t_d}[a], μamp	$D_j \times 10^6$, $cm^2 sec^{-1}$
0.240	- 0.582	3.96	21.20	4.992
0.360	- 0.582	3.96	20.65	4.756
0.480	- 0.582	3.96	20.10	4.526
0.600	- 0.586	3.97	19.50	4.280
0.720	- 0.586	3.97	19.00	4.070
0.840	- 0.586	3.97	18.50	3.880
0.960	- 0.586	3.97	18.00	3.687

3.0043 mM $Cd(NO_3)_2$ in Na_2SO_4 solutions.

[a] Evaluated at E = -0.710 V with respect to SCE.

[b] Flow-rate determined from Eq. (3.2.3-1), with h = 42.76 cm, to be 2.051 $mg \cdot sec^{-1}$.

TABLE 13 (continued)

C_{S_j}, M	$E_{1/2}$, V	t_d[a,b], sec	i_{j,t_d}[a], μamp	$D_j \times 10^6$, $cm^2 sec^{-1}$
0.240	- 0.582	3.95	28.20	4.943
0.360	- 0.582	3.95	27.50	4.720
0.480	- 0.582	3.95	27.00	4.563
0.600	- 0.586	3.95	26.35	4.363
0.720	- 0.586	3.95	25.60	4.137
0.840	- 0.586	3.95	24.60	3.842
0.960	- 0.586	3.96	24.25	3.739
1.080	- 0.586	3.96	23.40	3.496

4.0056 mM $Cd(NO_3)_2$ in Na_2SO_4 solutions.

[a] Evaluated at E = -0.710 V with respect to SCE.

[b] Flow-rate determined from Eq. (3.2.3-1), with h = 42.98 cm, to be 2.062 $mg \cdot sec^{-1}$.

C_{S_j}, M	$E_{1/2}$, V	t_d[a,b], sec	i_{j,t_d}[a], μamp	$D_j \times 10^6$, $cm^2 sec^{-1}$
0.240	- 0.582	3.98	35.30	4.974
0.360	- 0.582	3.98	34.65	4.807
0.480	- 0.582	3.98	33.75	4.580
0.600	- 0.586	3.98	32.65	4.309
0.720	- 0.586	3.98	31.95	3.140
0.840	- 0.586	3.98	31.00	3.915
0.960	- 0.586	3.98	30.30	3.753
1.080	- 0.586	3.98	24.05	3.471

5.0071 mM $Cd(NO_3)_2$ in Na_2SO_4 solutions.

[a] Evaluated at E = -0.710 V with respect to SCE.

[b] Flow-rate determined from Eq. (3.2.3-1), with h = 42.76 cm, to be 2.051 $mg \cdot sec^{-1}$.

TABLE 13 (continued)

C_{S_j}, M	$E_{1/2}$, V	t_d[a,b], sec	i_{j,t_d}[a], μamp	$D_j \times 10^6$, $cm^2 sec^{-1}$
0.240	- 0.586	3.99	42.00	4.921
0.360	- 0.586	3.99	41.20	4.750
0.480	- 0.586	3.99	40.00	4.499
0.600	- 0.586	3.99	39.00	4.294
0.720	- 0.586	4.00	38.00	4.089
0.840	- 0.586	4.01	36.55	3.802
0.960	- 0.586	4.01	35.70	3.640
1.080	- 0.586	4.02	34.70	3.450

6.0085 mM $Cd(NO_3)_2$ in Na_2SO_4 solutions.

[a] Evaluated at E = -0.710 V with respect to SCE.

[b] Flow-rate determined from Eq. (3.2.3-1), with h = 42.56 cm, to be 2.041 $mg \cdot sec^{-1}$.

TABLE 14

THE APPARENT DIFFUSION COEFFICIENTS OF Co^{++} IN $NaNO_3$ SOLUTIONS AT 20.0 ± 0.1°C

Concentration $NaNO_3$ C_{S_j}, M	Half-wave Potential $E_{1/2}$, V	Drop-time [a,b] t_d, sec	Instantaneous Current [a] i_{j,t_d}, μamp	Diffusion Coefficient $D_j \times 10^6$, $cm^2 sec^{-1}$
0.100	- 1.088	3.40	3.69	5.747
0.200	- 1.088	3.38	3.67	5.751
0.300	- 1.092	3.38	3.60	5.551
0.400	- 1.092	3.36	3.58	5.506
0.500	- 1.092	3.34	3.57	5.489
0.600	- 1.096	3.34	3.56	5.461
0.700	- 1.096	3.32	3.52	5.360

0.5017 mM $Co(NO_3)_2$ in 0.01% gelatin-$NaNO_3$ solutions.

[a] Evaluated at E = -1.272 V with respect to SCE.

[b] Flow-rate determined from Eq. (3.2.3-1), with h = 42.08 cm, to be 2.011 $mg \cdot sec^{-1}$.

Concentration $NaNO_3$ C_{S_j}, M	Half-wave Potential $E_{1/2}$, V	Drop-time [a,b] t_d, sec	Instantaneous Current [a] i_{j,t_d}, μamp	Diffusion Coefficient $D_j \times 10^6$, $cm^2 sec^{-1}$
0.100	- 1.100	3.40	7.37	5.830
0.200	- 1.104	3.38	7.36	5.827
0.300	- 1.108	3.38	7.26	5.683
0.400	- 1.108	3.36	7.25	5.683
0.500	- 1.112	3.34	7.19	5.605
0.600	- 1.112	3.34	7.16	5.563
0.700	- 1.116	3.33	7.11	5.497

1.0034 mM $Co(NO_3)_2$ in 0.01% gelatin-$NaNO_3$ solutions.

[a] Evaluated at E = -1.272 V with respect to SCE.

[b] Flow-rate determined from Eq. (3.2.3-1), with h = 41.79 cm, to be 1.997 $mg \cdot sec^{-1}$.

TABLE 14 (continued)

C_{S_j}, M	$E_{1/2}$, V	t_d[a,b], sec	i_{j,t_d}[a], μamp	$D_j \times 10^6$, $cm^2 sec^{-1}$
0.100	- 1.160	3.13	14.74	6.000
0.200	- 1.160	3.12	14.70	5.976
0.300	- 1.180	3.10	14.54	5.871
0.400	- 1.188	3.10	14.50	5.841
0.500	- 1.192	3.08	14.48	5.842
0.600	- 1.208	3.08	14.42	5.798
0.700	- 1.220	3.06	14.40	5.796

2.0068 mM $Co(NO_3)_2$ in 0.01% gelatin-$NaNO_3$ solutions.

[a] Evaluated at E = -1.430 V with respect to SCE.

[b] Flow-rate determined from Eq. (3.2.3-1), with h = 41.78 cm, to be 1.995 $mg \cdot sec^{-1}$.

C_{S_j}, M	$E_{1/2}$, V	t_d[a,b], sec	i_{j,t_d}[a], μamp	$D_j \times 10^6$, $cm^2 sec^{-1}$
0.200	- 1.200	3.12	22.10	6.001
0.300	- 1.208	3.10	21.90	5.915
0.400	- 1.220	3.08	21.85	5.906
0.500	- 1.228	3.08	21.80	5.882
0.600	- 1.228	3.07	21.75	5.863
0.700	- 1.232	3.07	21.70	5.839

3.0102 mM $Co(NO_3)_2$ in 0.01% gelatin-$NaNO_3$ solutions.

[a] Evaluated at E = -1.430 V with respect to SCE.

[b] Flow-rate determined from Eq. (3.2.3-1), with h = 41.78 cm, to be 1.995 $mg \cdot sec^{-1}$.

TABLE 14 (continued)

C_{S_j}, M	$E_{1/2}$, V	t_d[a,b], sec	i_{j,t_d}[a], μamp	$D_j \times 10^6$, $cm^2 sec^{-1}$
0.200	- 1.208	3.10	29.50	6.030
0.300	- 1.212	3.09	29.20	5.925
0.400	- 1.220	3.08	29.00	5.857
0.500	- 1.228	3.08	28.85	5.802
0.600	- 1.236	3.06	28.75	5.778
0.700	- 1.248	3.06	28.65	5.741

4.0136 mM $Co(NO_3)_2$ in 0.01% gelatin-$NaNO_3$ solutions.

[a] Evaluated at E = -1.430 V with respect to SCE.

[b] Flow-rate determined from Eq. (3.2.3-1), with h = 41.77 cm, to be 1.994 $mg \cdot sec^{-1}$.

C_{S_j}, M	$E_{1/2}$, V	t_d[a,b], sec	i_{j,t_d}[a], μamp	$D_j \times 10^6$, $cm^2 sec^{-1}$
0.300	- 1.236	3.11	36.50	5.954
0.400	- 1.248	3.09	36.30	5.907
0.500	- 1.252	3.09	36.15	5.862
0.600	- 1.256	3.06	36.10	5.866
0.700	- 1.268	3.06	35.70	5.748

5.0170 mM $Co(NO_3)_2$ in 0.01% gelatin-$NaNO_3$ solutions.

[a] Evaluated at E = -1.430 V with respect to SCE.

[b] Flow-rate determined from Eq. (3.2.3-1), with h = 41.54 cm, to be 1.982 $mg \cdot sec^{-1}$.

C_{S_j}, M	$E_{1/2}$, V	t_d[a,b], sec	i_{j,t_d}[a], μamp	$D_j \times 10^6$, $cm^2 sec^{-1}$
0.300	- 1.236	3.11	43.60	5.904
0.400	- 1.248	3.11	43.55	5.892
0.500	- 1.252	3.10	43.50	5.886
0.600	- 1.256	3.09	43.45	5.879
0.700	- 1.268	3.09	43.40	5.876

6.0204 mM $Co(NO_3)_2$ in 0.01% gelatin-$NaNO_3$ solutions.

[a] Evaluated at E = -1.430 V with respect to SCE.

[b] Flow-rate determined from Eq. (3.2.3-1), with h = 41.54 cm, to be 1.982 $mg \cdot sec^{-1}$.

TABLE 15

THE APPARENT DIFFUSION COEFFICIENTS OF Co^{++} IN Na_2SO_4 SOLUTIONS AT 20.0 ± 0.1°C

Concentration Na_2SO_4 C_{S_j}, M	Half-wave Potential $E_{1/2}$, V	Drop-time [a,b] t_d, sec	Instantaneous Current [a] i_{j,t_d}, μamp	Diffusion Coefficient $D_j \times 10^6$, $cm^2 sec^{-1}$
0.120	- 1.176	2.72	3.44	5.399
0.240	- 1.212	2.69	3.32	5.064
0.360	- 1.270	2.67	3.20	4.745
0.480	- 1.310	2.65	3.07	4.406
0.600	- 1.326	2.65	2.98	4.170
0.720	- 1.348	2.64	2.91	3.995
0.840	- 1.352	2.64	2.82	3.768
0.960	- 1.360	2.64	2.74	3.571

0.5004 mM $CoSO_4$ in 0.001% gelatin-Na_2SO_4 solutions.

[a] Evaluated at E = -1.586 V with respect to SCE.

[b] Flow-rate determined from Eq. (3.2.3-1), with h = 43.02 cm, to be 2.052 $mg \cdot sec^{-1}$.

Concentration Na_2SO_4 C_{S_j}, M	Half-wave Potential $E_{1/2}$, V	Drop-time [a,b] t_d, sec	Instantaneous Current [a] i_{j,t_d}, μamp	Diffusion Coefficient $D_j \times 10^6$, $cm^2 sec^{-1}$
0.120	- 1.180	2.70	6.98	5.550
0.240	- 1.228	2.70	6.72	5.176
0.360	- 1.270	2.66	6.62	5.063
0.480	- 1.310	2.66	6.37	4.716
0.600	- 1.326	2.65	6.18	4.464
0.720	- 1.348	2.65	6.13	4.398
0.840	- 1.352	2.64	5.85	4.037
0.960	- 1.360	2.64	5.87	3.986

1.0008 mM $CoSO_4$ in 0.01% gelatin-Na_2SO_4 solutions.

[a] Evaluated at E = -1.586 V with respect to SCE.

[b] Flow-rate determined from Eq. (3.2.3-1), with h = 42.98 cm, to be 2.050 $mg \cdot sec^{-1}$.

TABLE 15 (continued)

C_{S_j}, M	$E_{1/2}$, V	[a,b] t_d, sec	[a] i_{j,t_d}, μamp	$D_j \times 10^6$, $cm^2 sec^{-1}$
0.240	- 1.232	2.67	13.44	5.195
0.360	- 1.270	2.65	13.24	5.069
0.480	- 1.310	2.65	12.70	4.694
0.600	- 1.326	2.65	12.40	4.491
0.720	- 1.348	2.65	12.14	4.318
0.840	- 1.352	2.65	11.80	4.097
0.960	- 1.360	2.65	11.50	3.905

2.0016 mM $CoSO_4$ in 0.001% gelatin-Na_2SO_4 solutions.

[a] Evaluated at E = -1.586 V with respect to SCE.

[b] Flow-rate determined from Eq. (3.2.3-1), with h = 42.98 cm, to be 2.050 $mg \cdot sec^{-1}$.

C_{S_j}, M	$E_{1/2}$, V	[a,b] t_d, sec	[a] i_{j,t_d}, μamp	$D_j \times 10^6$, $cm^2 sec^{-1}$
0.240	- 1.236	2.67	20.40	5.337
0.360	- 1.270	2.67	19.95	5.123
0.480	- 1.310	2.67	19.45	4.888
0.600	- 1.326	2.67	18.60	4.501
0.720	- 1.348	2.64	18.20	4.340
0.840	- 1.352	2.64	17.60	4.078
0.960	- 1.360	2.64	17.30	3.950

3.0024 mM $CoSO_4$ in 0.001% gelatin-Na_2SO_4 solutions.

[a] Evaluated at E = -1.586 V with respect to SCE.

[b] Flow-rate determined from Eq. (3.2.3-1), with h = 42.81 cm, to be 2.042 $mg \cdot sec^{-1}$.

TABLE 15 (continued)

C_{S_j}, M	$E_{1/2}$, V	t_d[a,b], sec	i_{j,t_d}[a], μamp	$D_j \times 10^6$, $cm^2 sec^{-1}$
0.240	- 1.236	2.62	27.25	5.395
0.360	- 1.270	2.60	26.80	5.246
0.480	- 1.310	2.60	25.55	4.804
0.600	- 1.326	2.60	24.85	4.563
0.720	- 1.348	2.60	24.35	4.395
0.840	- 1.352	2.60	23.95	4.262
0.960	- 1.360	2.60	23.55	4.131

4.0032 mM $CoSO_4$ in 0.001% gelatin-Na_2SO_4 solutions.

[a] Evaluated at E = -1.586 V with respect to SCE.

[b] Flow-rate determined from Eq. (3.2.3-1), with h = 42.78 cm, to be 2.040 $mg \cdot sec^{-1}$.

C_{S_j}, M	$E_{1/2}$, V	t_d[a,b], sec	i_{j,t_d}[a], μamp	$D_j \times 10^6$, $cm^2 sec^{-1}$
0.360	- 1.270	2.61	33.10	5.125
0.480	- 1.310	2.61	32.00	4.815
0.600	- 1.326	2.61	31.25	4.608
0.720	- 1.348	2.61	30.65	4.446
0.840	- 1.352	2.61	29.55	4.155
0.960	- 1.360	2.61	29.20	4.064

5.0040 mM $CoSO_4$ in 0.001% gelatin-Na_2SO_4 solutions.

[a] Evaluated at E = -1.586 V with respect to SCE.

[b] Flow-rate determined from Eq. (3.2.3-1), with h = 42.78 cm, to be 2.040 $mg \cdot sec^{-1}$.

TABLE 15 (continued)

C_{S_j}, M	$E_{1/2}$, V	t_d[a,b], sec	i_{j,t_d}[a], μamp	$D_j \times 10^6$, $cm^2 sec^{-1}$
0.360	- 1.270	2.64	39.60	5.077
0.480	- 1.310	2.62	38.55	4.843
0.600	- 1.326	2.62	37.00	4.490
0.720	- 1.348	2.62	36.05	4.278
0.840	- 1.352	2.62	35.35	4.125
0.960	- 1.360	2.62	34.55	3.954

6.0048 mM $CoSO_4$ in 0.001% gelatin-Na_2SO_4 solutions.

[a] Evaluated at E = -1.586 V with respect to SCE.

[b] Flow-rate determined from Eq. (3.2.3-1), with h = 42.78 cm, to be 2.040 $mg \cdot sec^{-1}$.

APPENDIX II

The Diffusion Coefficients of Cd^{++} and Co^{++} at Zero Concentration of the Supporting Electrolyte as Functions of Concentrations at 20°C

TABLE 16

THE DIFFUSION COEFFICIENT OF Cd^{++} AT ZERO CONCENTRATION OF THE SUPPORTING ELECTROLYTE AS A FUNCTION OF CONCENTRATION AT 20°C

Concentration $\bar{C}_j$, mM	Diffusion Coefficient[a] $D_j \times 10^6$, $cm^2 sec^{-1}$	Concentration $\bar{C}_j$, mM	Diffusion Coefficient[b] $D_j \times 10^6$, $cm^2 sec^{-1}$
0.5003	6.195	0.5007	6.007
1.0006	6.093	1.0014	5.972
2.0012	6.358	2.0028	6.129
3.0018	6.417	3.0043	6.354
4.0024	6.461	4.0056	6.250
5.0030	5.410	5.0071	6.312
6.0036	6.455	6.0085	6.324

[a] At zero concentration of $NaNO_3$.

[b] At zero concentration of Na_2SO_4.

TABLE 17

THE DIFFUSION COEFFICIENT OF Co^{++} AT ZERO CONCENTRATION OF THE SUPPORTING ELECTROLYTE AS A FUNCTION OF CONCENTRATION AT 20°C

Concentration $\bar{C}_j$, mM	Diffusion Coefficient[a] $D_j \times 10^6$, $cm^2 sec^{-1}$	Concentration $\bar{C}_j$, mM	Diffusion Coefficient[b] $D_j \times 10^6$, $cm^2 sec^{-1}$
0.5017	6.063	0.5004	6.461
1.0034	6.074	1.0008	6.465
2.0068	6.134	2.0016	6.603
3.0102	6.146	3.0024	6.872
4.0136	6.334	4.0032	6.765
5.0170	6.276	5.0040	6.798
6.0204	5.970	6.0048	6.891

[a] At zero concentration of $NaNO_3$.

[b] At zero concentration of Na_2SO_4.

APPENDIX III

Graphs of the Apparent Diffusion Coefficients as Functions of the Concentrations of the Supporting Electrolytes at 20°C

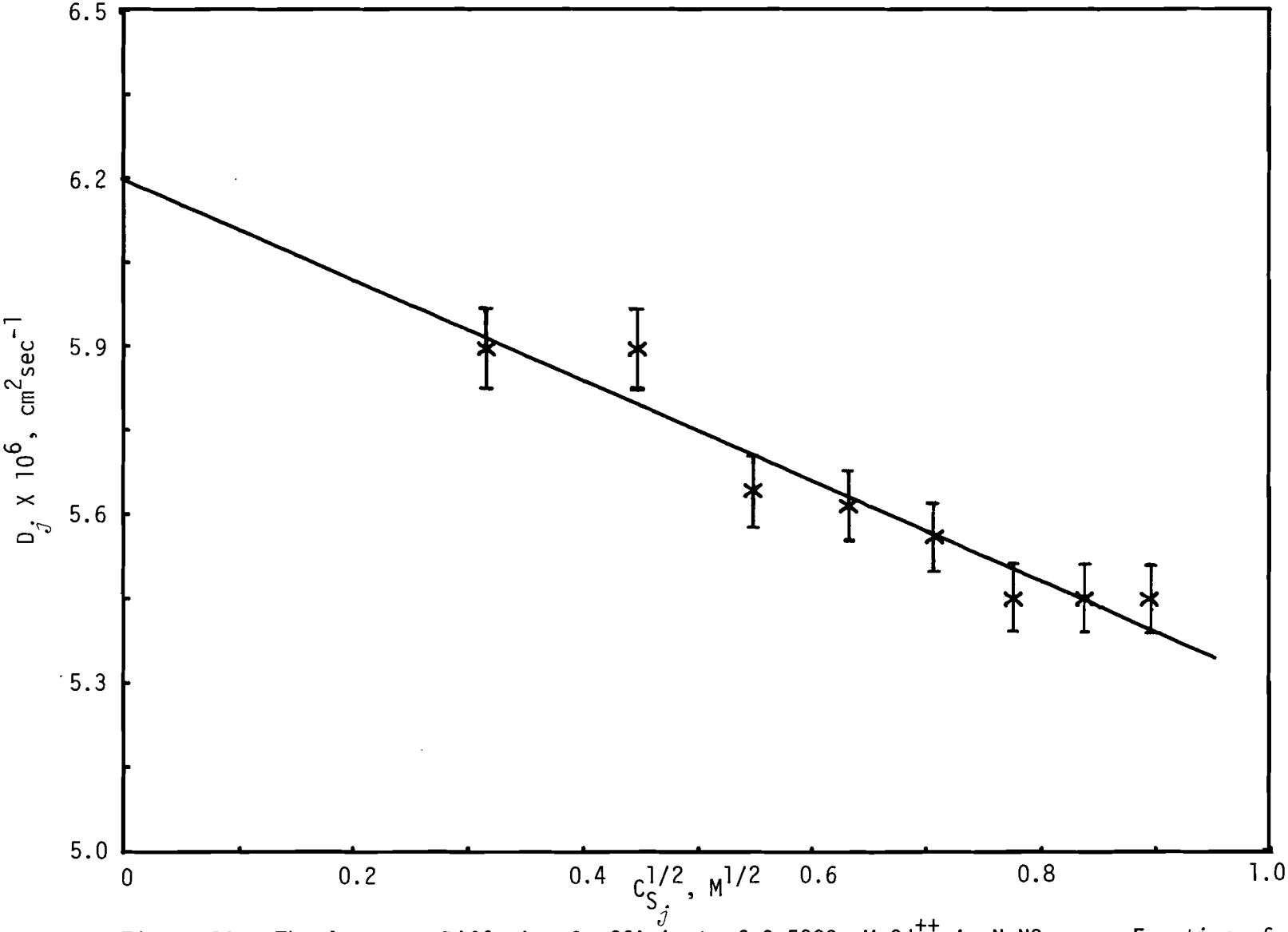

Figure 13. The Apparent Diffusion Coefficient of 0.5003 mM Cd^{++} in $NaNO_3$ as a Function of Concentration at 20°C.

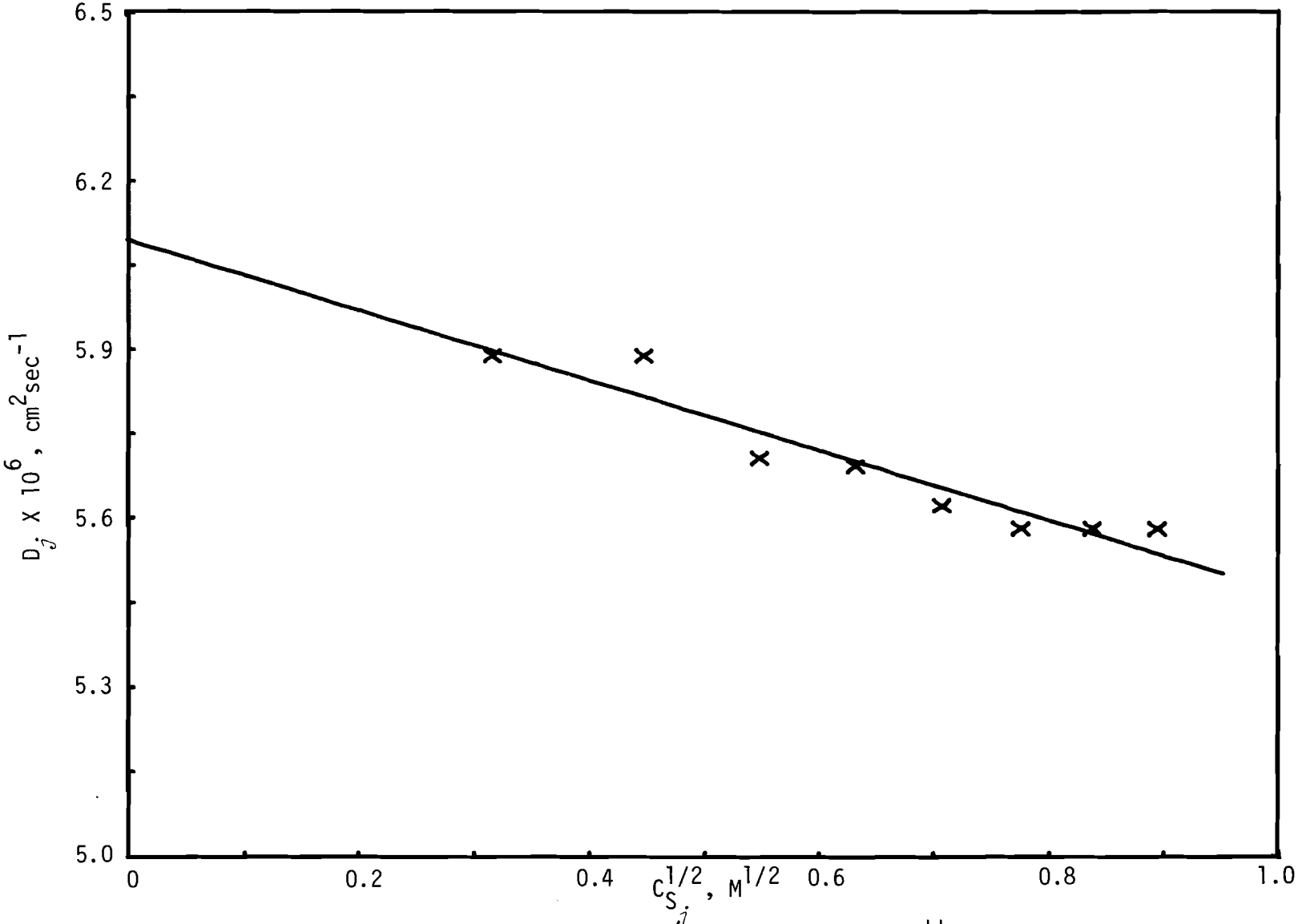

Figure 14. The Apparent Diffusion Coefficient of 1.0006 mM Cd^{++} in $NaNO_3$ as a Function of Concentration at 20°C.

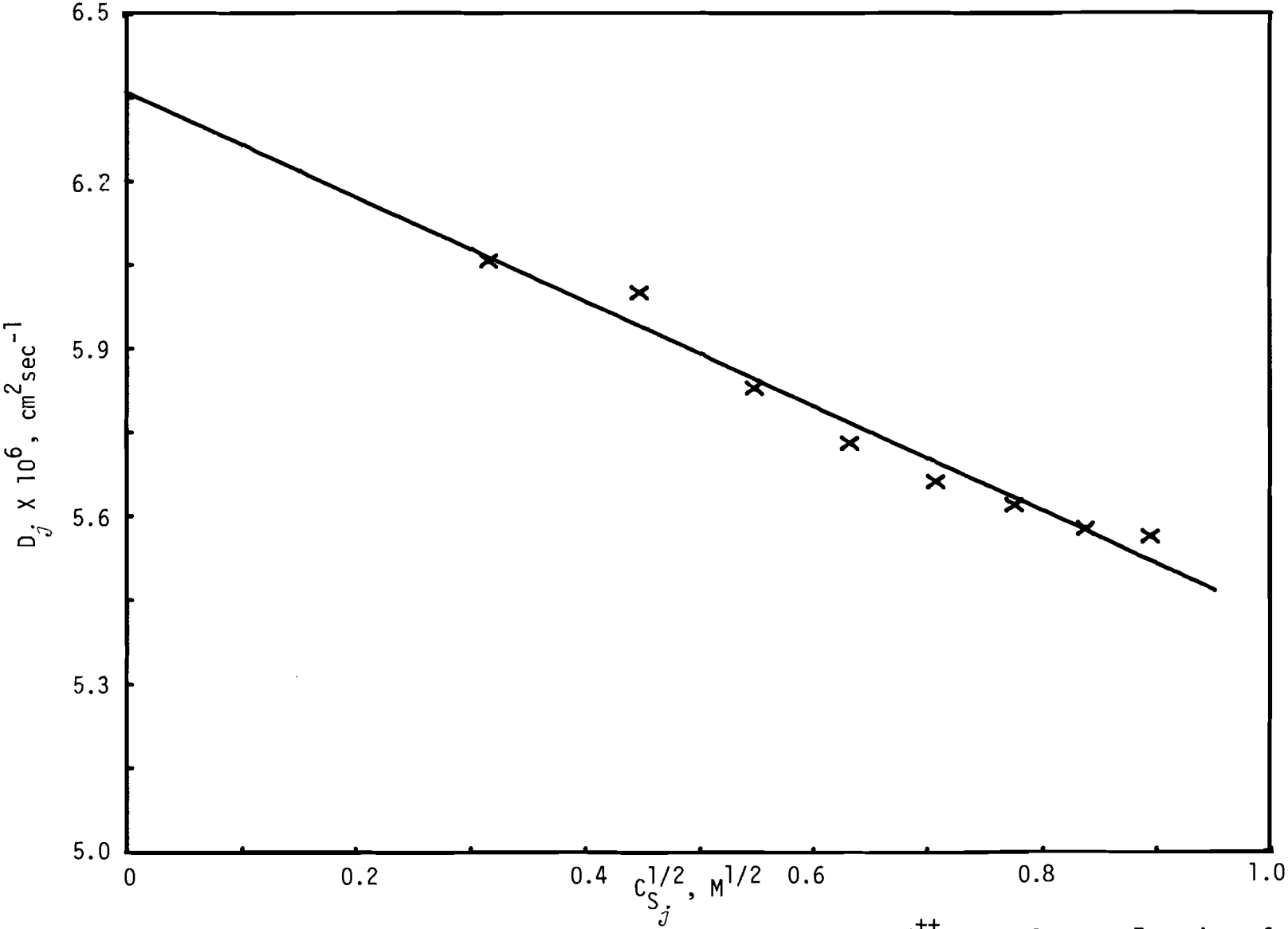

Figure 15. The Apparent Diffusion Coefficient of 2.0012 mM Cd^{++} in $NaNO_3$ as a Function of Concentration at 20°C.

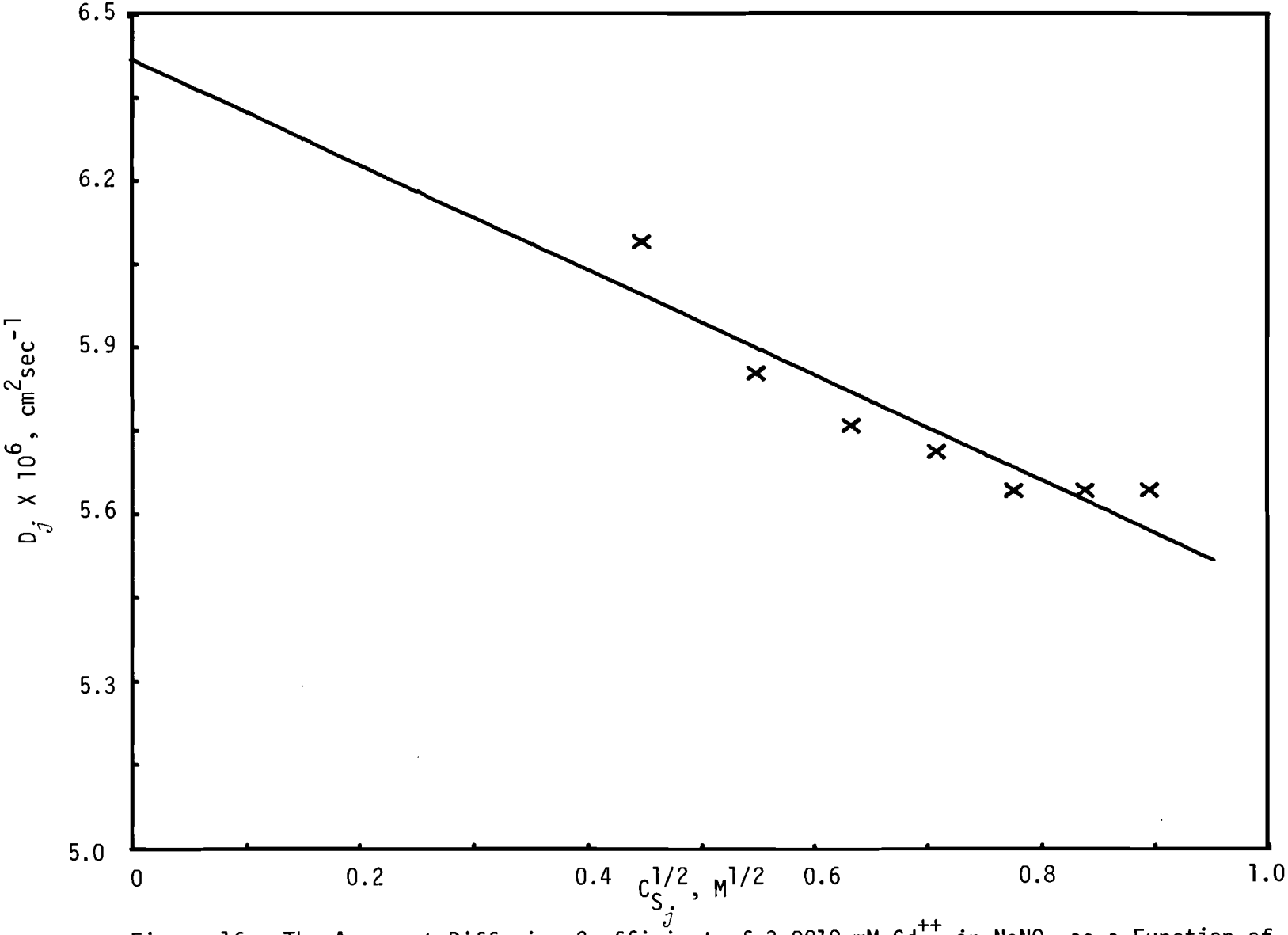

Figure 16. The Apparent Diffusion Coefficient of 3.0018 mM Cd^{++} in $NaNO_3$ as a Function of Concentration at 20°C.

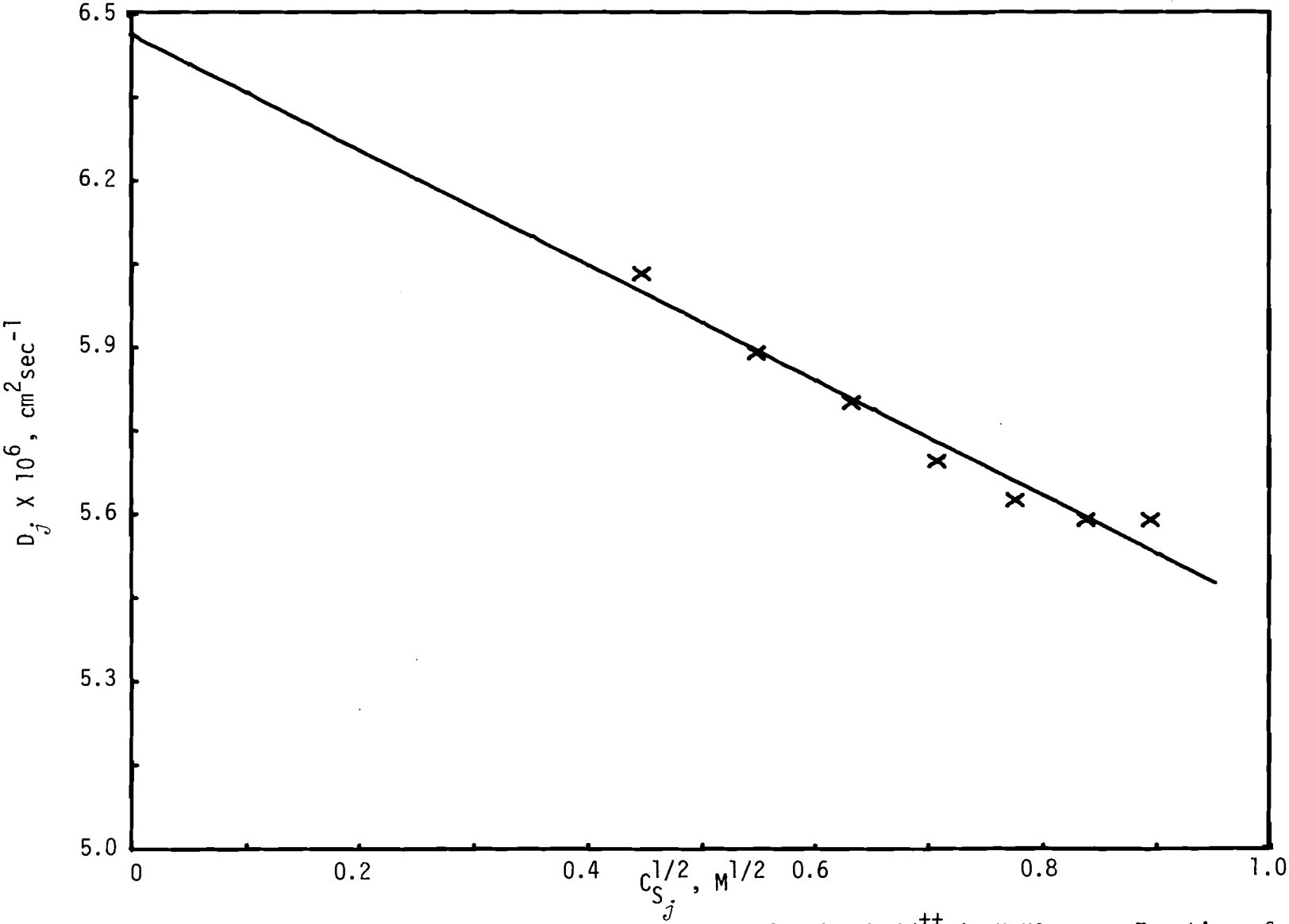

Figure 17. The Apparent Diffusion Coefficient of 4.0024 mM Cd^{++} in $NaNO_3$ as a Function of Concentration at 20°C.

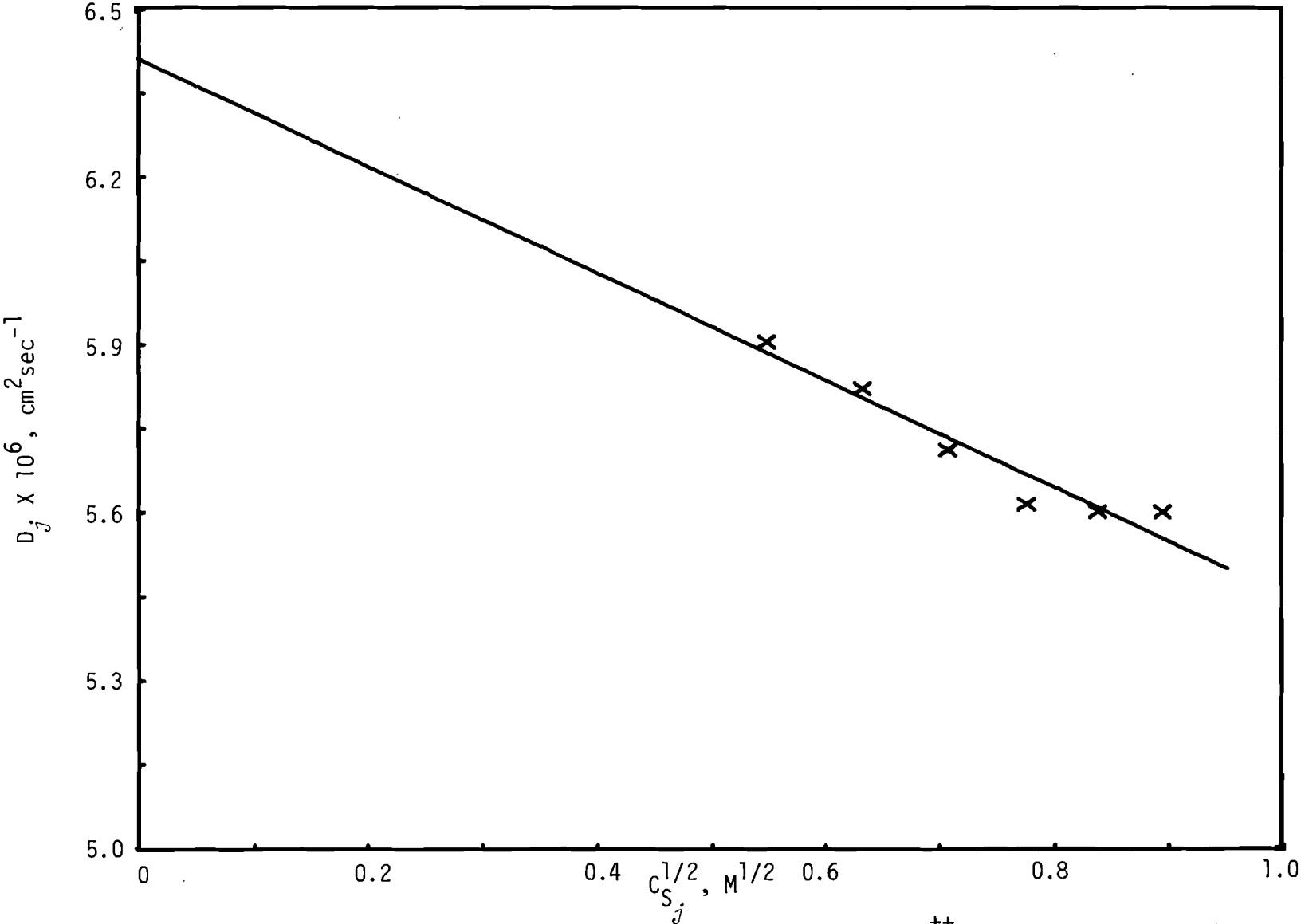

Figure 18. The Apparent Diffusion Coefficient of 5.0030 mM Cd^{++} in $NaNO_3$ as a Function of Concentration at 20°C.

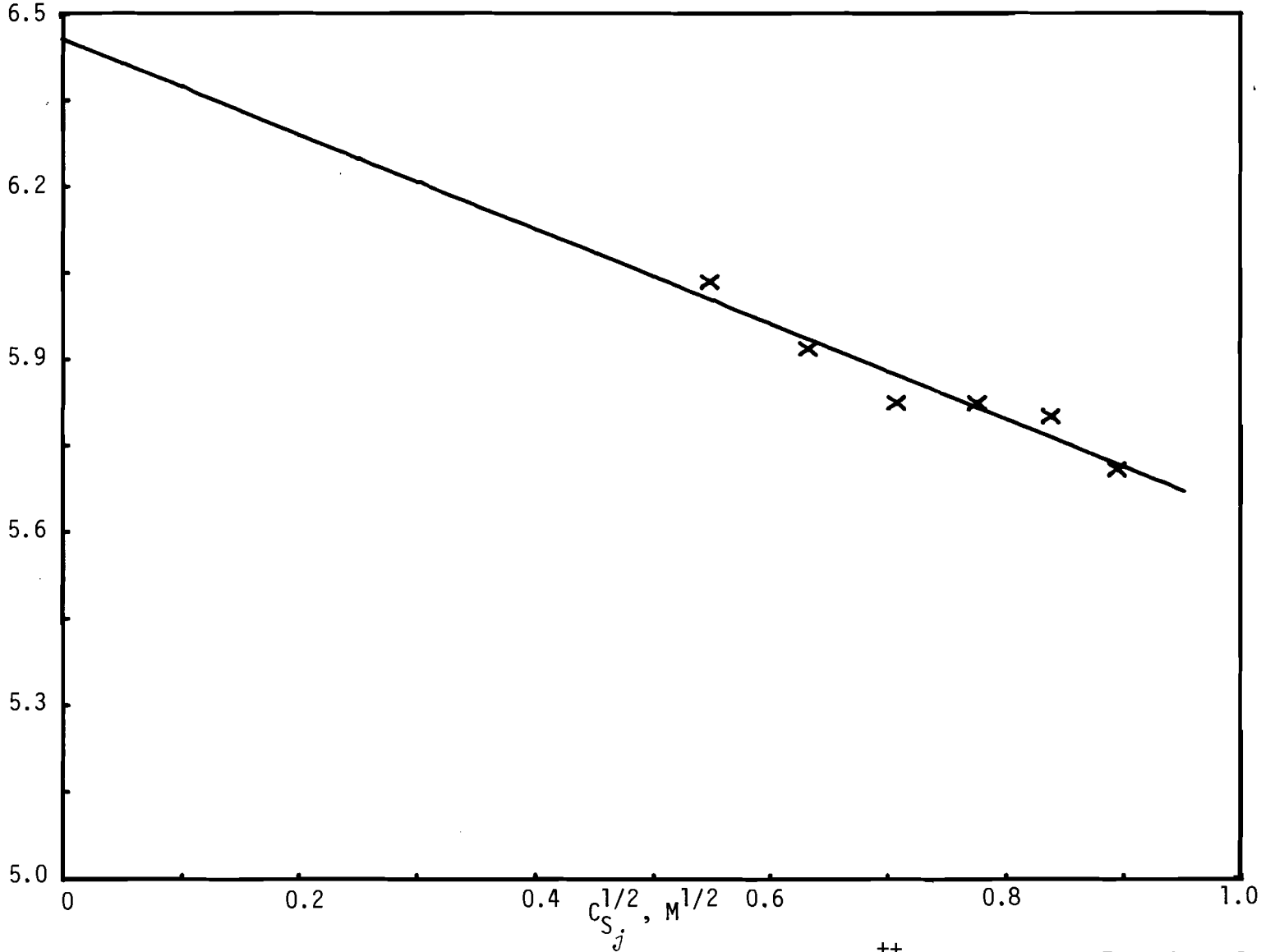

Figure 19. The Apparent Diffusion Coefficient of 6.0036 mM Cd^{++} in $NaNO_3$ as a Function of Concentration at 20°C.

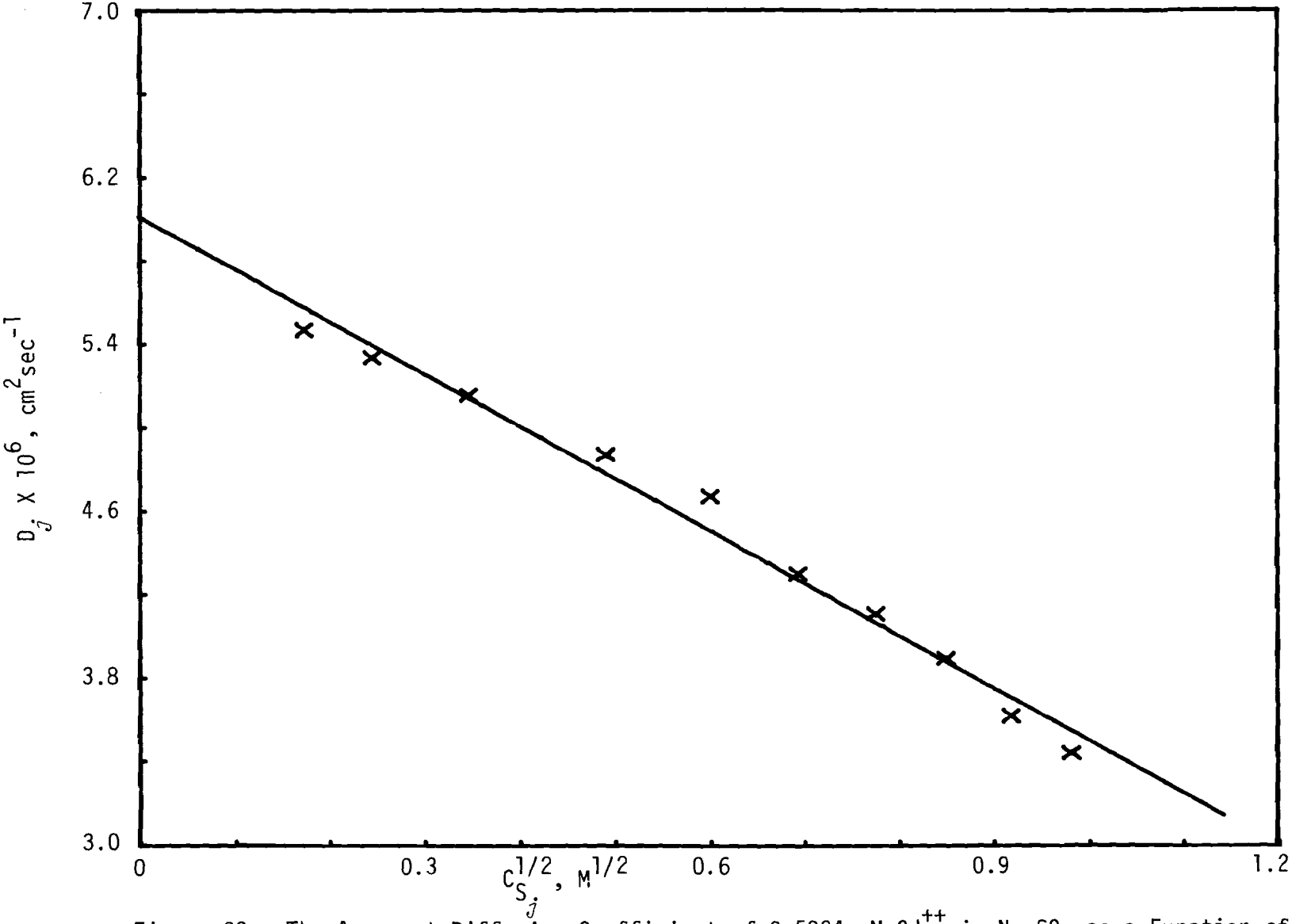

Figure 20. The Apparent Diffusion Coefficient of 0.5004 mM Cd^{++} in Na_2SO_4 as a Function of Concentration at 20°C.

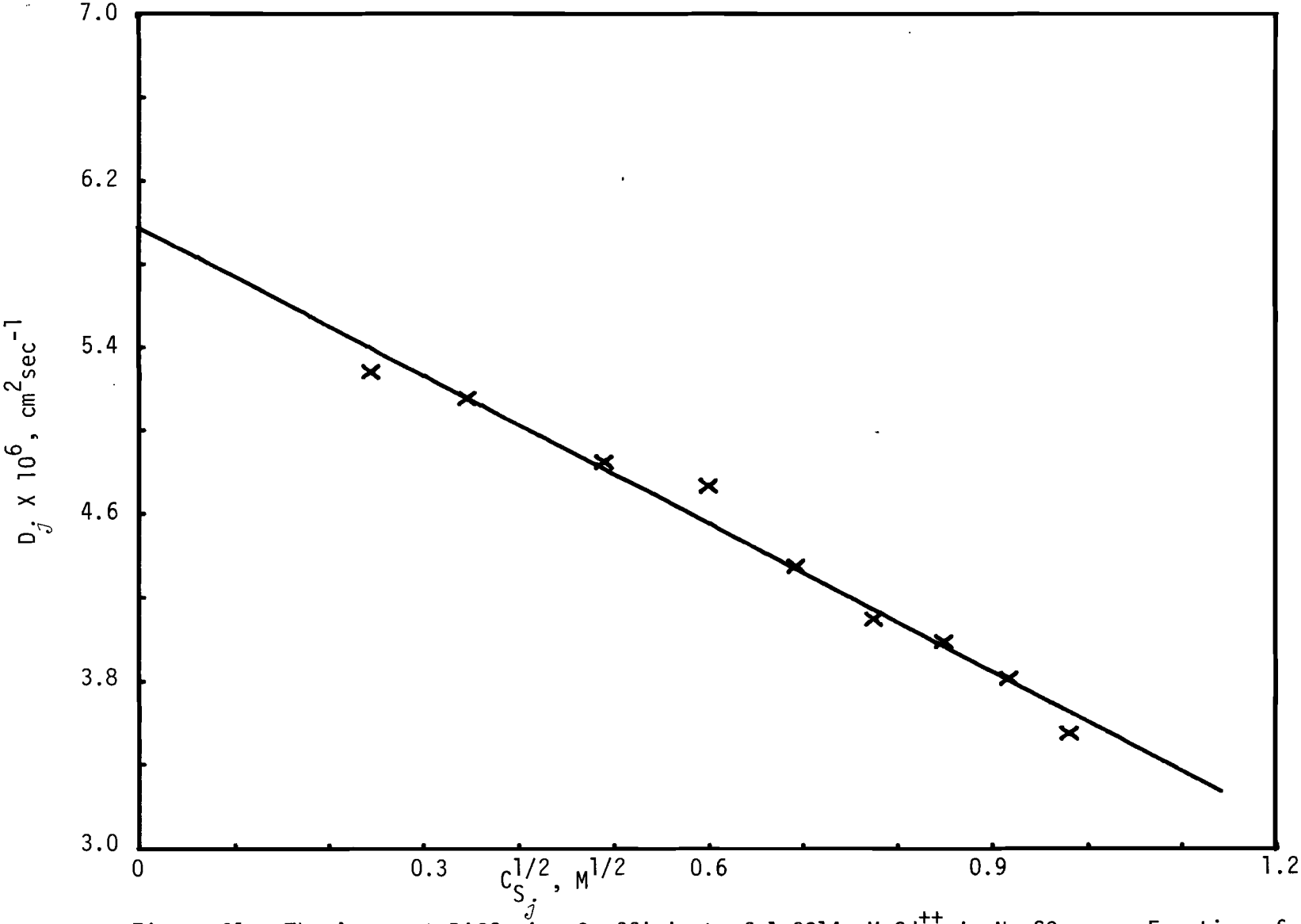

Figure 21. The Apparent Diffusion Coefficient of 1.0014 mM Cd^{++} in Na_2SO_4 as a Function of Concentration at 20°C.

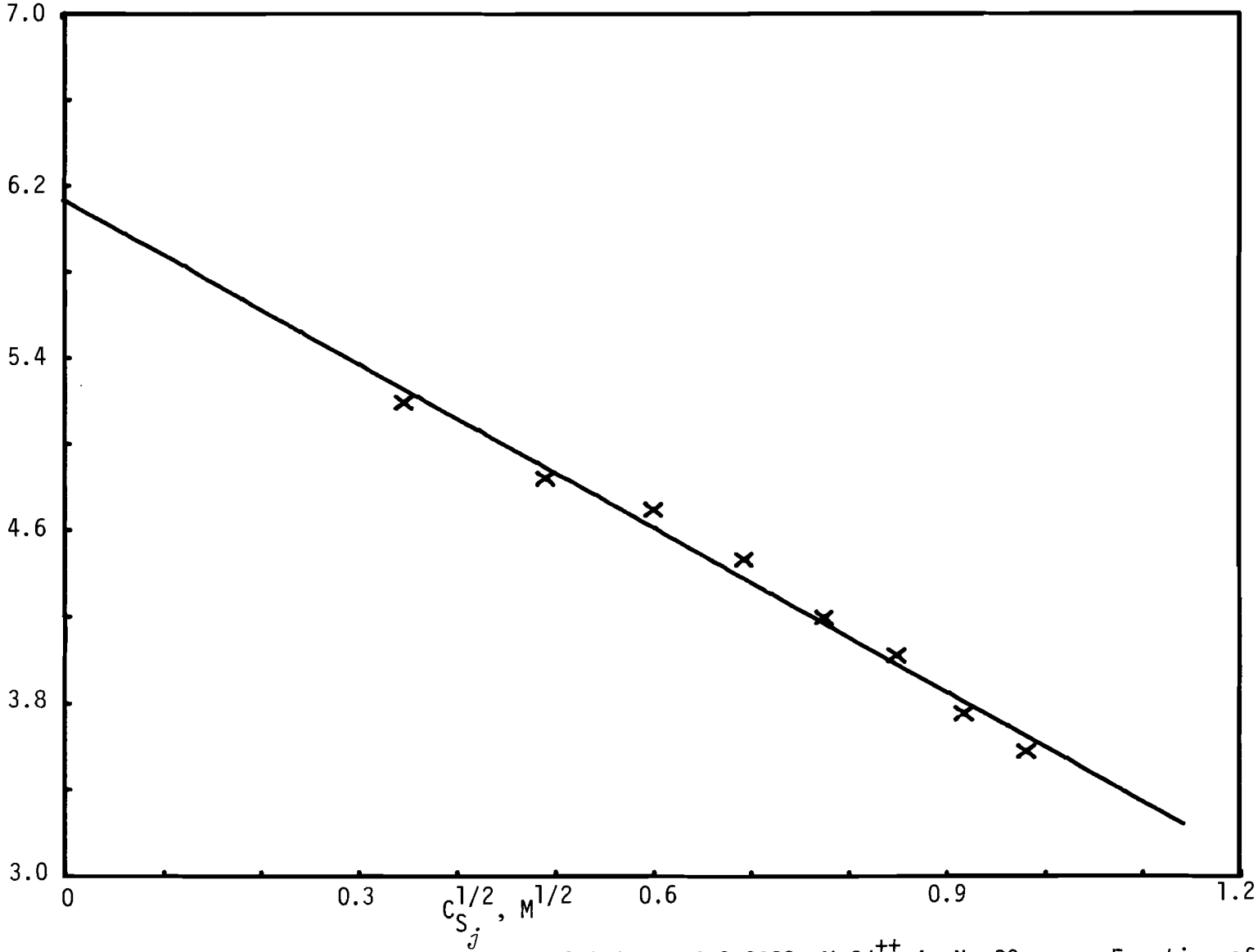

Figure 22. The Apparent Diffusion Coefficient of 2.0028 mM Cd^{++} in Na_2SO_4 as a Function of Concentration at 20°C.

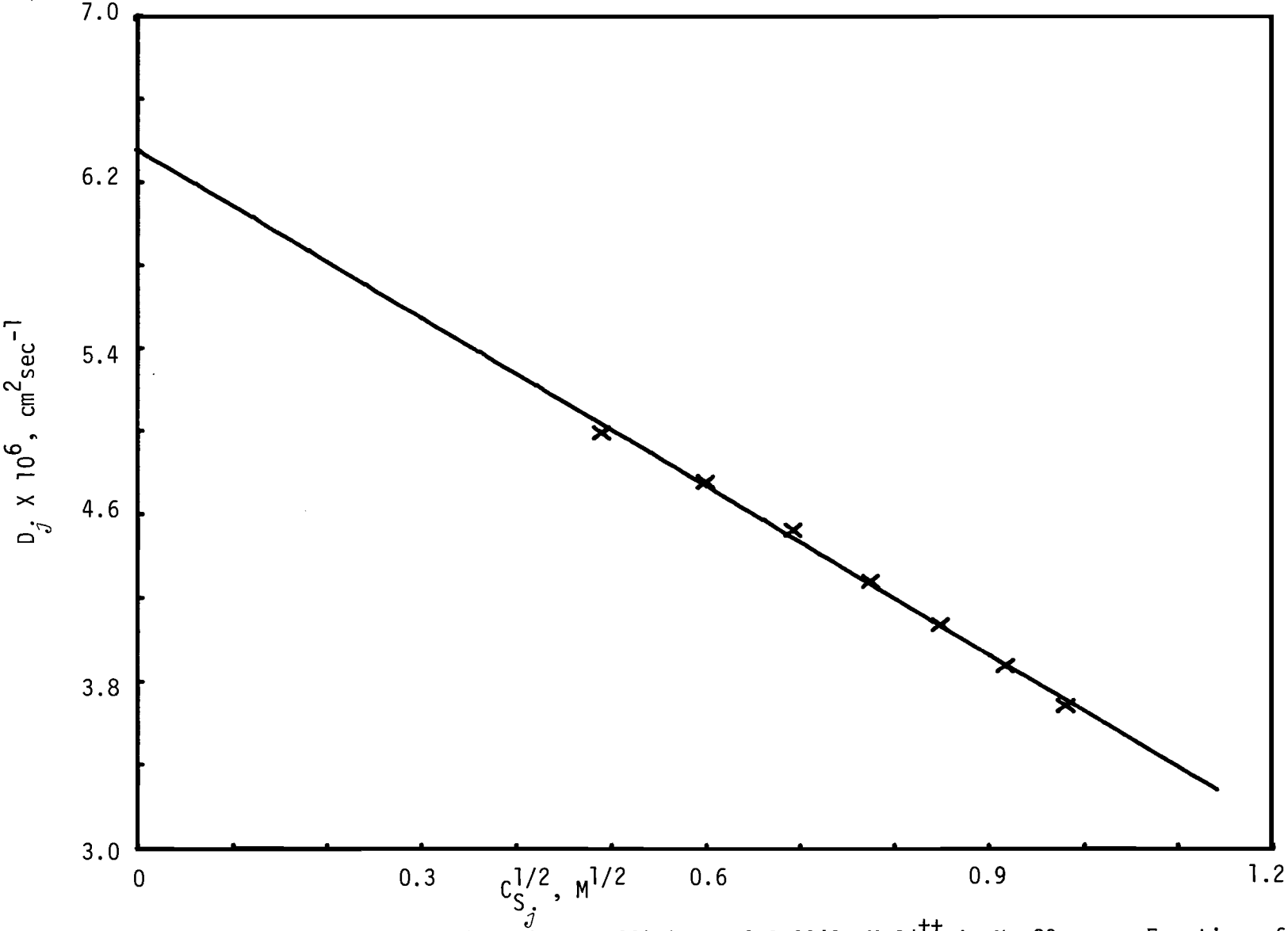

Figure 23. The Apparent Diffusion Coefficient of 3.0043 mM Cd^{++} in Na_2SO_4 as a Function of Concentration at 20°C.

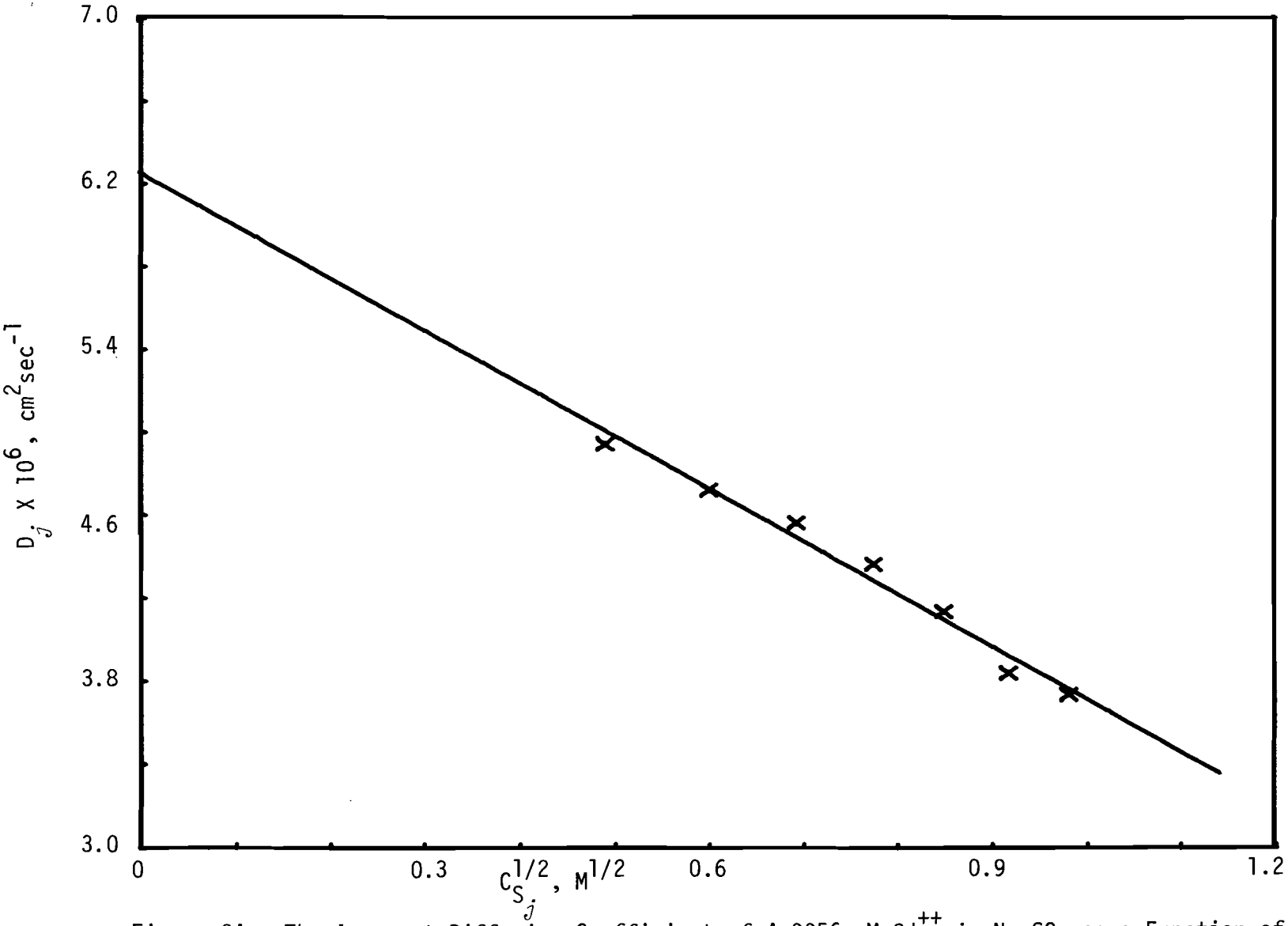

Figure 24. The Apparent Diffusion Coefficient of 4.0056 mM Cd^{++} in Na_2SO_4 as a Function of Concentration at 20°C.

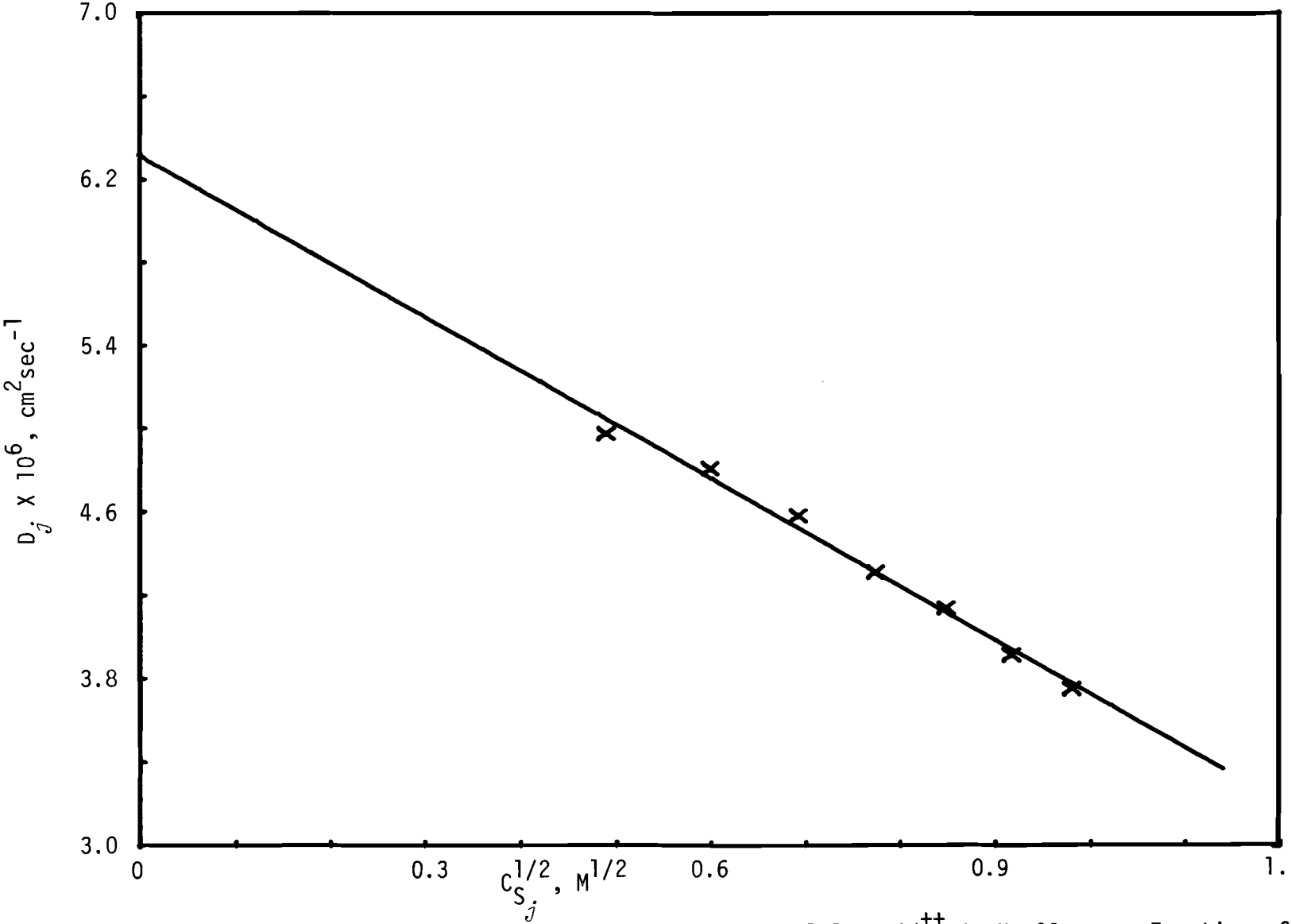

Figure 25. The Apparent Diffusion Coefficient of 5.0171 mM Cd^{++} in Na_2SO_4 as a Function of Concentration at 20°C.

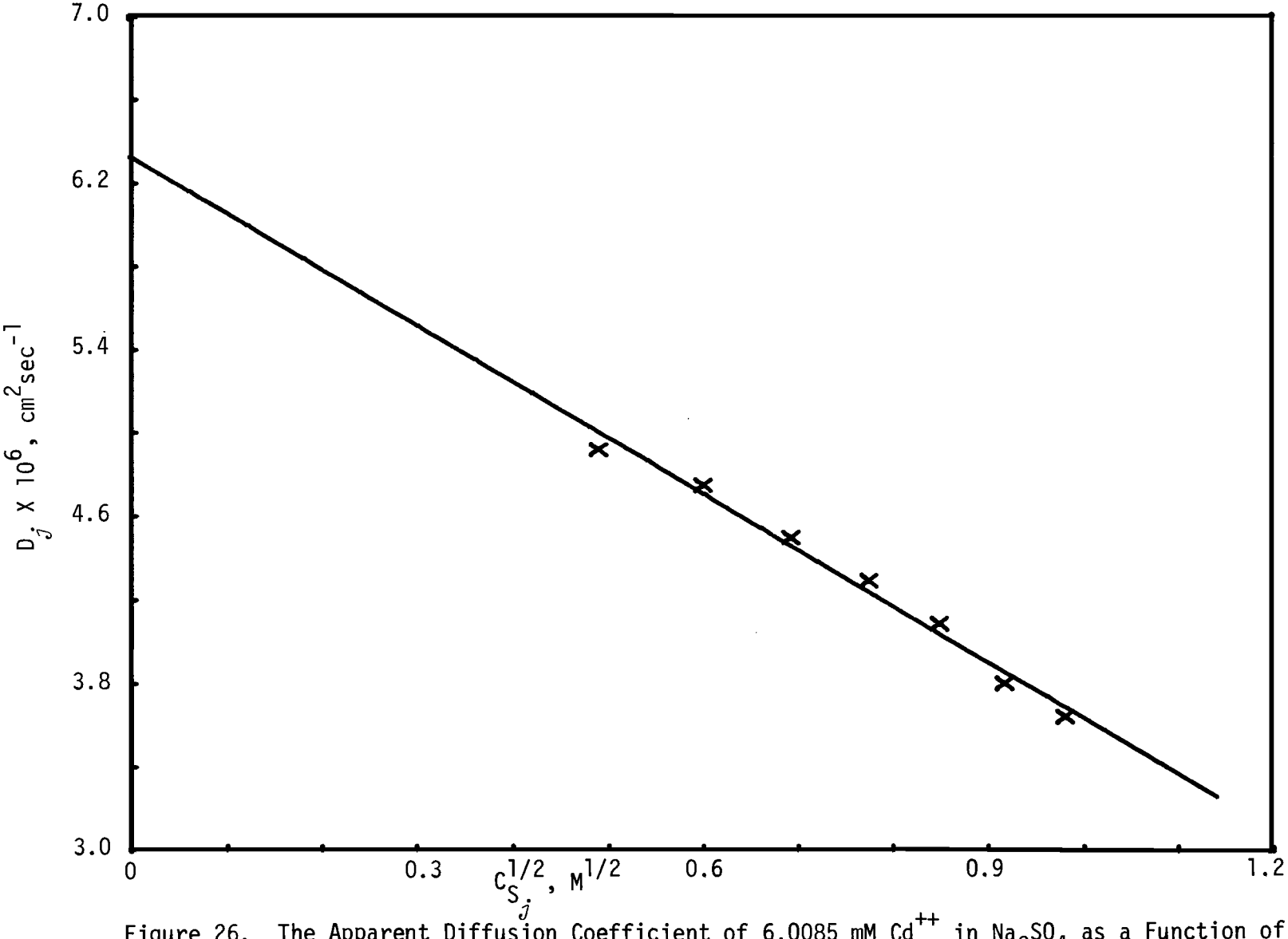

Figure 26. The Apparent Diffusion Coefficient of 6.0085 mM Cd^{++} in Na_2SO_4 as a Function of Concentration at 20°C.

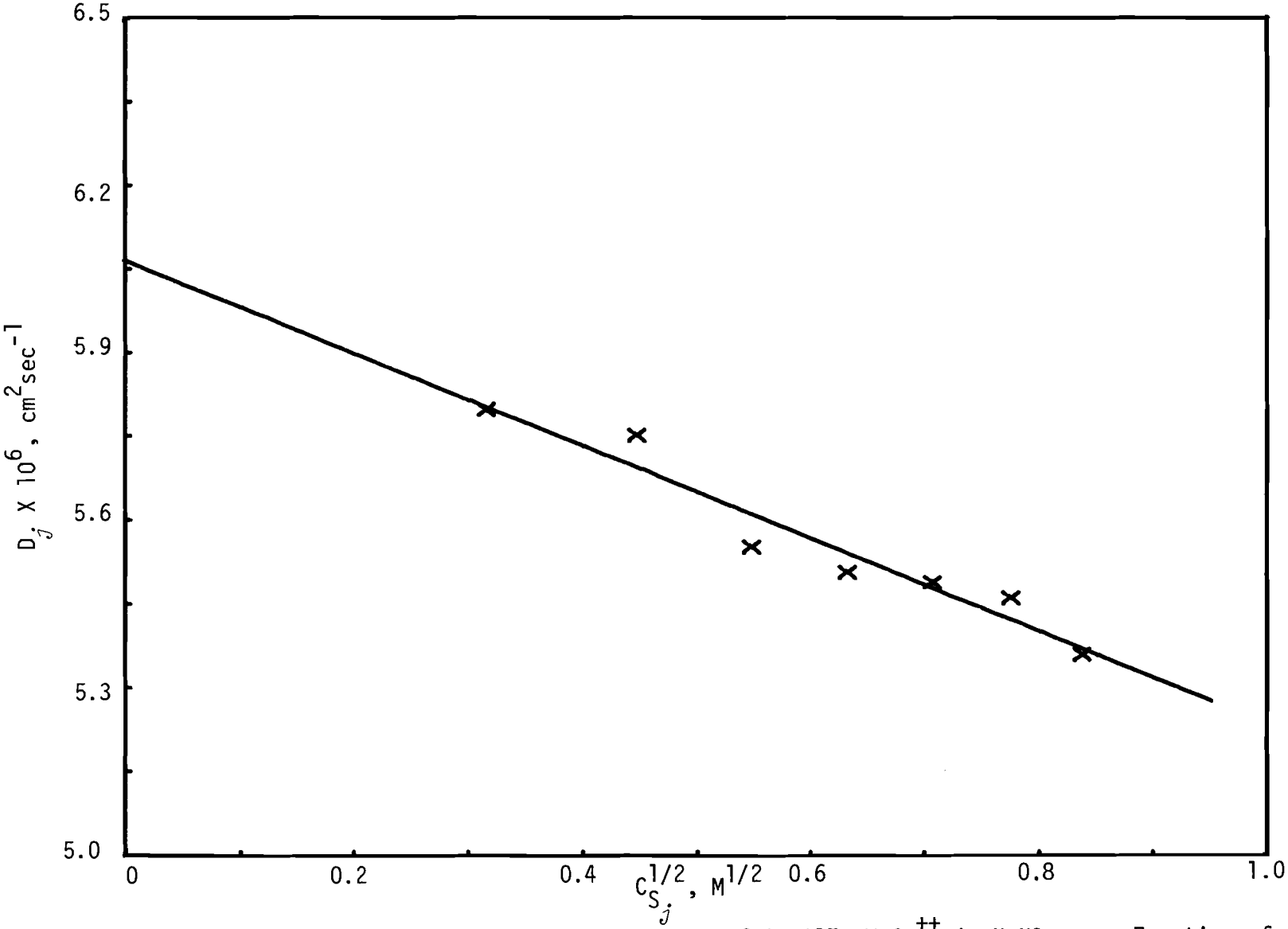

Figure 27. The Apparent Diffusion Coefficient of 0.5017 mM Co^{++} in $NaNO_3$ as a Function of Concentration at 20°C.

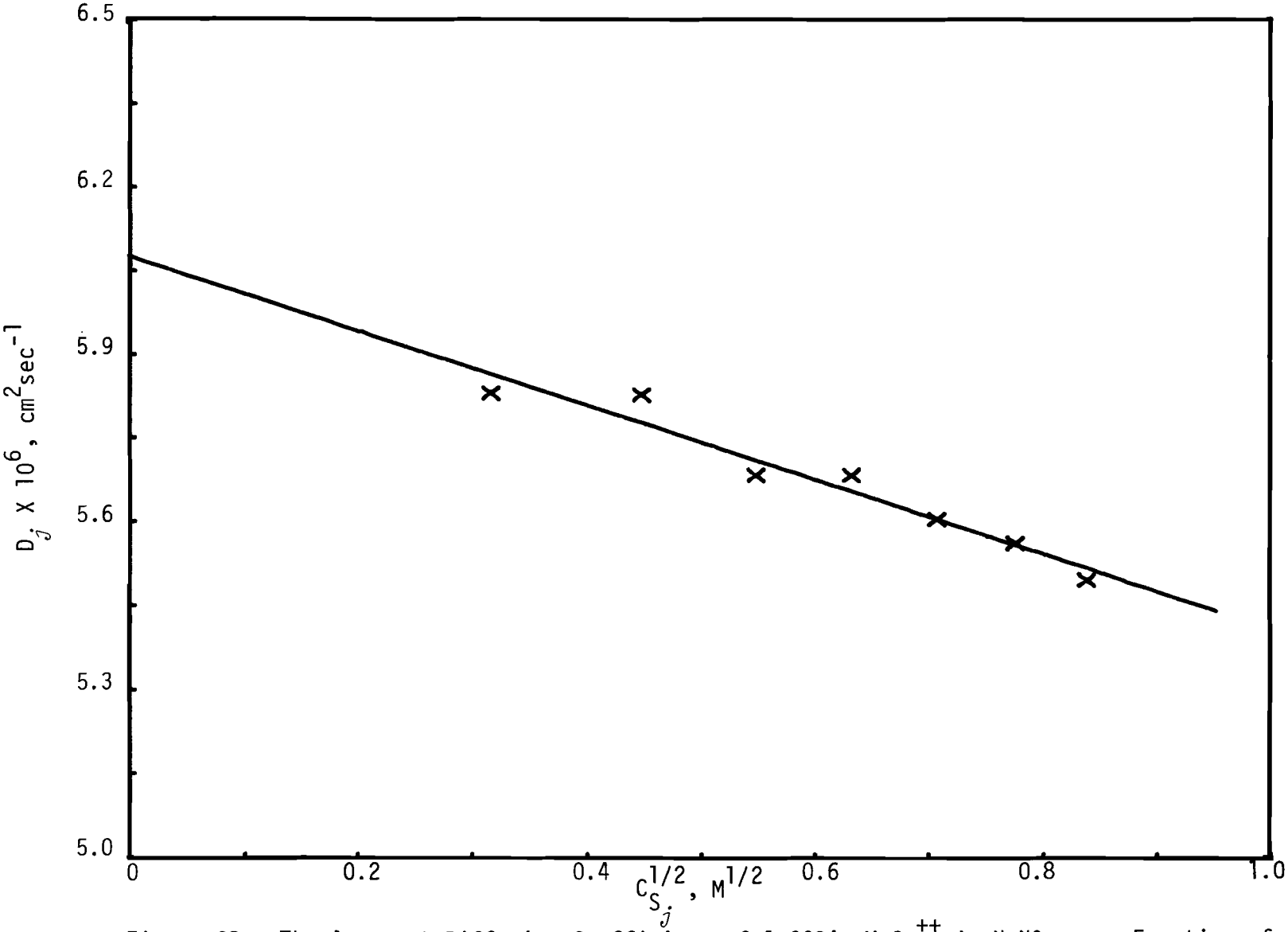

Figure 28. The Apparent Diffusion Coefficient of 1.0034 mM Co^{++} in $NaNO_3$ as a Function of Concentration at 20°C.

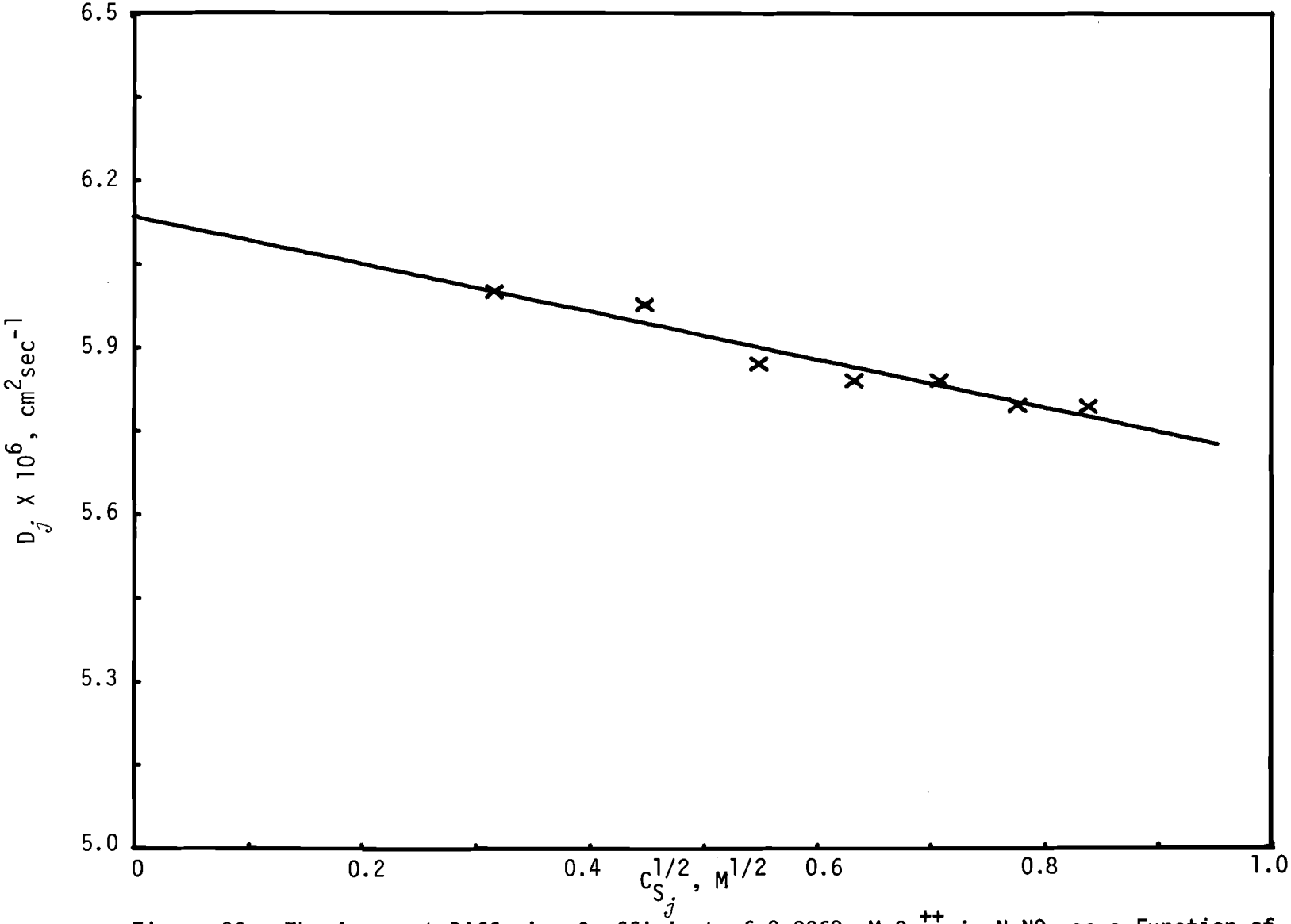

Figure 29. The Apparent Diffusion Coefficient of 2.0068 mM Co^{++} in $NaNO_3$ as a Function of Concentration at 20°C.

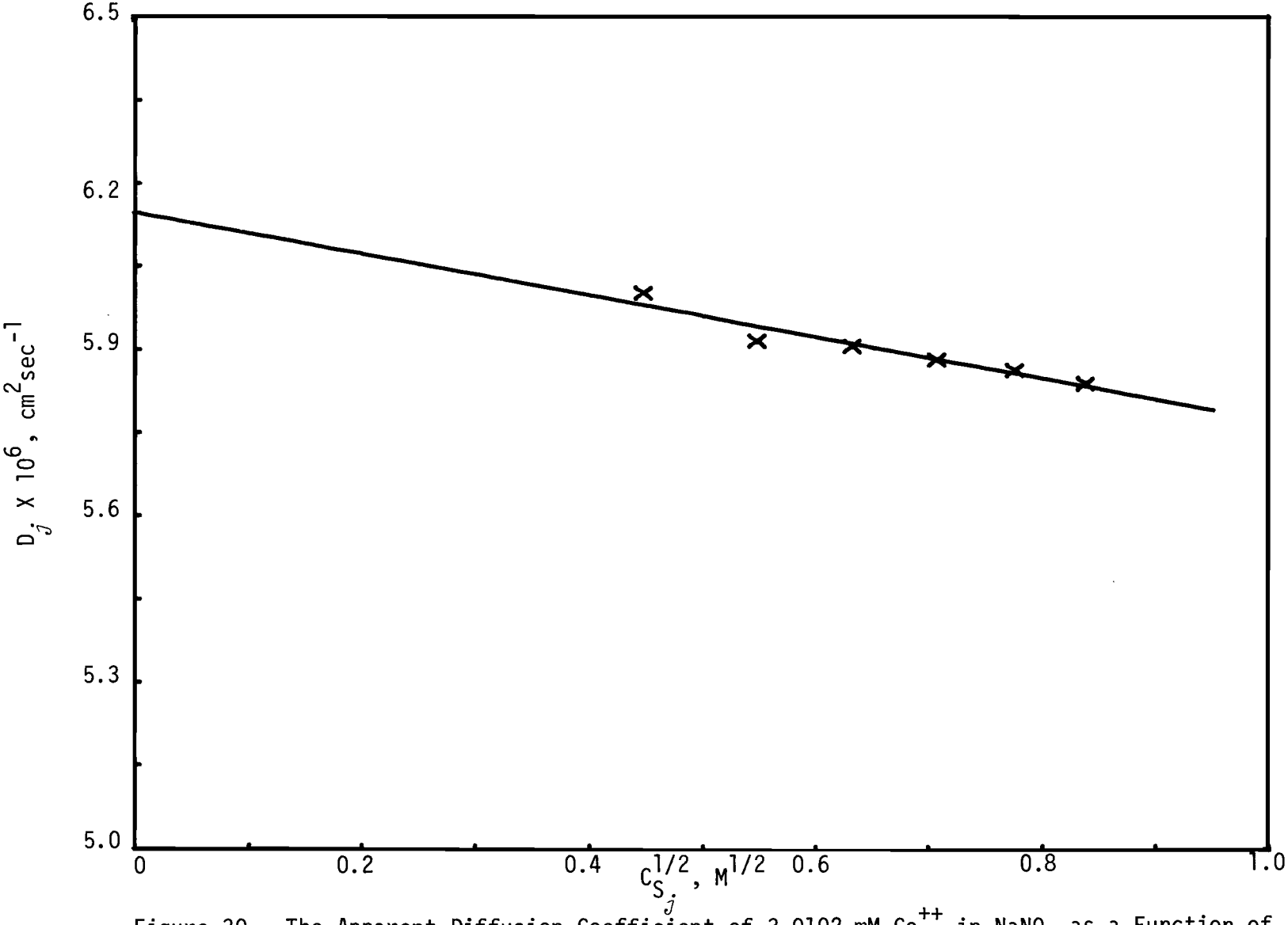

Figure 30. The Apparent Diffusion Coefficient of 3.0102 mM Co^{++} in $NaNO_3$ as a Function of Concentration at 20°C.

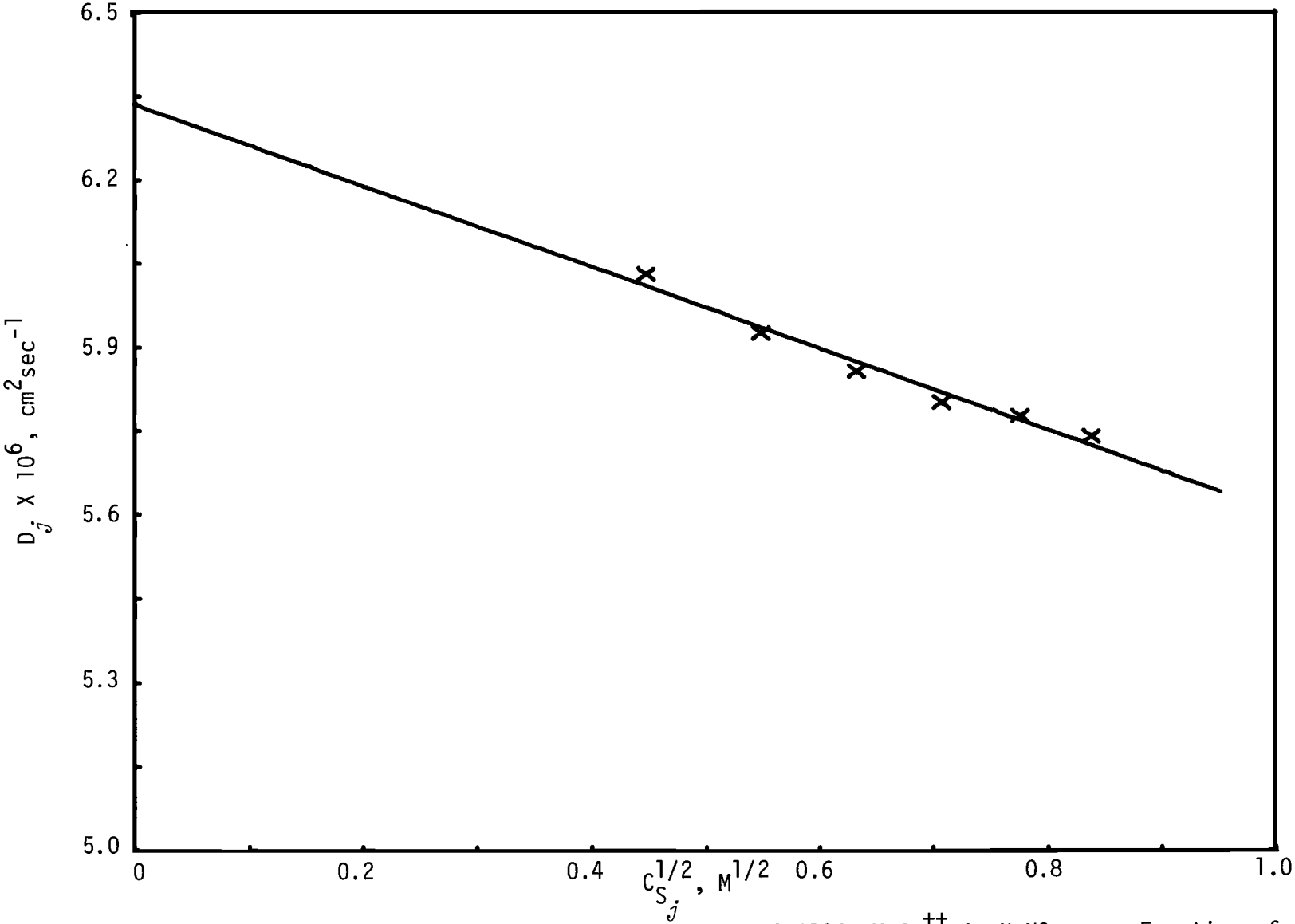

Figure 31. The Apparent Diffusion Coefficient of 4.0136 mM Co^{++} in $NaNO_3$ as a Function of Concentration at 20°C.

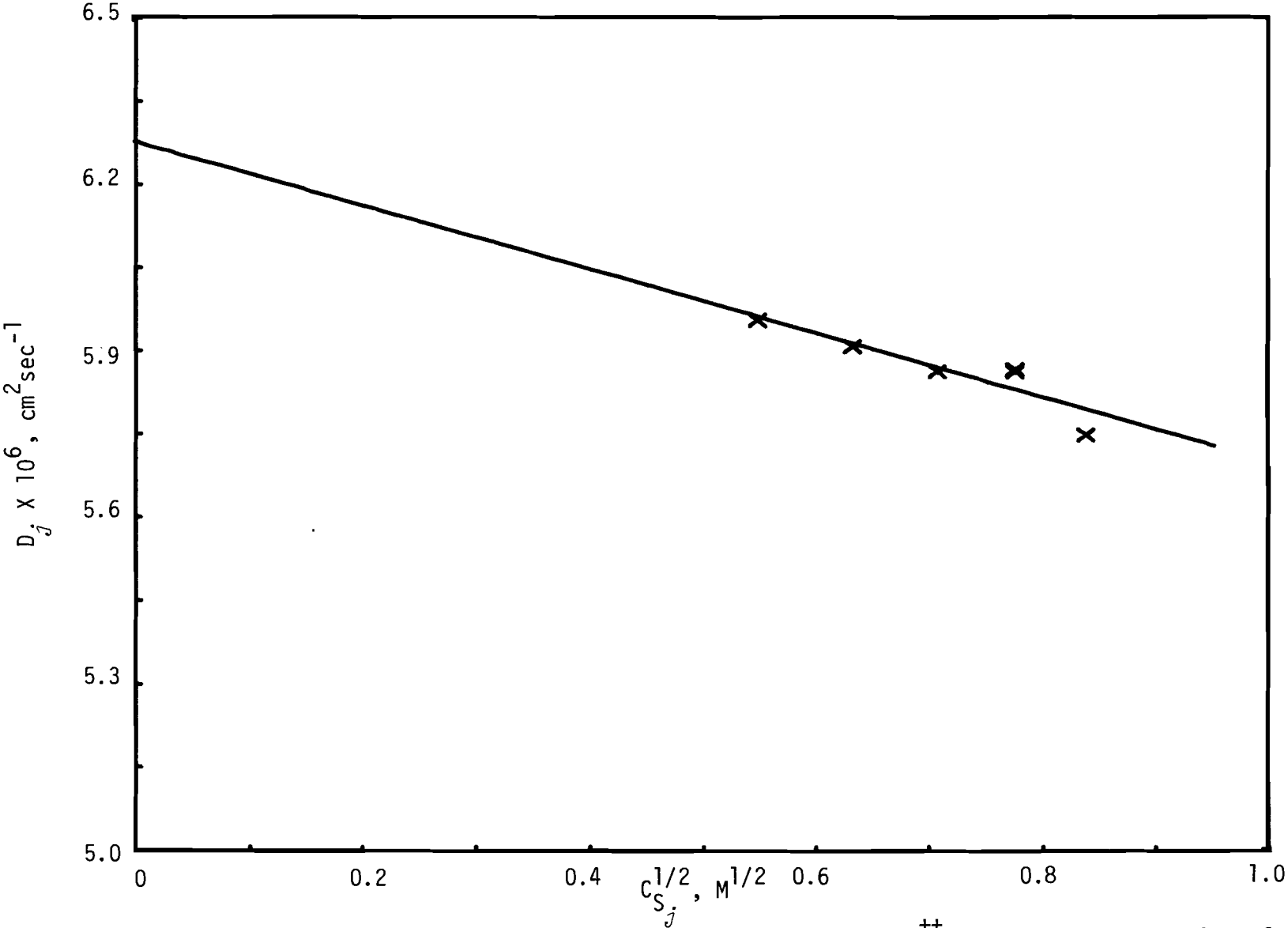

Figure 32. The Apparent Diffusion Coefficient of 5.0170 mM Co^{++} in $NaNO_3$ as a Function of Concentration at 20°C.

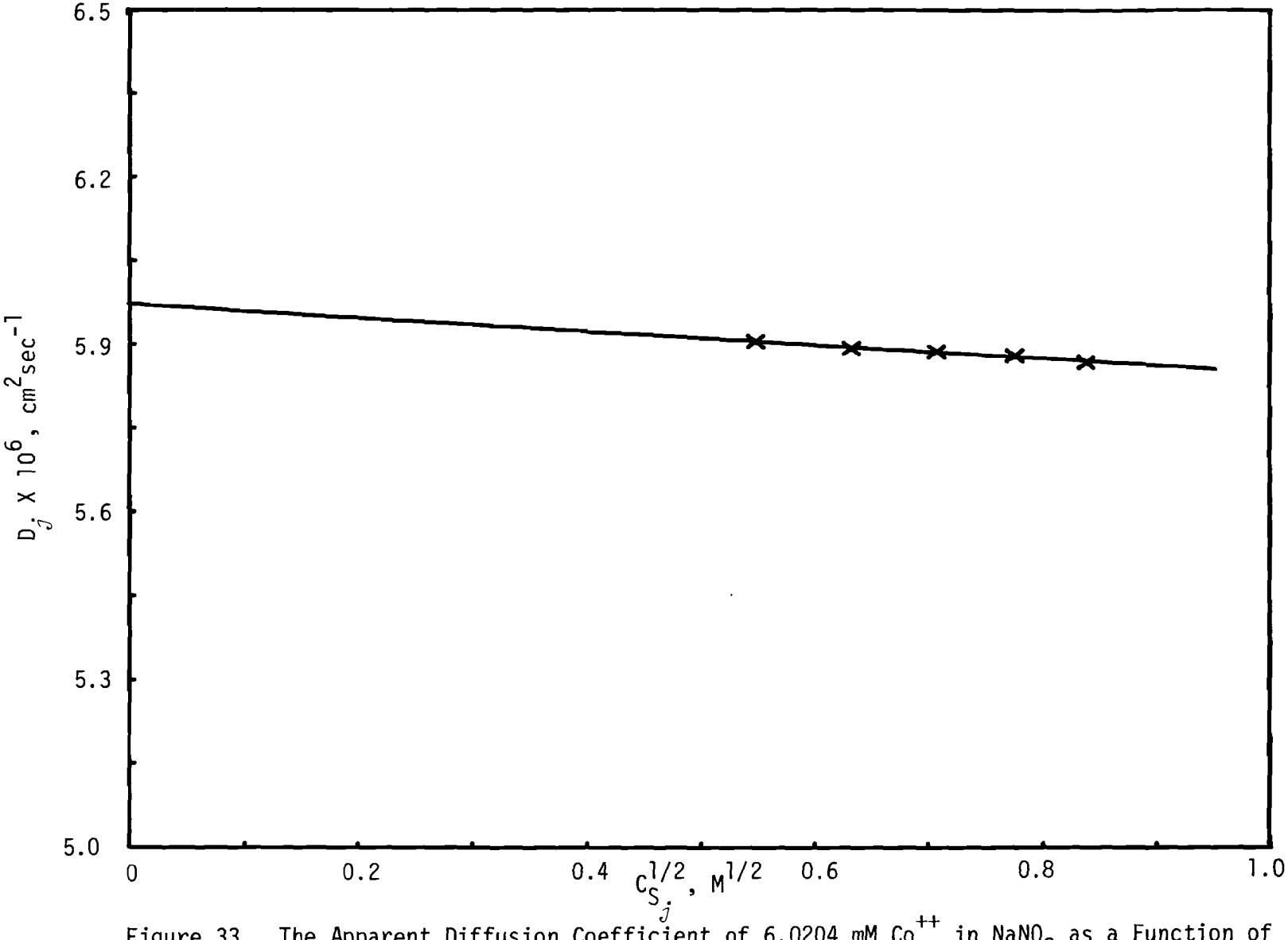

Figure 33. The Apparent Diffusion Coefficient of 6.0204 mM Co^{++} in $NaNO_3$ as a Function of Concentration at 20°C.

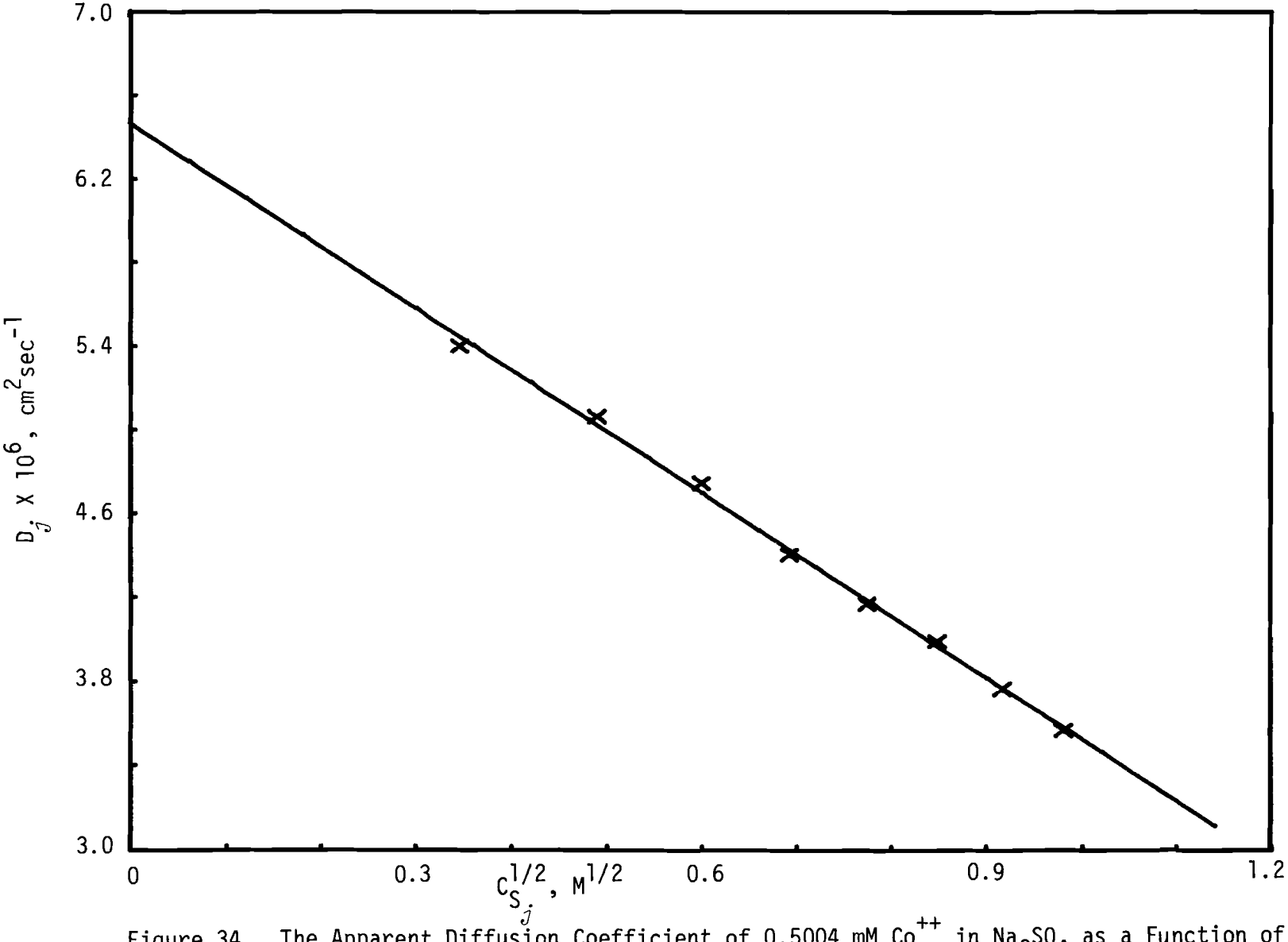

Figure 34. The Apparent Diffusion Coefficient of 0.5004 mM Co^{++} in Na_2SO_4 as a Function of Concentration at 20°C.

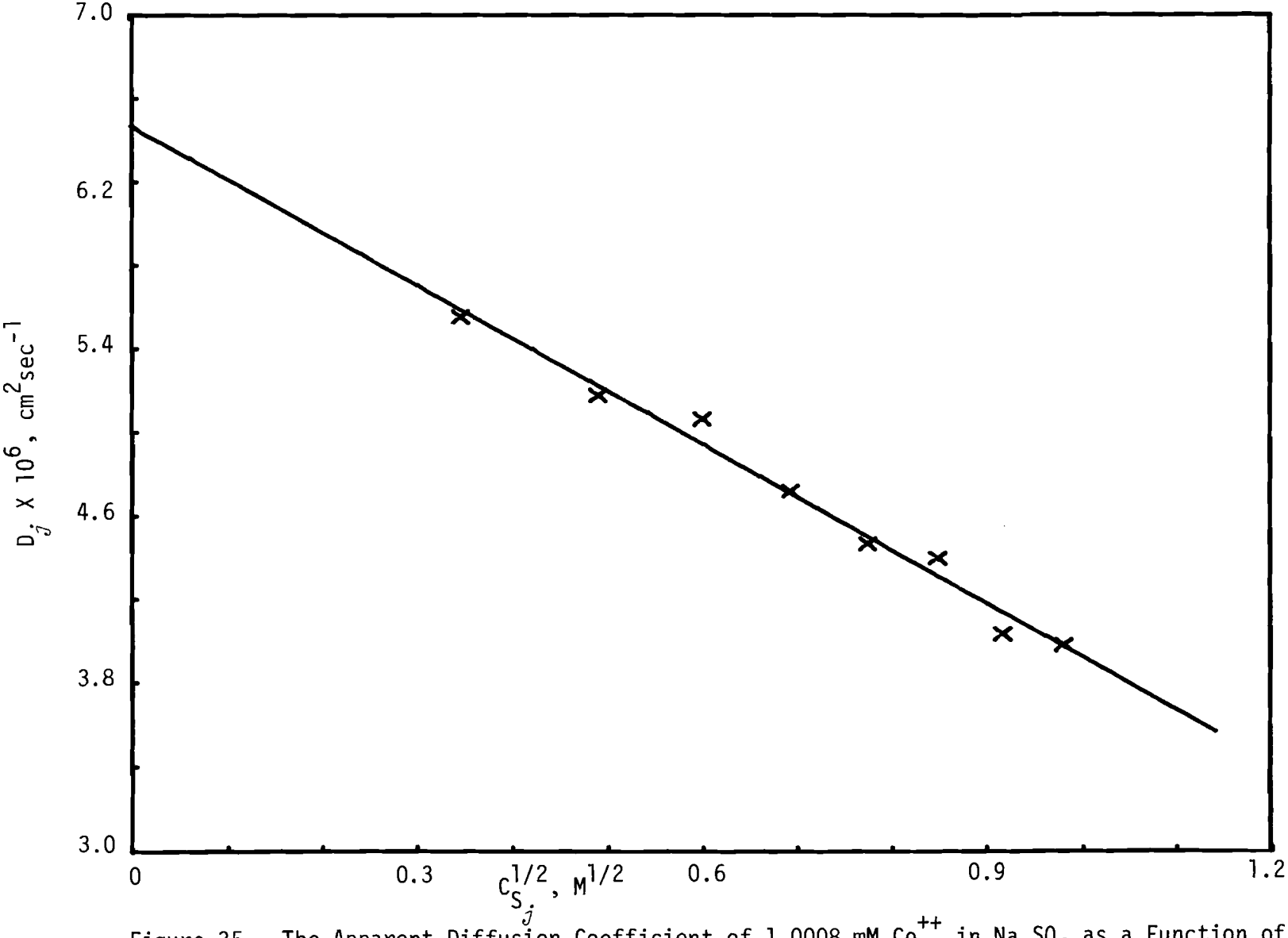

Figure 35. The Apparent Diffusion Coefficient of 1.0008 mM Co^{++} in Na_2SO_4 as a Function of Concentration at 20°C.

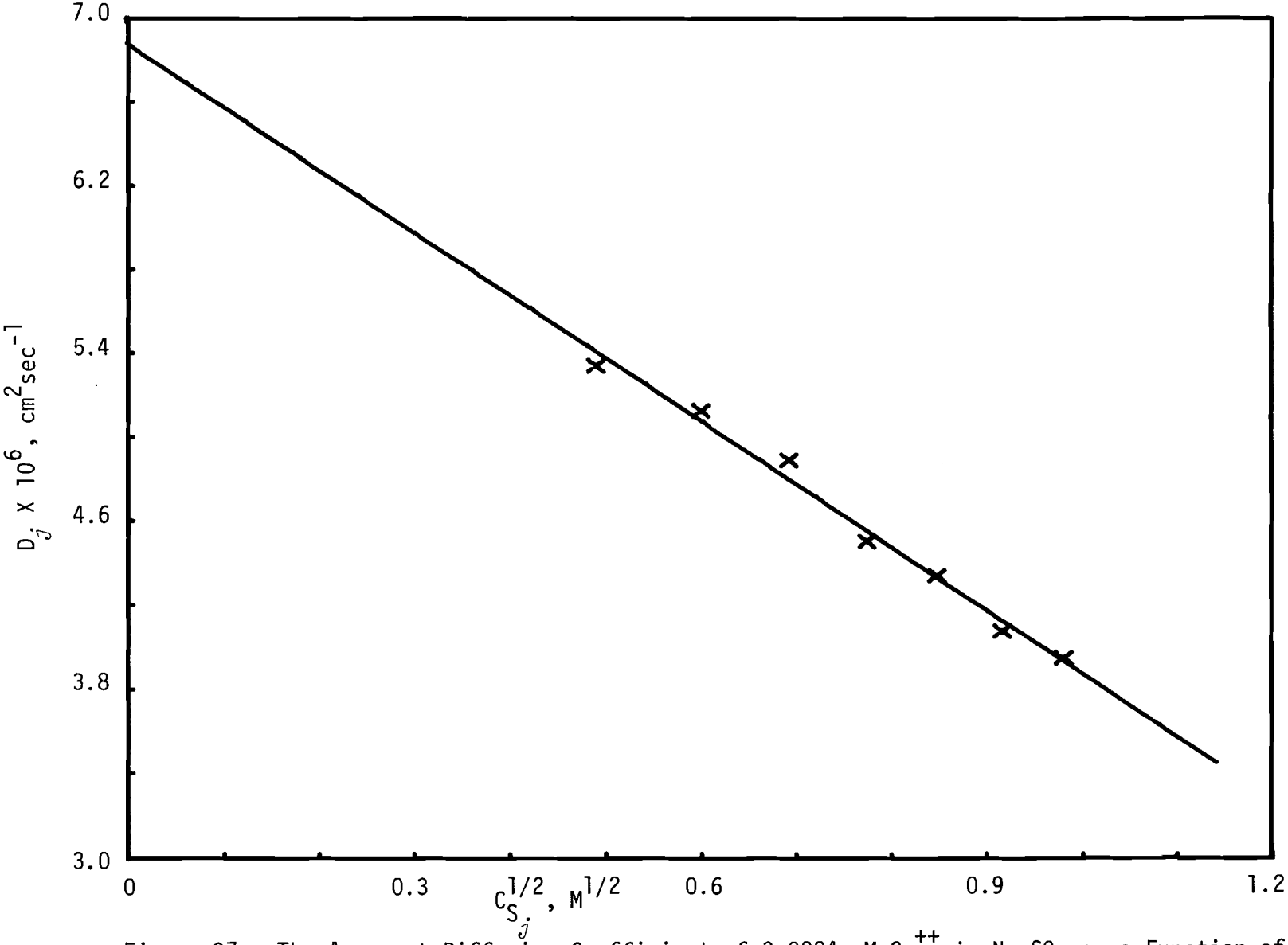

Figure 37. The Apparent Diffusion Coefficient of 3.0024 mM Co^{++} in Na_2SO_4 as a Function of Concentration at 20°C.

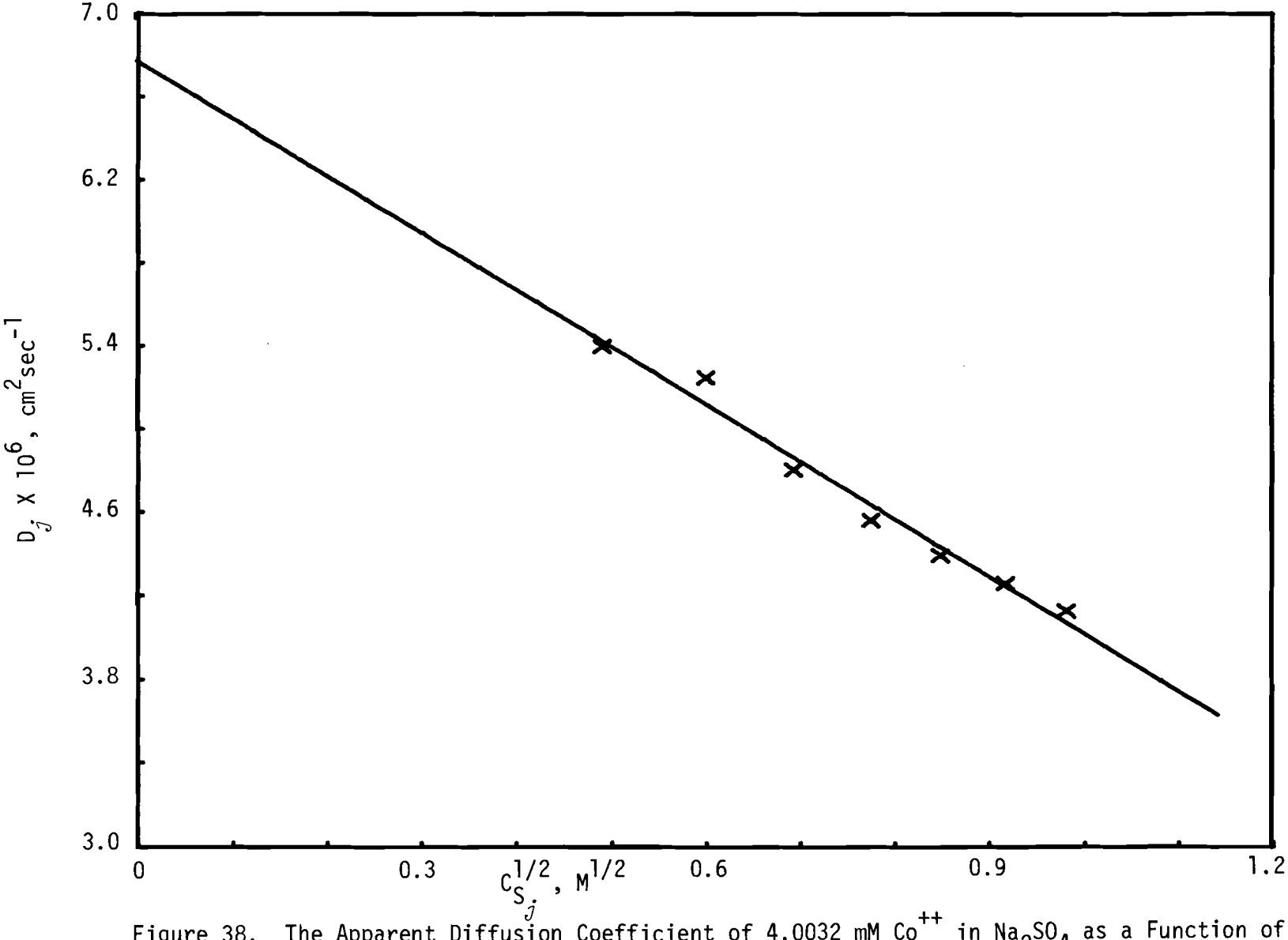

Figure 38. The Apparent Diffusion Coefficient of 4.0032 mM Co^{++} in Na_2SO_4 as a Function of Concentration at 20°C.

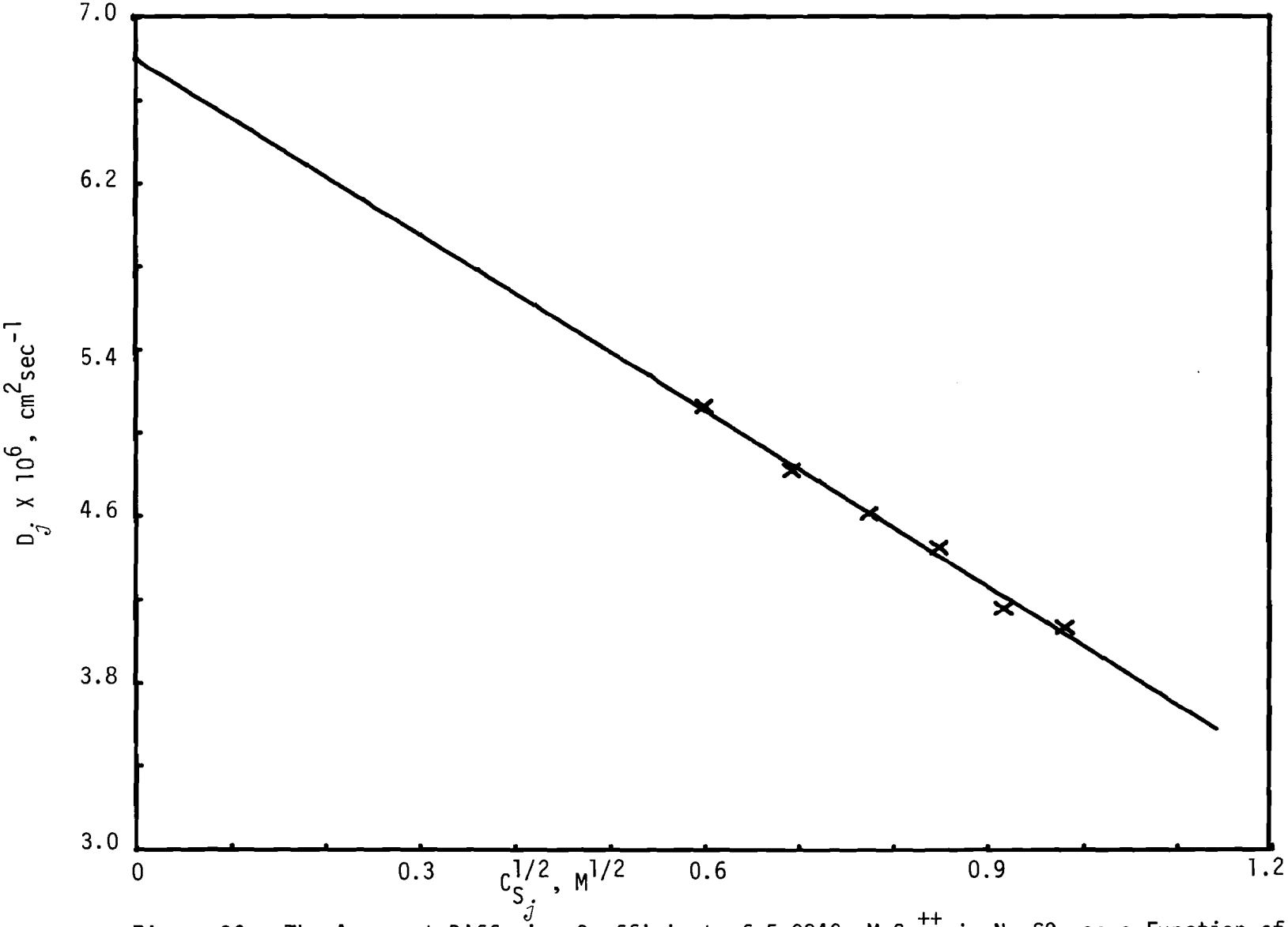

Figure 39. The Apparent Diffusion Coefficient of 5.0040 mM Co^{++} in Na_2SO_4 as a Function of Concentration at 20°C.

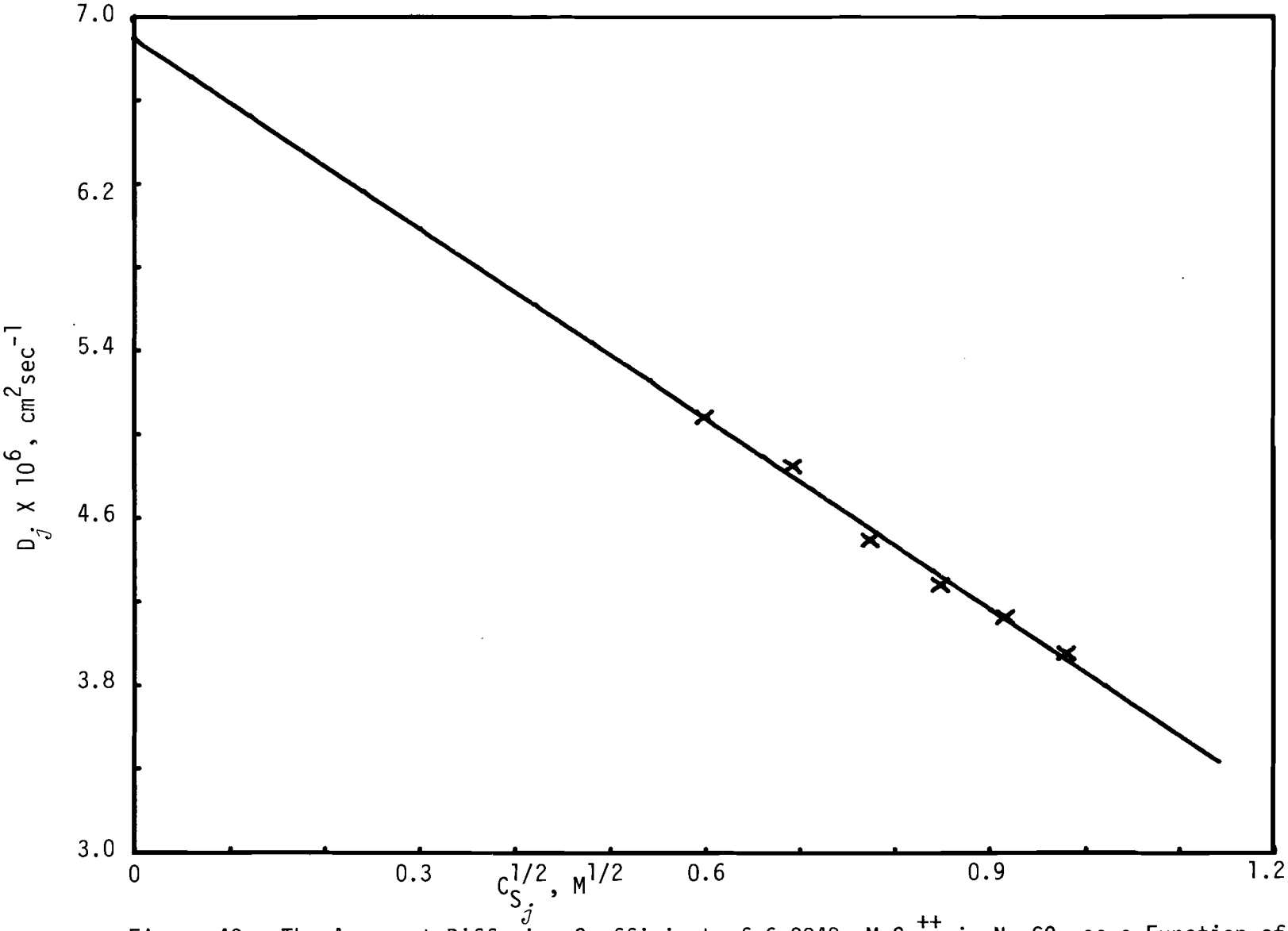

Figure 40. The Apparent Diffusion Coefficient of 6.0048 mM Co^{++} in Na_2SO_4 as a Function of Concentration at 20°C.

APPENDIX IV

List of Symbols

A = Avogadro's number

a_j = activity

b = inverse of the Debye length

C_j = concentration in general

$\overline{C}_j$ = bulk concentration ($\overline{C}_j \equiv C_{M_j}$)

C_{M_j} = concentration of the electroactive component M_j

C_{S_j} = concentration of the supporting electrolyte S_j

D_j = diffusion coefficient

D_j^* = diffusion coefficient under a relaxation effect

$D_{j,1}$ = diffusion coefficient at zero concentration of the supporting electrolyte

D_j° = limiting diffusion coefficient

d = density

E = potential energy

F = the Faraday

$\overline{F}_j$ = diffusive force under an ideal behavior

F_j'' = diffusive force under a non-ideal behavior

F_j^* = diffusive force under a relaxation effect

G = Gibb's free energy

g = the gravitational constant

h = apparent height of the mercury level

i_j = diffusion current

$\overline{i}_j$ = diffusion current density

$\overline{i}_{j,t_d}$ = instantaneous current of a single mercury drop

k = Boltzman constant

l = capillary length

M_j = electroactive metal

n = number of electrons transferred

R = the gas constant

r = mercury drop radius

r_c = capillary radius

S_j = supporting electrolyte

$\overline{v}_j$ = velocity of the diffusing ion

T = temperature

z = signed charge ($z \equiv \frac{n}{\nu_j}$)

ε = dielectric constant of a vacuum

ε_0 = dielectric constant of solution

μ_j = chemical potential

η = viscosity coefficient

η' = overvoltage

δ_j = mobility

γ_j = activity coefficient

ν_j = stoichiometric factor

Ψ = Galvanic potential

λ_j^0 = ionic conductance at infinite dilution

f_j = flux

t_d = drop-time

m = flow-rate